FOP PACIFIC CELL

October 12-14, 1984

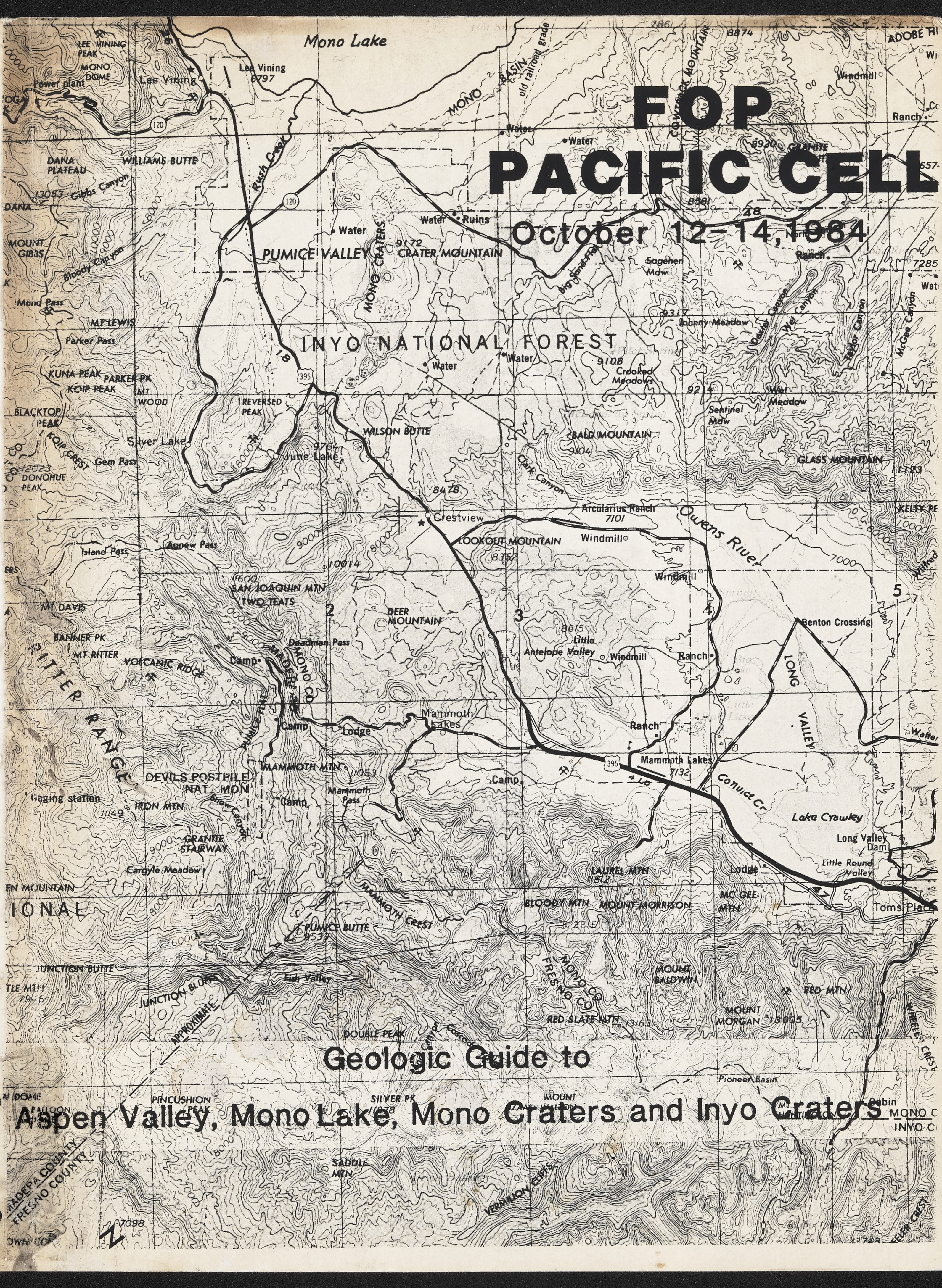

Geologic Guide to

Aspen Valley, Mono Lake, Mono Craters and Inyo Craters

10/22/94

HOLOCENE PALEOCLIMATOLOGY AND TEPHROCHRONOLOGY EAST AND WEST OF THE CENTRAL SIERRAN CREST*

by

Scott Stine[1]
Spencer Wood[2]
Kerry Sieh[3]
C. Dan Miller[4]

with contributions by
Marcus Bursik[3]
David Picket[3]
and
Edward Stolper[3]

Field Trip Guidebook for the
FRIENDS OF THE PLEISTOCENE
PACIFIC CELL
October 12-14, 1984

*Portions of this guidebook have not been reviewed for conformity with U.S. Geological Survey standards and nomenclature. Many preliminary ideas and data are discussed herein, and no part of this guidebook should be used or referenced without permission of the authors.

[1] Department of Geography, University of California, Berkeley, CA 94720
[2] Department of Geology and Geophysics, Boise State University, Boise ID 83725
[3] Division of Geological and Planetary Sciences, California Institute of Technology, Pasadena, California 91125
[4] U.S. Geological Survey, Denver Federal Center, Denver, CO 80225

PREFACE

Welcome to the Friends of the Pleistocene Pac-Cell field trip for 1984. On this year's trip we explore two dominant themes--Holocene climatic change and late Holocene volcanism. The setting is the trans-central Sierra Nevada, an area famous for its scenery as well as for classics of Quaternary geology. It is a region that boasts one of the most varied Quaternary records anywhere: few other places of comparable size in the world display evidence of multiple glaciation, large-scale lake fluctuations, rampant volcanism, and large-scale faulting. That this evidence should be displayed so vivedly in a landscape of such grandeur only increases the appeal of the region.

The trans-central Sierra is nothing if not dynamic. During the three days of the trip we will cross a range that is rising at around 1000 feet per million years; descend into basins that are subsiding at greater than that rate; view (at least from a distance) deposits associated with at least nine separate Pleistocene glaciations; hike onto the youngest portions of what may be the youngest mountain range in North America; examine evidence of climatic changes in the form of wholesale vegetation changes and lake level fluctuations; see evidence of sublacustrine volcanic eruptions including Mono Islands that are less than 200 years old; and trace near-vent and more widely dispersed tephras erupted in latest Holocene time.

We encourage your participation and input, and ask only that you drive carefully, and that you be aware of the impact that we as a large group might have on trails, vegetation, and other fragile parts of the landscape.

We thank the National Park Service for granting access to Aspen Valley; many thanks also to Brian Atwater, Jeanne Dunn, Mary Moulton, Clyde Wahrhaftig, and others who helped smooth the way for this trip.

Seventh printing June 1994
Velo-bound copies authorized by Scott Stine for Friends of the Pleistocene 5/14/85. Unfortunately, since the original photos were lost, there is no choice but to copy from a printed book, which does not give high quality photographs, but does give good quality text, drawings and graphs.

For prices and mail order information write:
Genny Smith Books, 23100 Via Explendor, #44, Cupertino, CA 95014

TABLE OF CONTENTS

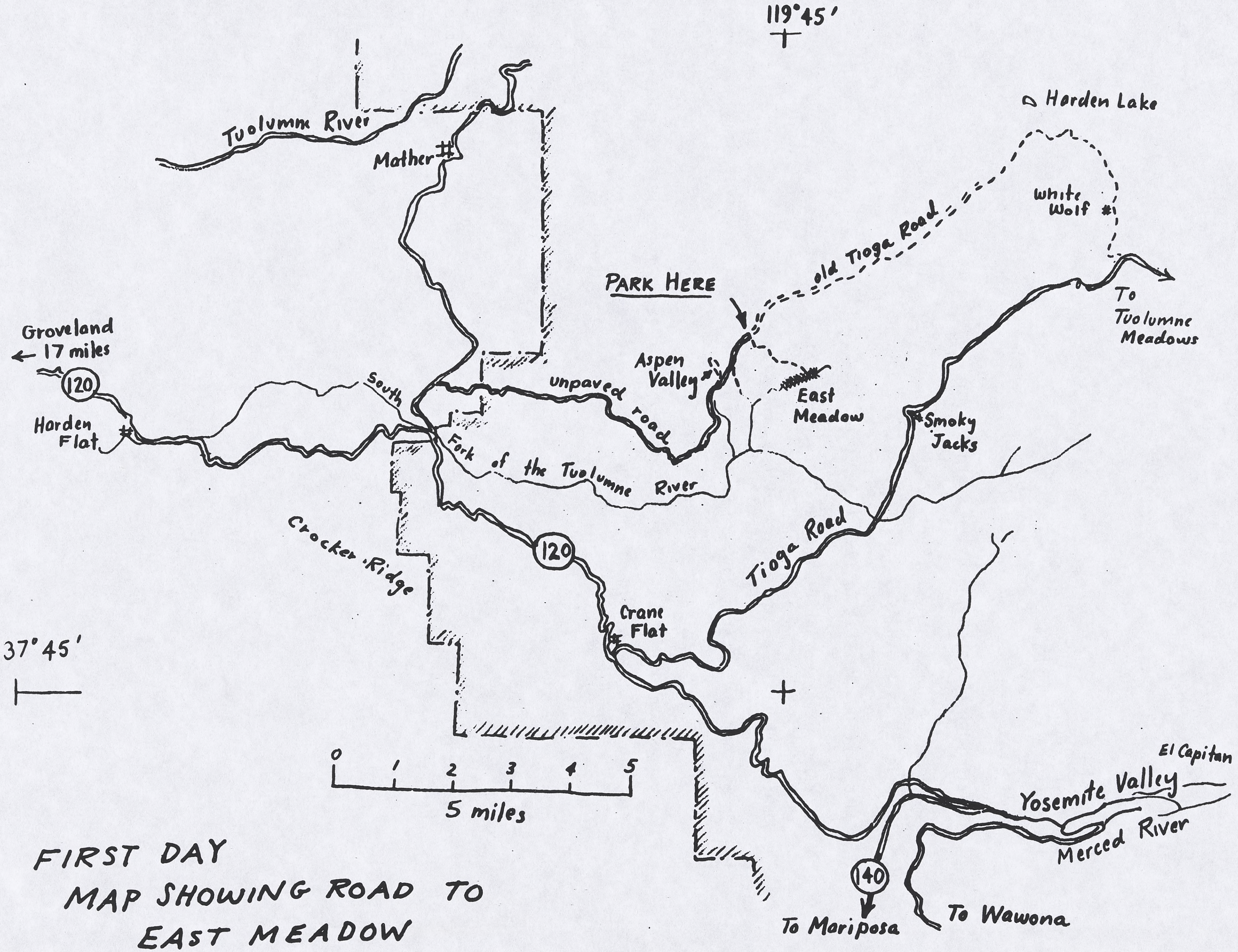

FIRST DAY
MAP SHOWING ROAD TO
EAST MEADOW

EAST MEADOW OF ASPEN VALLEY, WESTERN YOSEMITE NATIONAL PARK

by

Spencer H. Wood
Department of Geology and Geophysics
Boise State University
Boise, Idaho 83725

On the first day of this 1984 Friends of the Pleistocene trip we will walk about a mile from the Aspen Valley Road into the old East Meadow of Aspen Valley. The steep-walled gullies of East Meadow expose a fascinating stratigraphic section of layer upon layer of differing materials: sedge peat, gravels, forest soils, volcanic ash, and an early Holocene paleosol. Radiocarbon dates show that the valley fill contains an almost complete Holocene stratigraphic record. Similar sequences of meadow deposits occur beneath other montane meadows on the west slope of the Sierra Nevada. The sequence of valley fill beneath this meadow dispells the notion that meadows necessarily originate as sediment-filled glacial depressions, for there is no compelling evidence that a bedrock-silled basin or a lake ever existed beneath East Meadow and many other montane meadows of the Sierra Nevada. It is suggested that part of the variation in valley fill materials may be attributed to Holocene climatic fluctuations.

SETTING

The most representative and best exposed stratigraphic sequence beneath a Sierra meadow is in the walls of a gully dissecting, and conseqently destroying a 15-acre meadow in western Yosemite National Park. This is "East Meadow" of Aspen Valley which lies in an unglaciated embayment of the winding step front that rises abruptly from the 6000 to 8000-foot level on the west-sloping upland between Tuolumne (Hetch Hetchy) and Merced (Yosemite) canyons (figure 3-1). Bedrock within the 3.5 square-mile drainage basin above East Meadow is coarse-grained biotite-hornblende granodiorite with zones of mafic inclusions. A pervasive fabric to the drainages reflects a system of vertical bedrock joints oriented N 55° E. The valley of East Meadow is aligned along this strike.

The main stream which feeds the meadow forms in the thickly-forested valley bottom at the base of the rocky step. It flows one mile through forest to the meadow, two-thirds of a mile in the gully dissecting the meadow, and then a mile through a thickly forested reach before it cascades over a bedrock knickpoint. The stream above the meadow goes dry in mid-summer, but seepage into its gully maintains a perennial flow that dwindles to about 0.5 cfs by late summer.

Soils on the rocky slopes of the basin above the meadow are discontinuous patches of shallow grus upon exfoliating bedrock. On lower slopes and around the meadow disintegrated granodiorite accumulates by slope wash and is admixed with tree litter to form a coarse sandy loam in which the mixed-conifer forest is rooted. On the valley floor within the meadow, alluvial and organic deposits were accumulating prior to dissection on a smooth surface that sloped parallel to the stream with a gradient of 2.0 to 3.6 per cent.

The dry rocky slopes above East Meadow are covered with patches of Canadian zone mountain chaparall (Storer and Usinger, 1965, p. 27), Jeffery Pine, Lodgepole Pine, Sugar Pine, and Incense Cedar. Red Fir and White Pine are rare. On the forested valley bottom White Fir is most abundant. A few aspens are found around the meadow opening. The several willow clumps along the stream through the meadow may have been introduced to check erosion. The meadow

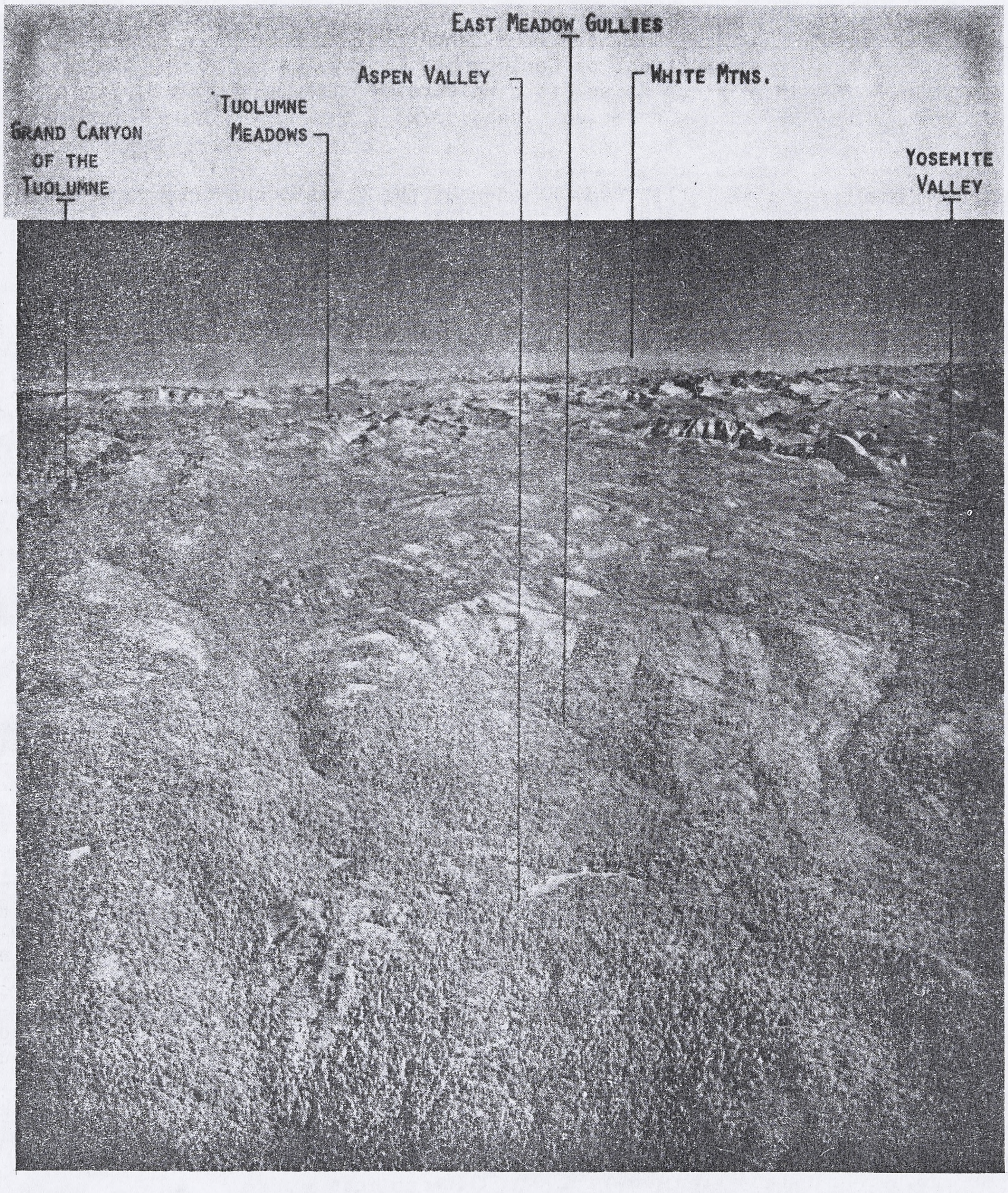

Figure 1. Oblique air photo looking east over west-central Yosemite National Park. The barren step front of granitic rock rises 1800 feet (550 m) behind the dissected 15-acre East Meadow of Aspen Valley. The main meadow of Aspen Valley is a typical montane meadow of 20 acres. (U.S. Geological Survey Photo GS-23, Nov.7, 1955).

community is dominated by sedge with forbs and grasses accounting for probably less than 35 per cent of the cover. By early summer, sedge stands knee-high in the two north branching undissected wet meadows. (See index map in figure 3-2.)

RECENT HISTORY

It is probable, but undocumented, that early sheepherders used the Aspen Valley meadows during the 1860s. The meadows were homesteaded in 1880 by Jeremiah Hodgdon. The Tioga Wagon Road was constructed in 1882-83 through Aspen Valley to mines at Bennetsville on Tioga Pass. According to Hodgdon's grandson, Robert Bright of Knights Ferry, California, hay was cut annually on East Meadow until 1910. In the winter or early spring of 1911, Bright recalls that the meadow was deeply gullied by floodwater from unusually heavy rains. This rainstorm must have been the January 31, 1911 storm that caused above normal stages on the Merced, Tuolumne, Stansislaus, Calavares, Consumnes and Pine rivers (Hoyt and Langbein, 1955, p. 358; and Young and Cruff, 1967, p. 135 and p. 121.)

A gully now runs the length of the meadow. Two headwater branches (figure 3-2) are currently encroaching upon the forested area above the meadow, largely by ground-water sapping. The slumped material produced by sapping is probably removed during floods. No major floods have occurred in East Meadow since 1952 as evidenced by an undamaged log roadway built across the gully during a 4-year selective logging operation that ceased in 1952.

Proximity to Pleistocene glaciers

This area lies outside the limit of Wisconsin glaciation shown by Matthes on an unpublished map compiled for Yosemite National Park. Wahrhaftig and Birman (1965) locate the Wisconsin climatic firn line, from elevation of the lowest cirques, at 8000 feet in this region which is too high to generate a glacier in East Meadow. A thorough search of the valley has revealed no erratic rocks, till, or other features of glacial origin supporting the conclusion of no Wisconsin glacial activity.

If, during older and more extensive glacial stages, ice accumulated on the step front, or high-country ice spilled into the valley from the southeast, all evidence of such an invasion has since been removed. The El Portal stage ice shown by Matthes (1930) was more extensive than Wisconsin ice and its edge would have lain near, but not quite in, this valley.

THE STRATIGRAPHIC SECTION

Presently, the main gully extends for 2500 feet through the meadow providing some exposure of the bedrock surface upon which the meadow deposits lie. This irregular surface has low spurs and knobs, and many core stones (Linton, 1955) 5 to 8 feet in diameter lie upon it. Most core stones are detached, but some, such as shown in figure 3-3, remain embedded in disintegrated granodiorite bedrock. Prior to development of the meadow fill, the stream apparently followed a course confined by spurs, knobs and core stones on a gradient of about 1 per cent. Near points "A" and "B" (figure 3-2) coarse, sub-angular gravels devoid of organic material, encountered by augering are thought to represent the bedload of this confined stream channel.

<u>The basal depositional unit and</u> paleosol.

The initial organic deposits of the meadow sequence are interbedded muck and thick sand layers. The top of this unit can be traced laterally to a burial soil profile developed upon the bedrock knobs and spurs. Muck layers rest upon a three-foot thickness of inorganic fine sand under point "B" (figure 3-2) in the middle of the meadow. In the upper meadow the muck rests upon inorganic sandy gravels. The muck layers represent the first deposits clearly involving vegetation at this site. The muck is black, humic, fine, cohesive material

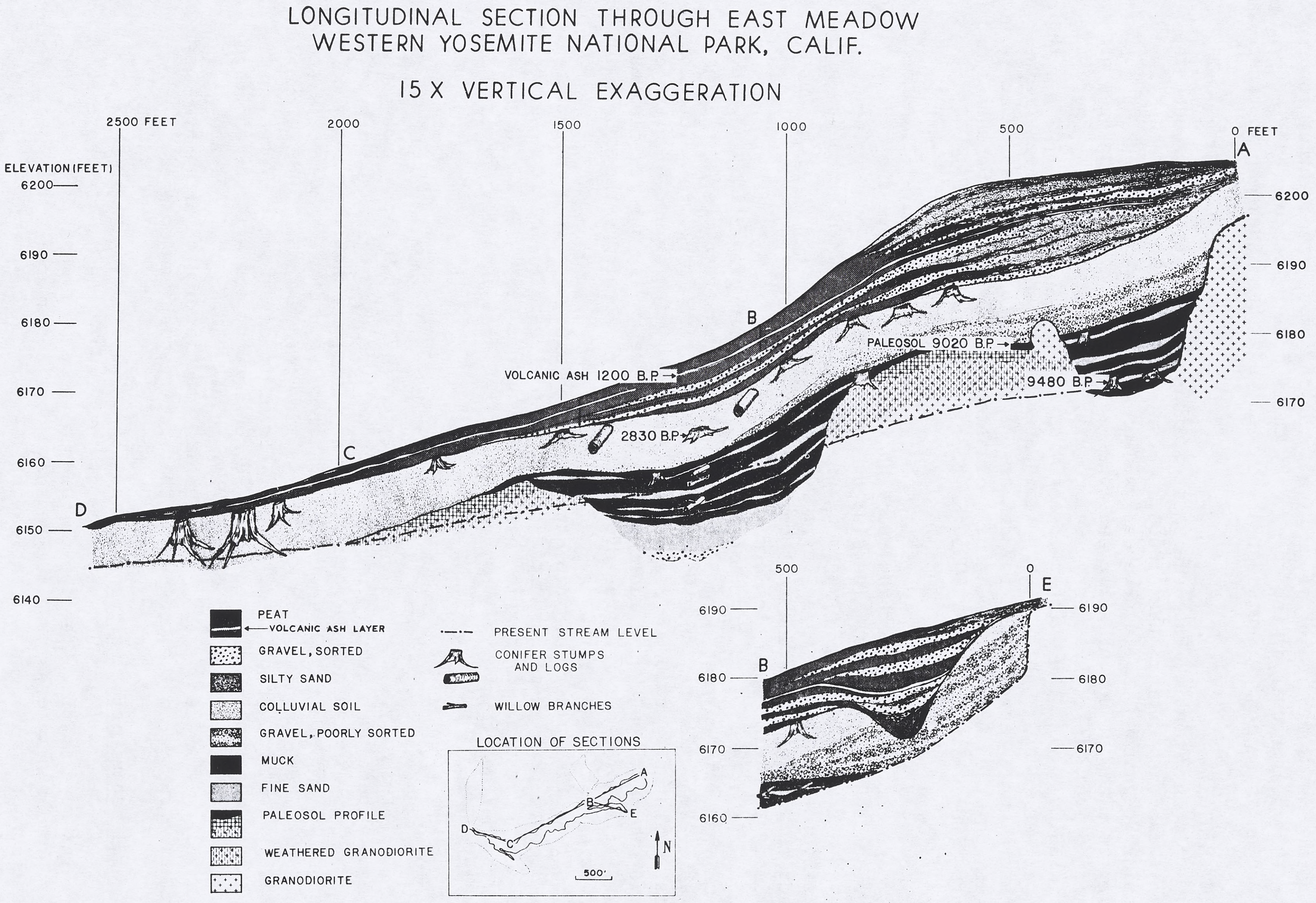

Figure 2. Longitudinal stratigraphic section through East Meadow. 15X vertical exaggeration.

Figure 3. Buried granodiorite core stones and the basal paleosol exposed in the gulley of East Meadow at a location 500 ft west of point A on Fig. 2. The "O" horizon of the 9020-yrs-B.P. (UGa-447) paleosol is the horizontal dark layer to the right of the 3.5-ft mark on the 6-foot white stadia staff. The burrow of an introduced beaver colony is at the left base of the stadia staff. The burrow is in the partially disintegrated granodiorite of the "C" horizon. A 7-foot thickness of gravel and forest soils of the middle depositional unit rests upon the core stone and paleosol. At and above the level marked by clumps of aspen saplings perched on the embankment are interbedded peaty meadow deposits and gravels of the upper depositional unit which here attains a thickness of 17 feet.

Figure 4. Photograph of the stratigraphic section of East Meadow at point "B" on Fig. 2. The 12-foot stadia staff shows scale. The upper depositional unit comprises the top one-third of the section. Here it is composed of three, light-colored, fine-gravel beds separated by two peat beds. The lowest gravel pinches out locally to the left. A massive 3-ft peat layer caps the section and contains the volcanic ash layer from Mono Craters which has been dated here as younger than underlying charcoal (1545 ± 90 yrs BP, I-6049) and probably the 1200 yr BP ash of Wood (1977).

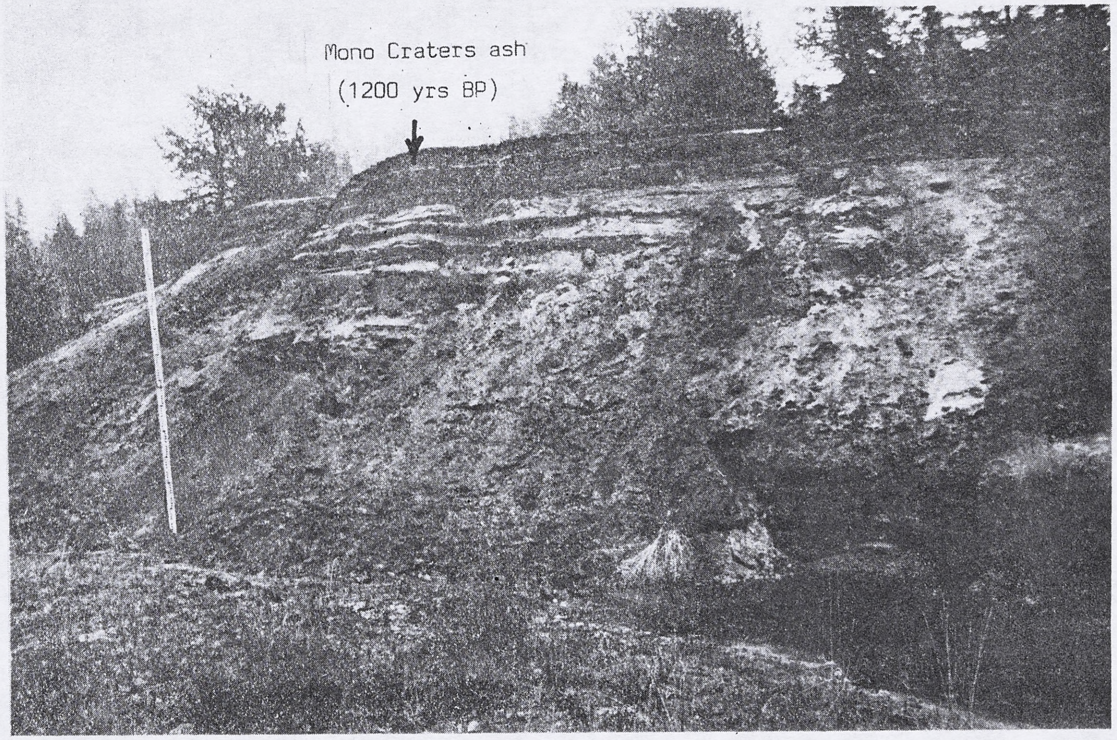

containing abundant sticks and small logs. A few in situ stumps identified as cedar and lodgepole pine are rooted at or near its base, and at the top of the muck unit is a rooted fir stump.

Intercalcated sand layers are composed mostly of fine grained, silty sand, except near the upper end of the meadow (250 feet from point "A", figure 3-2) where gravelly sand lenses with clasts less than 1 cm are exposed.

At a level concordant with the top of the muck unit, but resting upon bedrock protrusions is the complete profile of a well-preserved buried paleosol. This paleosol abuts against core stones (figure 3-3) but its parent material is the granodiorite bedrock upon which it rests. The soil formed on the better drained rocky irregularities of the valley bottom while muck and fine clastics were accumulating in the intervening low spots and stream channels. A field description of the paleosol profile is presented in figure 3-5. Stumps identified as Jeffery Pine and fir are rooted in it (table 3-1) implying fair drainage for part of its history. The black humic "O" horizon is lightly browner than the muck layers, and contains considerably more charcoal. It is crudely stratified and is an accreted horizon presumably formed under moist, but

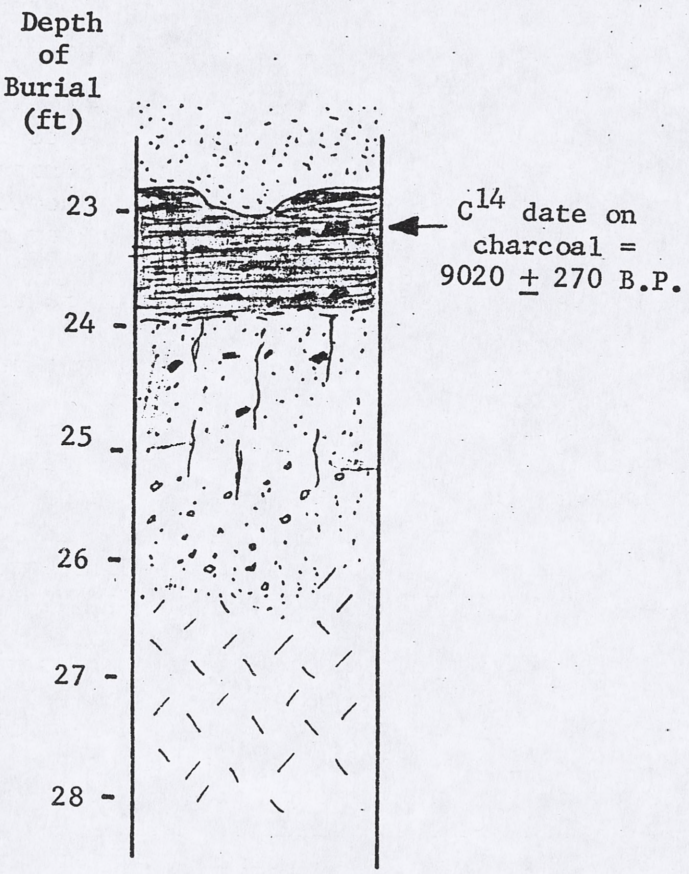

HORIZON DESCRIPTION

O: dark gray(10YR 3/1) finely divided humus and silt. Sticky but friable. Bark and charcoal abundant at top.

A: grayish-brown(2.5Y 5/2) sandy loam, friable, scattered charcoal throughout.

AC: pale olive(5Y 6/3) coarse sandy loam, slighty sticky but friable. Material is largely grus. Relict oxi-root channels penetrate this horizon

C: light gray(5Y 7/1) disinteggrated granodiorite. Can be cut with spade. Primary igneous features are preserved.

Figure 3-5. Profile description of basal paleosol at East Meadow.

moderately drained forested conditions. The underlying "A" and "AC" horizons contain a few rust stripes marking the sites of decomposed roots extending to a depth of 2.5 feet within the profile. At a downstream locality of the paleosol (station 1600 feet, figure 3-2) the "AC" horizon contains a few scattered sub-angular cobbles of aplite, apparently the remains of a thin dike that did not disintegrate with the granodiorite. These aplite cobbles have friable yellow-stained (10 YR 7/8) weathering rinds 3 to 5 mm thick which serve as a crude indication of the intensity of weathering undergone by a fine-grained felsic rock during this soil forming interval. Aplite cobbles in the overlying deposits have no visible weathering rind.

The "A" and "AC" horizons are differentiated primarily on the basis of color plus a slightly sticky consistency in the "AC" material. Admixed charcoal, and fine organic material give the parent gruss of the "A" horizon a slightly browner hue and darker color value than the "AC" horizon which has no visible organic component. There are 5-cm-diameter animal burrowings in the "A" horizon filled with "AC" horizon material.

<u>Chronologyof the basal unit</u>: Two radiocarbon age determinations have been made on material from this basal unit. A charcoal layer, shown in figure 3-5 near the top of the "O" horizon of the paleosol yields an age of 9020 B.P. (UGa-447). A lodgepole pine stump rooted in gravelly sand beneath 9 feet of basal-unit muck and sand (figure 3-2) yields an age of 9480 years B.P. (UGa-452). These two ages confirm the field conclusion that the paleosol organic horizon and the muck layers accumulated in the same time interval.

The middle unit

Resting upon the paleosol or upon the uppermost muck layer are 8 to 10 feet of poorly sorted, rudely bedded, gravelly sand and loamy sand deposits. The lower contact of this unit is everywhere sharp, and it is commonly accentuated by a basal cobble layer with sub-rounded clasts up to 10-cm diameter resting upon the dark-brown muck or the organic horizon of the paleosol. The top of this middle unit is well defined by a line of truncated tree stumps rooted in a slightly cohesive coarse loamy sand material.

Layers in the upper half of this unit are coarse textured, consisting of transported grus admixed with varying amounts of silt, partially decomposed tree litter, and carbonized wood. Layers in the lower half of the unit contain more silt and humus. Some of these lower layers are simliar in texture and color to those found in the present topsoils of dryer meadow habitats sparsely vegetated by xeric sedges and grass. The upper materials of the middle unit, however, are of forest origin and contain abundant charcoal. These layers, up to 2 feet thick, are well-mixed and unstratified suggesting turbation by tree-root growth or rodents.

The most striking feature of the middle unit are well-preserved stumps and logs, particularly abundant near its top. The distribution and the speciation of these coniferous stumps is shown in figure 3-6 and tabulated in table 3-1. The uppermost stump line is associated with a two-foot forest layer that can be traced the full 2500-foot length of the main gully. The valley bottom was entirely forested at the end of middle-unit deposition. Figure 3-7 shows a 5-foot diameter stump of a Jeffery Pine that thrived during the latterpart of middle-unit time. Several other pines reached 4-foot diameters. Jeffery Pine requires well-drained sites (U.S. Department of Agriculture, 1965). Wilde (1958, p. 207) indicates that water table depths of 5 to 7 feet are optimal for coniferous forest trees. It is reasonable to assume that the valley-bottom

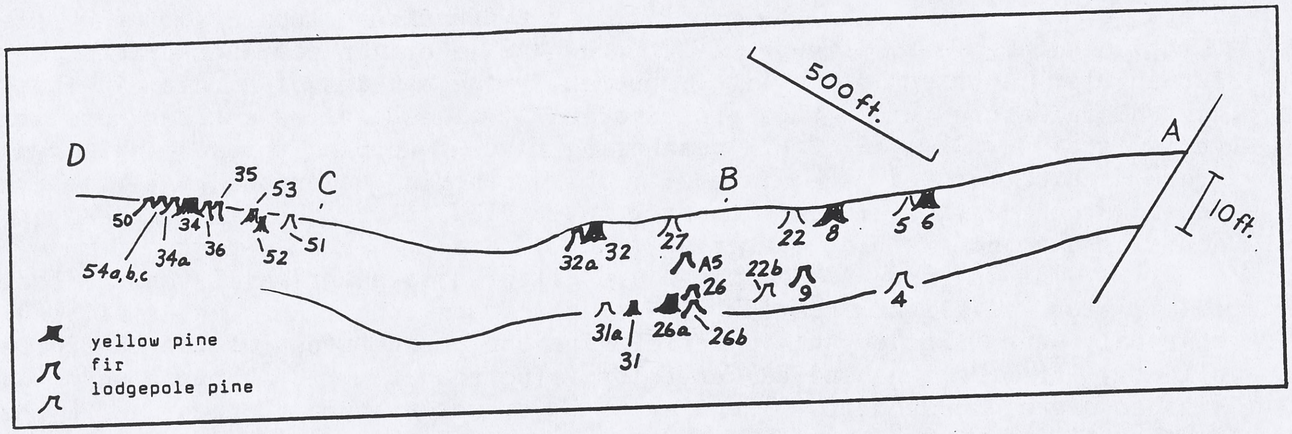

Figure 6. Distribution of in situ buried tree stumps within the middle depositional unit of East Meadow.

water table was deeper than 5 feet for the growth of these large pines in East Meadow. Water table depth is an important parameter of the valley bottom environment that will be used later in a discussion of hydrologic variations during the Holocene.

Chronology of the middle unit: A radiocarbon age of 2830 years B.P. (UGa-448) was obtained from the stump, numbered "A5", (figure 3-6), in the center of the middle unit. This is the root mass of a fir tree that grew in a soil layer just beneath, and truncated by, the uppermost soil layer that contains the prominent stump line. In a discussion of the chronology of the upper unit it will be shown that the death age of the uppermost stumps is about 2500 years B.P.

The length of time represented by the middle unit is not closely bracketed. At East Meadow, the interval must lie between 9020 years B.P. and c.a. 2500 years B.P. It is reasonable to ask whether the stratigraphic boundaries of this middle unit are really time lines as has been tacitly assumed in the preceding discussion. The possibility exists that the major boundaries in the section represent encroaching environments as the valley aggraded through time. If a transverse section were available across the valley such relationships might be seen as the valley bottom environments onlapped the side slopes during accumulation of the fill. However, the conformable relation of the litho-stratigraphic boundaries of the major units with the internal bedding within the deposits strongly suggests that these are time lines within 50 to 100 years.

The valley bottom environment during middle-unit time was well drained. No deep channels are observed in the section that would suggest good drainage was provided by incision. Instead, it appears that aggradation prevailed during this time, the material of which being largely coarse pervious debris derived by slope wash. There may be depositional hiatuses in the 6500-year stratigraphic record of the middle unit, but detection of such hiatuses would require more detailed radiocarbon dating.

The dryer environment and deeper water table indicated by middle unit deposits can be explained by a much diminished supply of ground water caused by

Table 3-1. in situ stumps of conifers in the middle depositional unit, East Meadow, Yosemite National Park.

No. on Map	Stump diameter (inches)	Largest resin ducts* (microns)	Genus	Probable species	Remarks
5	36	100	Pinus	contorta	
6		200	"	jeffreyi	charred top
8	48	200	"	"	charred top
9	21	none	Abies	?	
22	24	100	Pinus	contorta	charred top
22b	20	130	"	"	
26	35	none	Abies	magnifica	red root bark
26a	14	200	Pinus	jeffreyi	
26b	20	none	Abies	?	
A5	24	none	Abies	?	C^{14} age = 2830 yrs.
31	20	none	Abies	?	
31a	20	100	Pinus	contorta	
32	42	150	Pinus	jeffreyi	
32a	10	none	Abies	?	charred top
34	63	200	Pinus	jeffreyi	charred top
34a	48	none	Abies	?	
35	36	none	"	?	
36	24	none	"	?	
50	40	none	"	?	
51	6	100	Pinus	contorta	
52	5	200	Pinus	jeffreyi	
53	6	200	Pinus	jeffreyi	charred top
54a	14	none	Abies		
54b	30	none	Abies		
54c	16	none	Abies		

* Comparative wood anatomy from Panshin, De Zeeuw, and Brown (1964, p. 443-482)

a change in the amount of precipitation or pattern of snowmelt.

The upper unit

The contrast between the stratified dark peats of the upper unit with the underlying lighter colored, crudely stratified forest materials of the middle unit produces everywhere an obvious contact which is also marked by the conspicuous line of stumps beneath. The upper unit thickens from 3 feet in the lower part of the meadow to 15 feet near the upper end as shown in figure 3-2. The character of the sediment layers also change up-meadow. Sediments in the lower reach are parallel-bedded, massive, sedge-peat with intervening beds of well-sorted gravels, but headward the massive sedge-peat layers interfinger with, and grade into, sandy humic loam and sandy silt beds. The gravel layers are also siltier and less well-sorted up-meadow. Cut and fill cross-bedding relationships (amplitudes less than 1 foot) exist among the gravel and sand layers in the upper reaches in contrast to the horizontal bedding down-meadow. Individual gravel layers and the thinner peal layers are rarely continuous for more than a few hundred feet, except for the uppermost peat layers which can be followed continuously for about 1500 feet along the trunk gully. It attains a thickness of 4 feet in the center of the meadow. Below this massive peat are usually two or three prominent gravel layers separating two thinner peat beds (figure 3-3).

The massive peat layers are composed of interwoven fibers and roots of sedge. Around the upper margin of the meadow they become increasingly silty, and the thinner peat beds are generally silt-rich throughout. Some contain considerable wood and bark fragments and conifer needles. All gradations from pure organic sedge peat through humic sandy loams (greater than 5 per cent organic by dry weight) occur in this upper unit of East Meadow. Both peat and the humic sandy loams appear dark brown in the section because of their organic content and their capacity to hold moisture. The organic material in these layers has not sufficiently decomposed to produce muck like that in the basal unit.

<u>Volcanic Ash</u>: Within the peat is one prominent and nearly continuous layer of volcanic ash varying in thickness from 0.4 to 1.5 inches. The layer is assigned a maximum radiocarbon age of 1545 years B.P. from analysis of a lump of charcoal found within it (Wood, 1972). It is identified as tephra 2 (Chapter 4) closely bracketed elsewhere by radiocarbon dates at 1200 years B.P. Thus the 1545 years B.P. charcoal had already aged as heartwood of a tree with considerable longevity or as reworked surficial material before being incorporated within the waterlain ash layer.

Rate of accumulation of the peat above tephra 2 does not exceed 2 feet over the last 1200 years or 2 inches per century. Peat between tephra 2 and the top of the middle unit is bracketed between radiocarbon based ages of 1200 B.P. and 2830 B.P., thus its accumulation rate cannot exceed 5 inches per century.

At one section in the center of the meadow, a second, very thin and whispy layer of fine ash lies 0.6 feet beneath tephra 2. The two peat accumulation rates provide an age estimate for this whisp of ash of 1400 to 1670 years B.P.

<u>Diatom layers</u>: Easily mistaken for volcanic ash are several discontinuous whitish, diatom-rich layers which contrast sharply with the dark peats. A 15-cm thick layer of nearly pure diatom tests lies at the base of the upper unit. It apparently accumulated in a ponded area shown in the section B - E, figure 3-2. Elsewhere in the upper peat and humic silt loam deposits, diatom layers occur as thin, 1 to 2 cm thick, layers composed of mixed finely divided organic material and whole diatom tests. Several taxa of diatoms are relatively plentiful, but they have not been specifically identified. It is thought that concentrations of tests into discrete layers may represent intervals during which parts of the

meadow became water-logged or actually ponded, or perhaps forest-fire-induced changes in nutrient supply and water chemistry caused a flowering of diatoms. Detailed study of diatom stratigraphy might be useful in revealing subtle environmental variations during the accumulation of meadow deposits.

Charcoal bands: Thirteen separate charcoal-rich bands are found within peat layers of the upper unit. They are not continuous, but, assuming that these layers record major forest fires, it was hoped that each would serve as a time-correlative marker horizon. A 380-year fire history extending back from the present was determined from study of annual growth rings on recently logged, fire-scarred, sugar pine stumps that surround East Meadow. Charcoal bands within sections of the upper unit exposed along the main trunk gully are shown in figure 3-8. In four of the eight sections examined, exactly 5 bands are found above the 1200 year volcanic ash layer. In the remaining sections, 2 to 3 bands are found. This consistency is probably significant, but matching these layers to the known fire history is difficult because East Meadow fire history is imperfectly recorded prior to the late 16th Century. As shown in figure 3-9, fires were recorded on 3 or more stumps for the years 1779, 1803, 1842, and 1901 A.D. The latter 2 fires were also noted by Wagener (1961) in a similar study at Crocker's Station, 8 miles to the southwest. He considered only the 1842 and 1901 events to be major fires. Wagener found a prevailing 8-year natural fire frequency in the west slope Sierra timber zone which compares well with a 7 to 9 year frequency reported for the Sierra mixed Sequoia-conifer forest by Kilgore (1973).

Forest fires of this frequency are not recorded by charcoal layers. It is likely that only major fires, and perhaps, only those followed by a heavy slope-washing runoff, produce significant charcoal layers. If these layers represent major fires, then there have been five such events in the East Meadow watershed in the past 1200 years. It cannot be said with certainty which, if any, of the dendrochronologically recorded fires matches the uppermost charcoal layer in the section, but the thickness of peat capping that band would be consistent with the 1842 A.D. fire or one still older.

Gravel beds: Well sorted, sandy gravels derived from grus are interstratified with the peat. Three prominent gravels shown in figure 3-2, and figure 3-4, occur discontinuously as lenses up to one foot thick and several hundred feet long beneath the 1200-year marker ash. Two more gravel layers occur above the 1200-year ash in the upper reaches of the meadow producing thereby a thickening of the upper unit with the aid of intercalcated sand lenses. These sand and gravel layers do not extend to the center of the meadow.

Clasts in the gravel lenses rarely exceed 1 cm diameter. The size analysis given in figure 3-10 is typical. Median size of the granules is 1 to 2 mm reflecting the texture of the granodiorite from which they are derived. The gravels are well-sorted with a Trask sorting coefficient Q3/Q1 between 2 and 2.2.

The pure gravels show little stratification, but sandier beds are crudely layered. In the upper reaches of the meadow, some of the sands display small scale cross-bedding less than 1.0 foot in amplitude associated with correspondingly small scale scour and fill.

Material comprising relatively large gravel bars along the smaller Sierra streams is similar in texture and stratification to the gravels in the East Meadow section. Janda (1967) reports that relatively large flat-topped gravel bars and berms of present High Sierra mountain streams are constructed during floods with recurrence intervals of more than 10 years. The gravel beds in the East Meadow section probably represent flat-topped gravel bars of this origin.

It is surprising that only 5 significant gravel beds were spread over the meadow surface during the past 2500 years. This indicates that gravel transporting flows have been relatively infrequent during the deposition of the

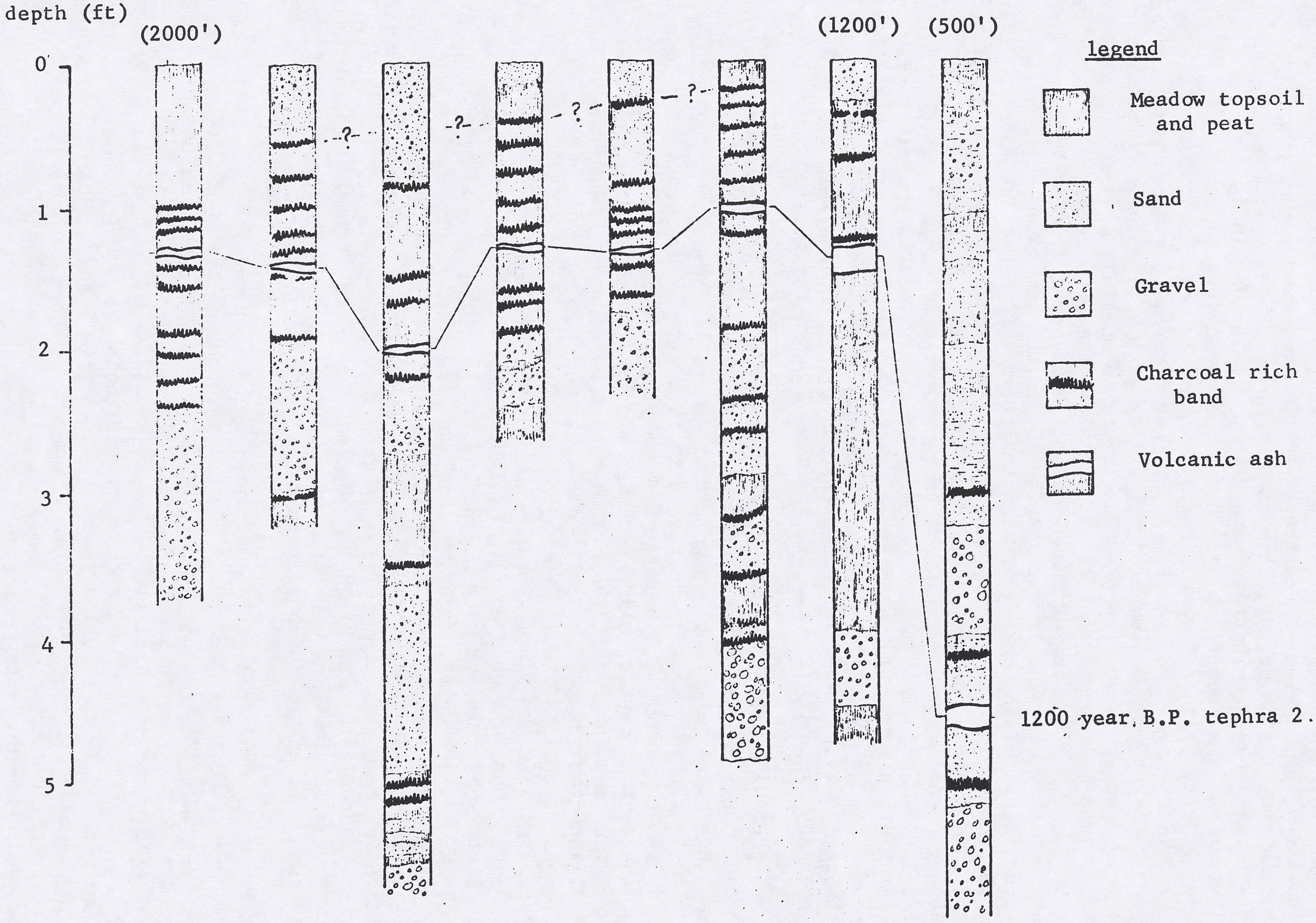

Figure 3-8 Detailed stratigraphy in the upper unit of East Meadow illustrating charcoal-rich bands above the 1200 year B.P. marker horizon. Numbers above columnar sections refer to horizontal distance west of point "A" on index map of figure 3-2.

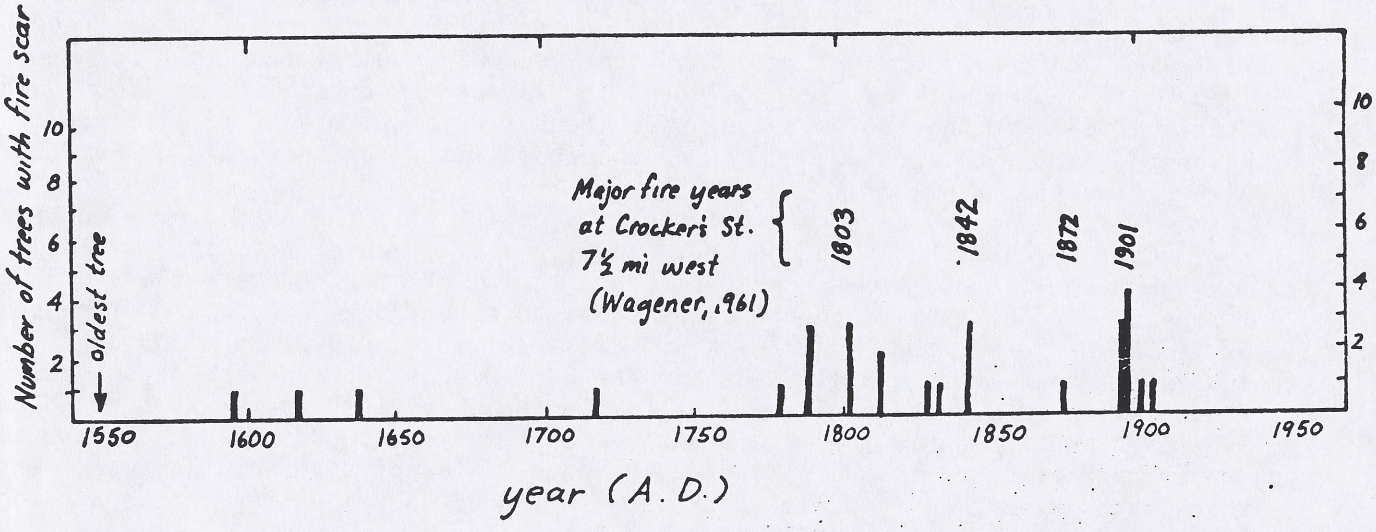

Figure 3-9. Forest-fire history at East Meadow of Aspen Valley, Yosemite National Park as read from fire scars on Sugar-Pine stumps. Uncertainty in dendrochronologic age of fire is probably ± 5 years for there is uncertainty of this order in the field tree-ring counts, and the logging operations spanned 1950 - 52 .

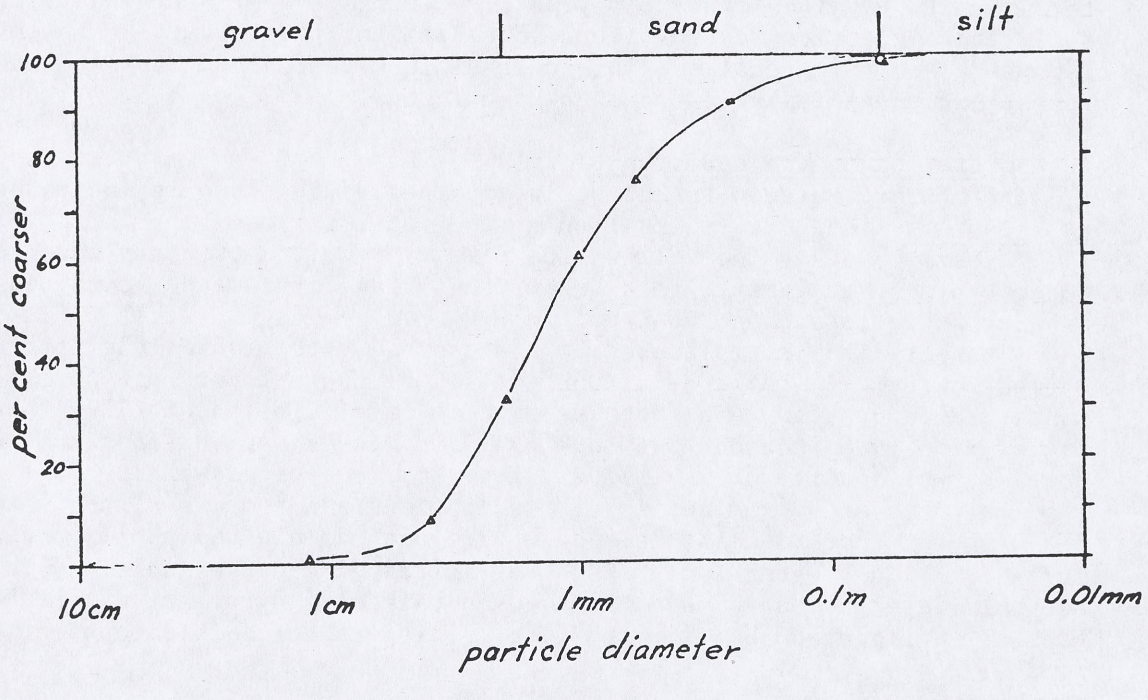

Figure 3-10. Size analysis of material in gravel bed immediately beneath the massive peat bed of the upper depositional unit, East Meadow.

upper unit within the meadow deposits. The recurrence interval for bar-building floods suggested by these five layers is about 500 years.

A 124-year historical record of Tuolumne drainage flood stages comes from La Grange (elev. 330 ft) where the Tuolumne discharges into the San Joaquin Valley. Major floods occurred in January, 1862, January, 1911, and December, 1955. The 1862 flood is considered the largest historical flood (Young and Cruff, 1967) in the Tuolumne drainage. Peak flow at La Grange is estimated by Wagoner (1908) to be 130,000 cfs or 85 cfs/sq. mi., but there are no data for higher elevation stations.

Since no gravel beds are found in a position in the East Meadow section that can be attributed to the 1862 flood, the five gravel beds in the section may be from flood flows greater than those of 1862. Were a flood of the intensity of the 1966 southern Sierra flood to occur at East Meadow a discharge of $(3.5\ \text{mi} \times 400\ \text{cfs/mi}^2) = 1400$ cfs might flow across the meadow. It is suggested that the gravel beds in the East Meadow section were deposited by flows of this magnitude. According to Dean and Scott (1971) the 1966 southern Sierra flood produced peak discharges three times greater than the computed 50-year recurrence flood discharge. Hence it is not unreasonable to suspect that each significant gravel layer in the meadow sections represents a flood event of several-hundred-year-recurrence interval.

Chronology of the upper unit: Ages within these deposits are established by; the 1200-year B.P. tephra 2, the surface of an historically known meadow that began eroding in 1911 A.D., and the age of underlying deposits. The date of the contact representing the change from forest to meadow conditions lies between the 2830 year B.P. age on the stump in the middle unit and the 1200 year B.P. tephra 2 layer. Radiocarbon dating the outer wood of any one of the many stumps would give a most accurate age, but it can as well be estimated without the additional cost. Since the 1200 year marker horizon is in the middle of the upper unit with perhaps slightly more peat beneath than above, the lower half represents an estimated 1300 years, giving an age of 2500 years B.P. for the total unit. Since the 2830 year B.P. stump is overlain by a layer of forest soil that contains an in situ 3-foot diameter pine stump, an interval of some 300 years seems reasonable. This date of 2500 years B.P. marks the death of the forest and the initiation of meadow conditions.

Interpretation of the upper unit

The contact between forest soils and the meadow topsoils indicates a rise of at least 5 feet in the shallow ground water table of the valley bottom about 2500 years ago. The yellow pine forest prior to its death required that the water table be at least 5 feet below the surface, but meadow conditions indicate a water table less than two feet.

Forest fire is implicated by the charred tops of 5 of the uppermost buried stumps of unit 2, table 3-1. But it will be shown later that forest fire alone cannot account for a 5-foot water table rise. The possibility that the water table rise was caused by damming or impeded soil drainage was considered. However, no vestige of any slides, log jams, or beaver workings are found below the meadow, and examination of the longitudinal profile of the valley, figure 3-2, shows that damming alone would not explain the poorly drained sloping surface. The water-table rise that initiated meadow-conditions in the valley bottomis interpreted to have been caused basically by climatic variation and was possibly triggered by forest fire. This mechanism is discussed in detail in Wood (1975)..

Figure 7. Photograph of Stump no. 34 (table 1) of a five-foot diameter yellow pine rooted in the top of the middle depositional unit of East Meadow about 2200 ft west of point "A" in Fig. 2. The surrounding soil and overlying meadow deposits have been entirely removed by erosion. A remnant of the meadow surface is behind the stump.

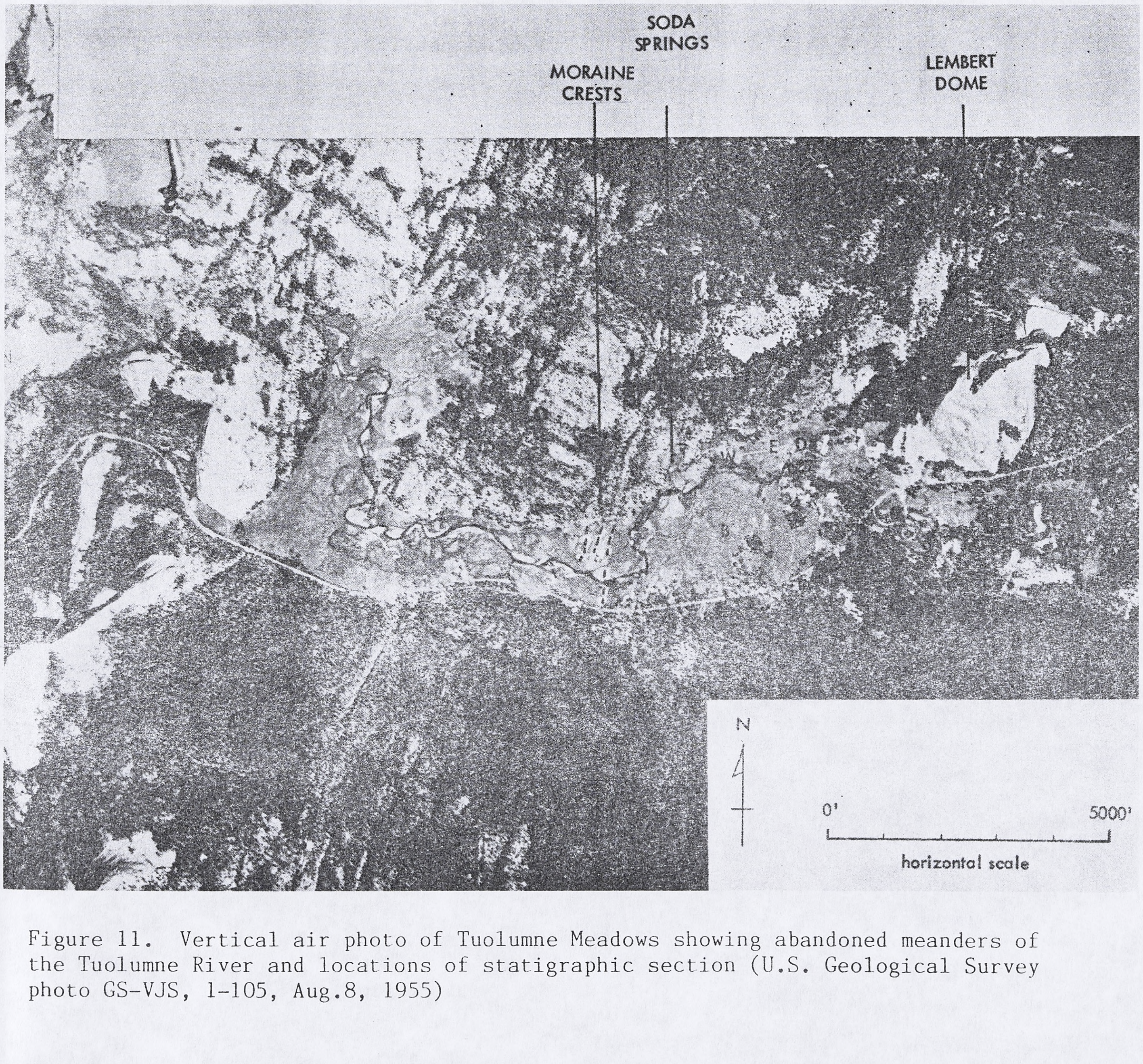

Figure 11. Vertical air photo of Tuolumne Meadows showing abandoned meanders of the Tuolumne River and locations of statigraphic section (U.S. Geological Survey photo GS-VJS, 1-105, Aug.8, 1955)

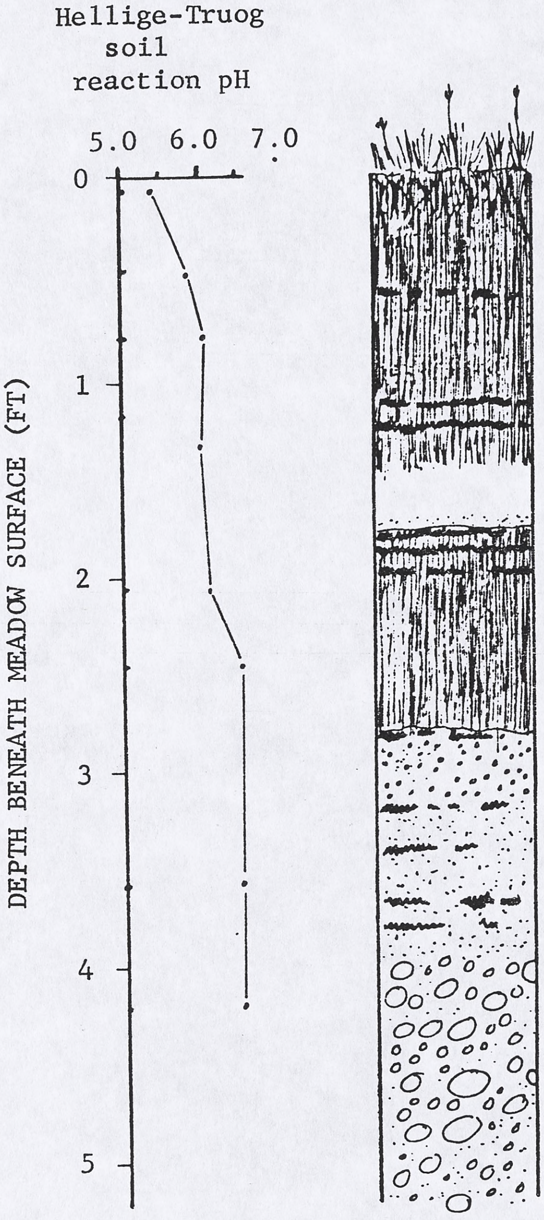

DESCRIPTION

Very dark greyish brown (10YR 3/2) humic silt and sand loam with a few thin fine sand lenses and charcoal-rich bands.

White pumiceous volcanic ash and lapilli (graded air-fall bed).

Dark brown (10YR 4/3) humic silt loam with dark red (10R 3/6) 3-mm wide mottles.

Coarse, well-sorted sand with charcoal layers.

— C^{14} date on charcoal = 3930 ±80 B.P.

— water table (September)

Gravels, sub-round, metamorphic clasts outnumber granitic clasts 8 to 1.

Figure 12. Description and stratigraphy of meadow topsoil at site B of Tuolumne Meadows (Fig. 11), eastern Yosemite National Park.

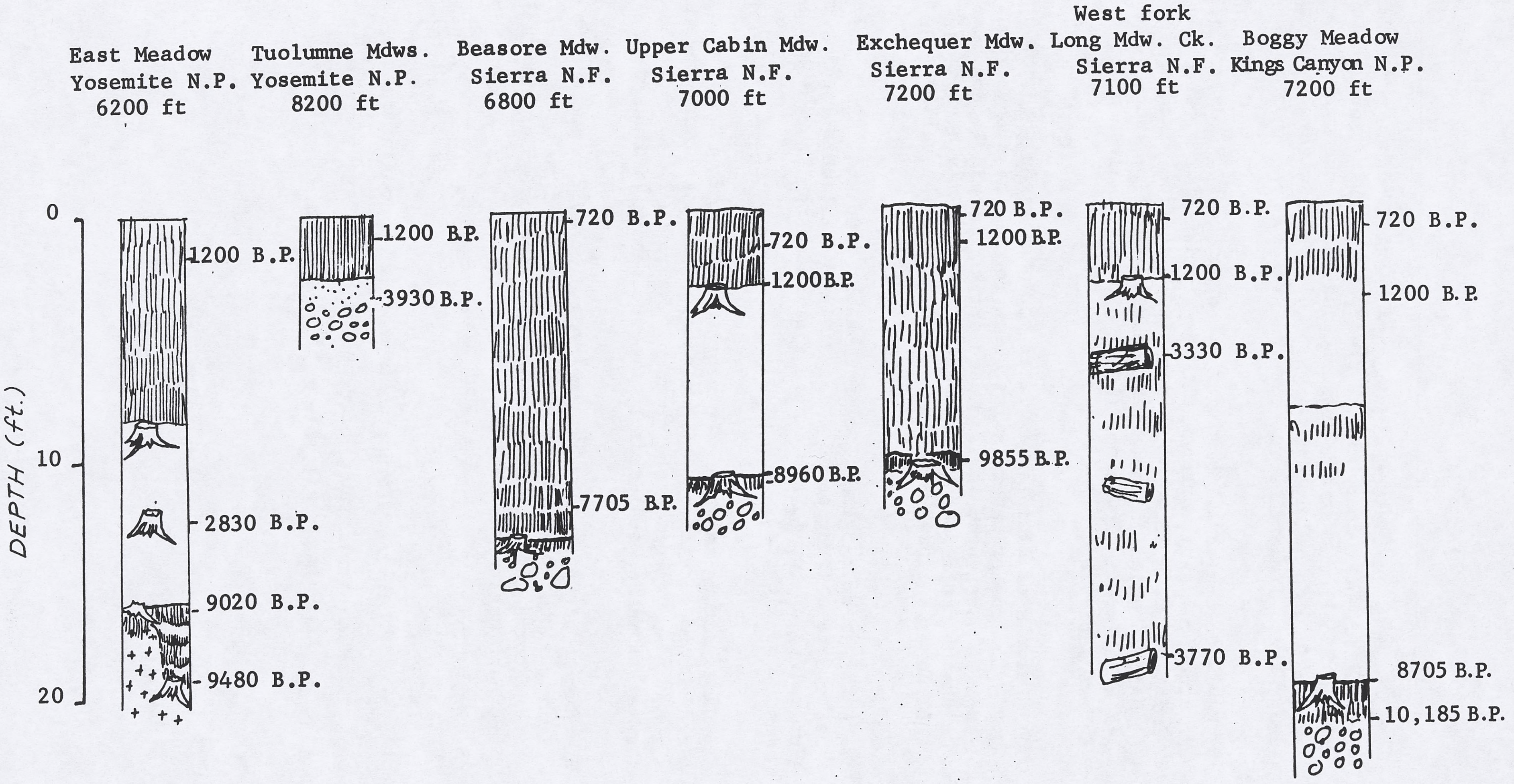

Fig. 13. Summary of stratigraphy and chronology of meadow sections along the west slope of the southern Sierra Nevada.

1. During the late Wisconsin ice age, peak flows of the stream are sufficiently competent to transport coarse alluvium along a 1 to 2 per cent stream gradient and out of the valley. Deposits are limited to bed-load cobbly gravels. The watershed is sparsely vegetated. Timberline is near the present upper montane belt.

2. Early post-glacial warming, just prior to 10,200 years B.P. , is accompanied by montane-belt forestation of the watershed. Diminished peak flows allow deposition of fine clastics and organic material in the stream channel. Willow and sedge meadows and bogs form in low areas. Soil profile develops on riparian forest sites.

3. Intervals of diminished winter snowpack begin about 8700 years B.P. Low summer water tables allow forest invasion of bogs and meadows. Continued low snowpack during the middle Holocene maintains the forest environment on the valley bottom. Forest soil and slope wash alluvium accumulate on the valley floor.

4. Extremes of neoglacial climate about 2500 and 1200 years B.P. cause late melting snows and a rising water table leading to mortality of the forest on the flat and establishment of open meadow conditions.

5. Late melting snows of the neoglacial sustain high ground water and meadow conditions. Organic topsoils, peats, and sheets of flood gravel aggrade the surface. Aggradation on a protective cover of meadow sod leads to oversteepening of the surface slope.

6. Summer use of meadow by livestock damages the protective sod. During winter plant dormancy, flood waters from torrential winter rain storms initiate gullies leading to erosion of the valley fill and destruction of the meadow.

Figure 14. The developmental history of a montane meadow interpreted from the stratigraphy of deposits in valleys on the west slope of the southern Sierra Nevada, California.

TUOLUMNE MEADOWS, YOSEMITE NATIONAL PARK

The second stop of the first day will be at Tuolumne Meadows, the largest, and perhaps the most scenic of the subalpine meadows of the Sierra Nevada. The section of fluvial gravel and meadow soil at sight "B" marked on the air photo of Fig. 11 is illustrated in Fig. 12.

GENERALIZED INTERPRETATION OF MEADOW DEPOSITS

Comparison of radiocarbon dated meadow stratigraphy from exposed sections of meadow deposits in the southern Sierra Nevada is shown in Fig. 13. Coincidence of age of similar stratigraphic units in the meadow deposits strongly argues for paleoclimatic variation as the underlying cause of many of changes observed in the deposits. A summary of events as interpreted mostly at East Meadow is in figure 14.

ACKNOWLEDGEMENTS

I thank Carl Sharsmith for first showing me the East Meadow area and for many enjoyable discussions in the field. I thank Robert P. Sharp for several memorable trips to the field, timely advice, and critically reading earlier versions of the description of East Meadow. Partial support of research expenses was provided by National Science Foundation grant GA-35449, Geological Society of America Penrose grant 1721-73, and the California Institute of Technology.

REFERENCES CITED

Dean, W. W., and Scott, K.M., 1971, Floods of December, 1966 in the Kern-Kaweah area, Kern and Tulare Counties, California: U. S. Geological Survey Water-supply Paper 1870-C, 79 p.

Hoyt, W.G., and Langbein, W.B., 1955, Floods, Princeton University Press, Princeton, New Jersey. 469 p.

Janda, R., 1967, Gravel transport in high mountain streams, Sierra Nevada, California (abs.): Geological Society of America, Special Paper 115, p. 334.

Kilgore, B.M., 1973, The ecological role of fire in Sierran conifer forests: Quaternary Research, v. 3, p. 499-513.

Linton, D.L., 1955, The problem of tors: Geographical Journal, London, v. 121, p. 470-487.

Matthes, F. E., 1930, Geologic history of Yosemite Valley: U.S. Geological Survey Professional Paper 160, 137 p.

Panshin, A. J., de Zeeuw, C., and Brown, H. P., 1964, Textbook of Wood Technology, volume 1: New York, McGraw Hill Book Co., 643 p.

Storer, T.I., and Usinger, R.L., Sierra Nevada Natural History: Berkeley, University of California Press, 374 p.

Wagener, W. W., 1961, Past fire incidence in Sierra Nevada forests: Journal of Forestry, v. 59, p. 739-748.

Wagoner, L., 1908, Flood of March, 1907: American Society of Civil Engineers Transactions, v. 61, p. 353.

Wahrhaftig, C. and Birman, J.H., 1965, The Quaternary of the Pacific mountain system in California: p. 299-340 _in_ Wright, H.E., Jr., and Frey, D.G., (editors) The Quaternary of the United States: Princeton University Press, 922 pages.

Wilde, S. A., 1958, _Forest Soils_: New York, Ronald Press, 537 p.

Wilde, S. A., Steinbrenner, E. C., Pierce, R. S., Dosen, R. C., and Pronin, D. T., 1953, Influence of forest cover on the state of the ground water

table: Soil Science Society of America Proceedings, v._ _ p. 65-67.

Wood, S.H., 1972, Preliminary Holocene volcanic ash chronology for the Yosemite National Park region, Sierra Nevada, California (abs.) Geological Society of America Abstracts with Programs, v. 4, p. 263.

Wood, S.H., 1975, Holocene stratigraphy and chronology of mountain meadows, Sierra Nevada, California (Ph.D. dissertation): Pasadena, California Institute of Technology, 180 p. University Microfilms order no._ _ _ __. Reprinted in 1979 as Earth Resources Monograph no. 4, U.S. Forest Service, Western Forest Information System, Berkeley Service Center, PO.Box 245, Berkeley, California.

Wood, S.H., 1977, Distribution, correlation, and radiocarbon dating of late Holocene tephra, Mono and Inyo Craters, California: Geological Society of America Bulletin, v. 88, p. 89-95.

Young, L.E., and Cruff, R.W., 1967, Magnitude and frequency of floods in the United States, Part 11, Pacific slope basins in California, Volume 2, Klamath and Smith River basins and Central Valley drainage from the east: U. S. Geological Survey Water-supply Paper 1686, 308 p.

Late Holocene Lake Level Fluctuations and Island Volcanism at Mono Lake, California

by

Scott Stine
Department of Geography
University of California
Berkeley, CA

Abstract

During the past 3500 years the surface of Mono Lake has fluctuated over a vertical range of more than 130 feet in response to variations in climate. Sedimentary sequences exposed in recently dissected deltas, together with biotic, geomorphic, tephrochronologic, radiometric, and historic evidence, permit a detailed reconstruction of these fluctuations. The lake level curve, in combination with tephrachronologic evidence, can in turn be used to illuminate the history of volcanism associated with the islands of Mono Lake. This history includes no fewer than 30 separate eruptive events, many of which occurred during the past 220 radiocarbon years.

Introduction

Between 1941, when the City of Los Angeles began to divert water from the Mono Basin, and 1982, when abnormally wet weather temporarily curtailed stream diversions, the surface of Mono Lake fell 45 feet--from an elevation of 6417 feet to 6372 feet. In response to the drop in base level, Rush, Mill, and Lee Vining Creeks--the lake's principal tributaries--incised the downstream portions of their Holocene deltas to depths ranging from 5 to 30 feet. Exposed in the walls of these fresh stream cuts are sequences of riverine, littoral, lacustrine, and volcanic sediments. These sedimentary sequences, in combination with geomorphic, biotic, historic, and radiocarbon evidence, have been used to construct a detailed fluctuation curve for Mono Lake that spans the past 3500 radiocarbon years (Figure 1). Construction of the lake level curve, its paleoclimatic significance, and its bearing on the ages of the Mono Islands, are the topics of today's leg of the Friends of the Pleistocene trip.

Field work for this study was undertaken in the summers of 1980-1983. Three of these years--1980, '82, and '83--were characterized by abnormally high runoff from the Mono Sierra. The Los Angeles Department of Water and Power, unable to divert the full stream flow, was forced to release large amounts of water down the creeks. High flows scoured the walls of the stream cuts, clearing away talus and colluvium, and permitting access to the delta stratigraphy. In contrast, runoff during the past season (1983-84) was not sufficient to force substantial releases of water. As a result, thick blankets of talus today cover many of the most illuminating exposures. I have tried to clean up some of the best cuts so that we will have a chance for examination and a basis for discussion.

A Few Important Lake Surface Elevations

6380'	present-day lake elevation (October, 1984).
6372'	lake elevation in early 1982. Note the rise of 8' in the past 2 years.
6404'	the lowest level to which the lake has fallen under natural (pre-diversion) conditions during historic times.
6417'	lake level in 1940 when water diversions began. Also the approximate level the lake would be today had no diversions occurred.
6428'	the historic highstand, attained on July 16, 1919.

Road Log

START: Intersection of Highways 120 and 395, just south of the town of Lee Vining. Turn left (north) toward Lee Vining.

MILEAGE

0.2 mi.	Crossing Lee Vining Creek, the second largest of Mono Lake's tributary streams.
0.35	Enter Lee Vining, named after miner and sawmill operator Leroy Vining (Fletcher, 1982). The town lies at an elevation of 6800 feet on the plain of the Late Pleistocene (Tioga/Wilson Creek) delta of Lee Vining Creek.
0.8	To the left is a clear view of depositional shoreline terraces associated with Late Pleistocene Lake Russell. The highest terrace visible in this vicinity lies at about 7070 feet. A higher terrace (at 7180 feet--the overflow elevation of the lake) can be seen in a few places around the basin (Lajoie, 1968).

Figure 1

Surface Fluctuations of Mono Lake,
3500 BP- present.
● = Radiocarbon date

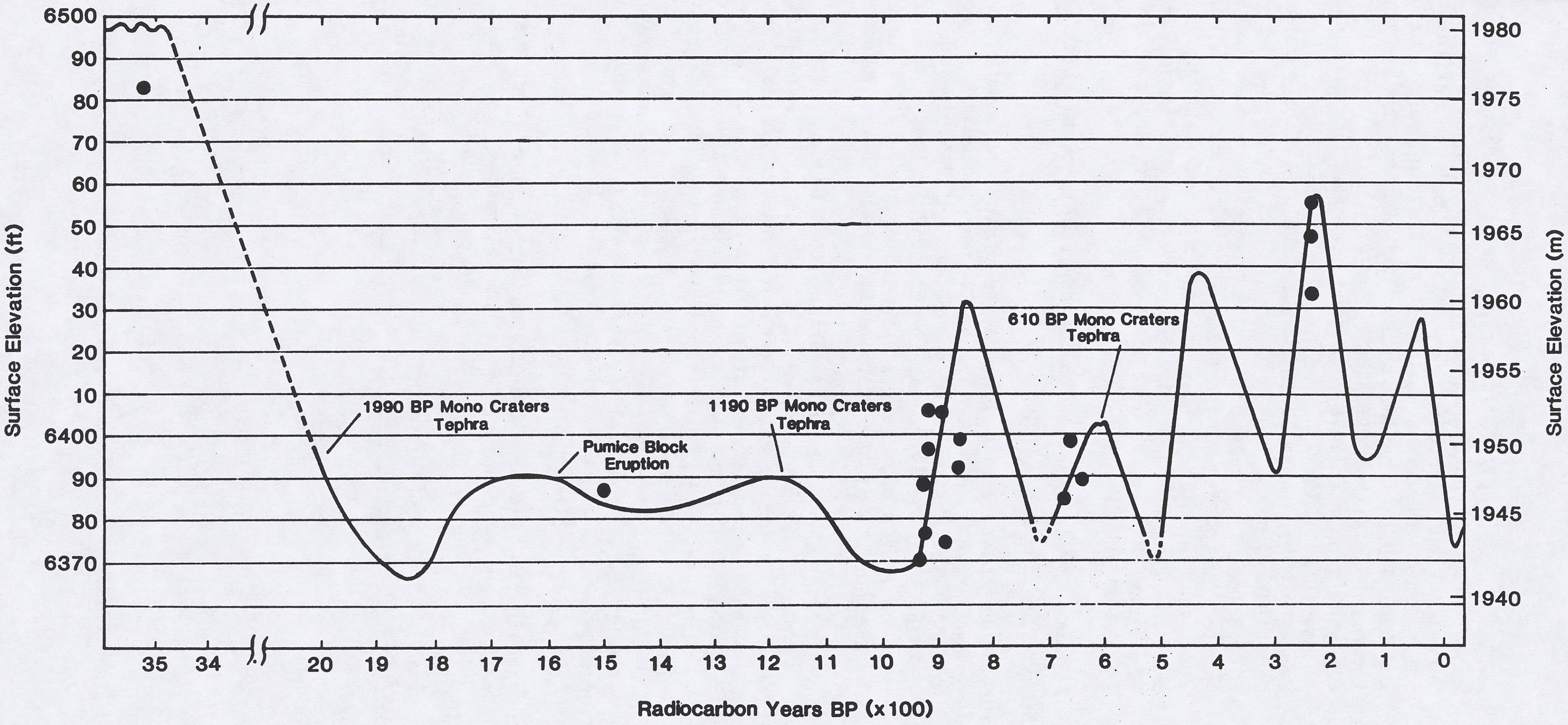

2.05 WATCH OUT! BAD TURN! Turn right off Hwy 395 onto the county road.

2.25 Road forks; bear right.

3.51 Turn left (but before you do, notice the large Jeffrey Pine tree on your right. It was established in 1884--the year after Israel Russell and W.D. Johnson completed field work for their classic monograph on the Mono Basin (Russell, 1889).

~3.80 Crossing a berm at 6428 feet--the elevation of the historical highstand of Mono Lake.

~3.85 Crossing a berm at 6417 feet--the lake elevation during the period 1938-1946.

4.0 STOP 1 (Locality 1, Map 1). Los Angeles Department of Water and Power brineshrimp ponds. These ponds were built by DWP to conduct experiments on the salinity tolerance of the Mono Lake brineshrimp, *Artemia monica*. Park here. Walk southeast along the shoreline, crossing Lee Vining Creek near its mouth; climb onto the delta plain just southeast of the creek.

Walkstop 1a. (Locality 1a, Map 1) Rooted stumps associated with the lowstands of ~1000 BP and ~700 BP.

A quick reconnaisance of the lower delta plain immediately south of the mouth of Lee Vining Creek reveals a dozen or more large, rooted stumps protruding from the ground surface. These stumps are the remains of Jeffrey Pine trees that grew during past lowstands of the lake. At the base of several of the stumps the outward flaring of the root system is evident. Clearly, very little sediment has accumulated on the surface of the delta plain since the time the trees grew.

Note the thick (up to 8 cm) rind of tufa that has accumulated on the outside of many of the stumps. (Note too the "cast" of the wood grain visible on the inner surface of some of the broken pieces of tufa.) This calcium carbonate precipitate forms when calcium-bearing fresh water mingles with the saline water of the lake (Dunn, 1953; Scholl and Taft, 1964; Cloud and Lajoie, 1980). Mixing commonly occurs at the orifice of a sublacustrine spring; in these cases the product is a "tufa tower", many of which can be seen in the "tufa grove" to the east. In the case of these stump rinds, however, the mingling mechanism may involve "wicking" of ground water by the stumps into the lake water. That some of the stumps are still acting as wicks is suggested by the relatively dense stands of rush (*Scirpus* sp.) growing at their bases.

Radiocarbon dates have been calculated for eight of the tree and shrub stumps rooted here and at other sites on the Lee Vining Creek delta. These dates are listed below.

Stump elevation at rooted base	Radiocarbon date	no. of growth rings	Radiocarbon Lab No.
6395'	910±60	~50	USGS 1275
~6402'	950±50	~50	USGS 1487
6397.21'	860±60	~50	USGS 1276
6371'	940±60	12	USGS 1319
6392.07'	850±50	~50	USGS 1274
~6400'	920±90	~50	UCLA 118*
6402.23	700±60	~30	USGS 1277
6388'	640±60	~20	USGS 1167

*Reported in *Radiocarbon*, 1962, V. 4, p. 112.

Map 1

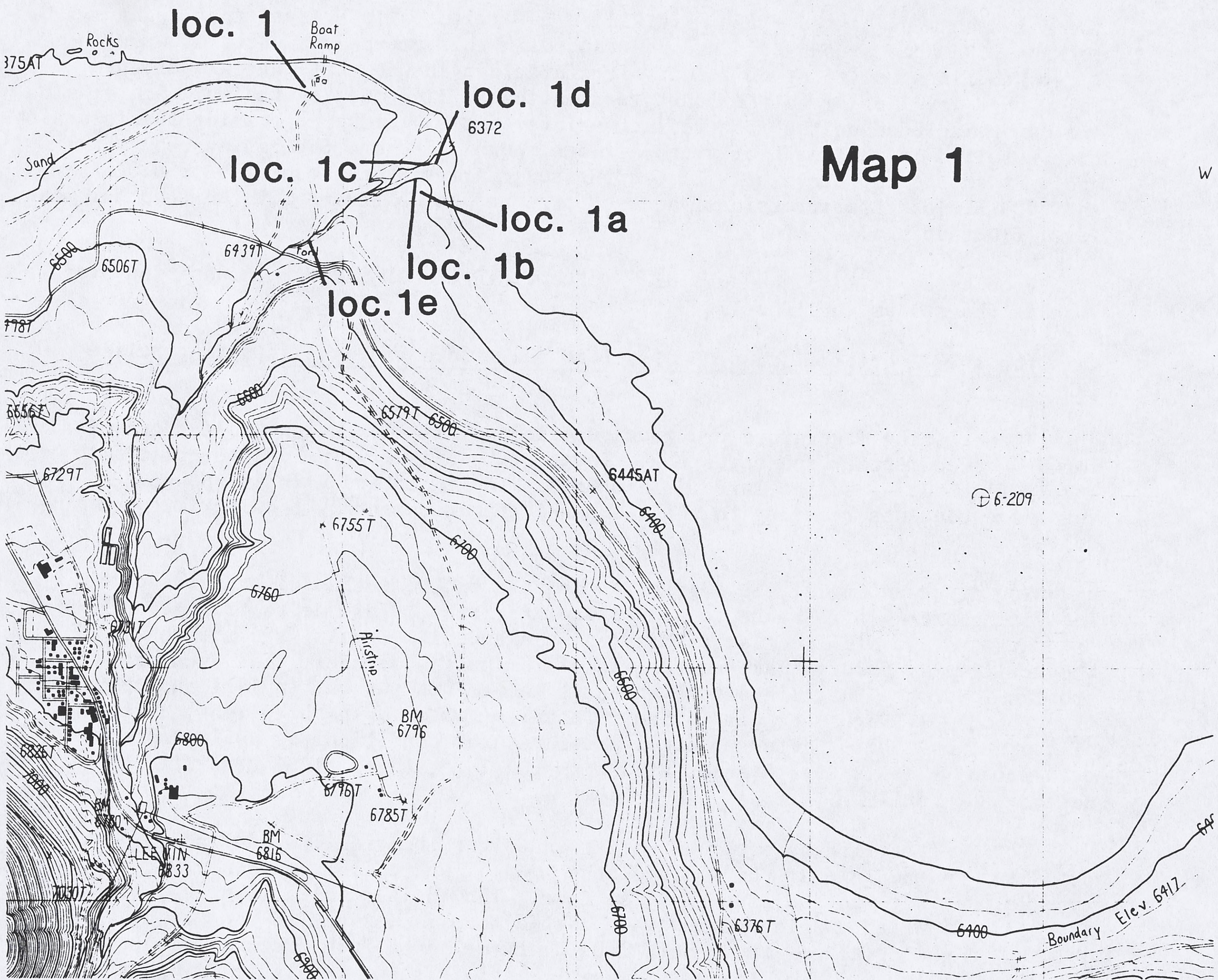
loc. 1
Boat Ramp
Rocks
375AT
loc. 1d
6372
loc. 1c
Sand
loc. 1a
loc. 1b
loc.1e
6500
6506T
6439T
Ford
6656T
6729T
6579T
6500
6600
6445AT
6400
6755T
6700
6760
Airstrip
BM 6796
6800
6796T
6785T
6826T
BM 6780T
LEE VIN
6833
BM 6816
7030T
6600
6700
6376T
6-209
6400
Boundary Elev. 6417
W

Map 2

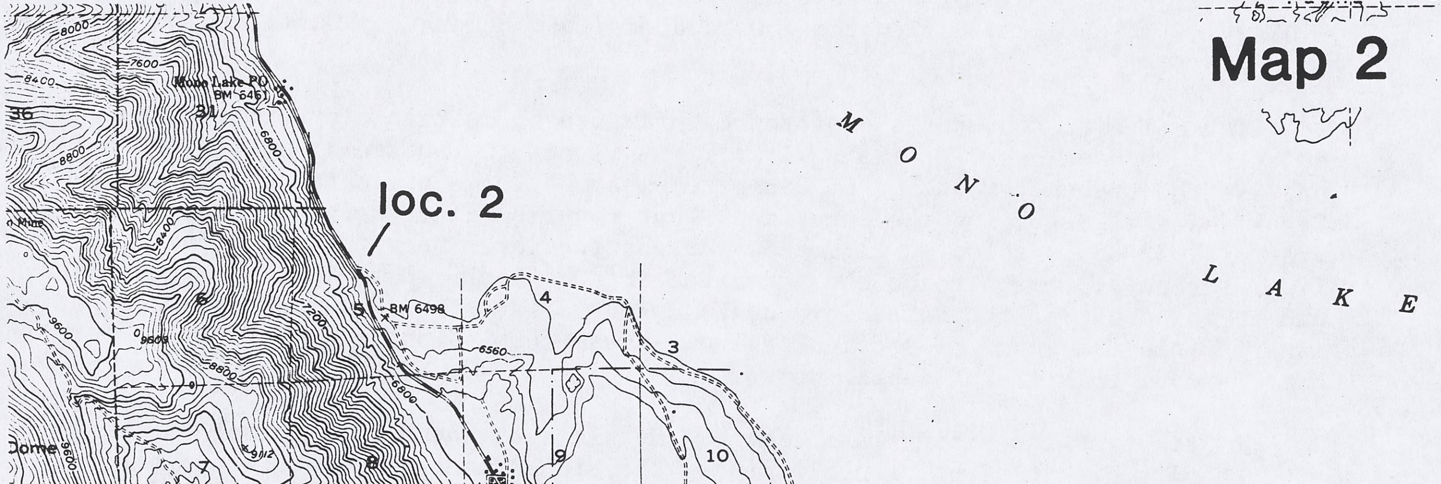
loc. 2
Mono Lake PO
BM 6461
36
31
MONO LAKE
6
5
BM 6498
4
3
6560
Dome
7
8
9
10
Lee Vining
BM 6781
Gravel Pit
13
16
17
16
15
14
State Fish Hatchery
BM
6447
13
18
6560
6800
6788

The six specimens listed first were killed by a rise in lake level that began perhaps 950 radiocarbon years ago. Included in this group is a shrub stump with 12 growth rings rooted at 6372 feet--irrefutable evidence that the lake dropped below that level prior to the transgression that killed the vegetation. The final two dates included on the list reflect a later cycle of lake regression/transgression that resulted in the death of trees between roughly 700 and 640 radiocarbon years ago. At subsequent stops we will examine sedimentary evidence of the ~950 BP and ~700 BP lake transgressions, and see tree and shrub stumps related to other lake level fluctuations.

From here, walk to the edge of Lee Vining Creek and take a position overlooking the stream cut (Locality 1b, Map 1).

Walkstop 1b. A brief discussion of deltas built into widely fluctuating saline lakes.

The existing literature provides surprisingly little insight to the geomorphic forms and sedimentary sequences that characterize Gilbert-type deltas built into widely fluctuating saline lakes. This brief stop is intended to introduce some terms and concepts relating to the geomorphic and sedimentary peculiarities of such deltas.

You are standing at the edge of a "delta trench", a channel that was cut by Lee Vining Creek in response to a drop in lake level. This delta trench, and the trenches that we will see later today on Rush and Mill Creeks, are the result of the artifically induced lake regression of the past 4 decades. The prominant erosional terrace that lines both sides of the trench was cut in 1967 and 1969, when abnormally high snowmelt forced releases of water down the stream. Trenches, of course, must be expected to occur under natural conditions as well; indeed, evidence of a delta trench associated with the lowstand of ~1000 BP will be presented momentarily.

Sediment carried by a stream during and after incision of a delta is deposited in the lake at the mouth of the trench, where it forms a new Gilbert-type delta graded to the lower lake surface. The incised delta is here called the "parent delta", while the newly-deposited form is designated the "subsidiary delta". A photograph of the modern subsidiary delta on Rush Creek as it appeared prior to the lake rise of the past several years is shown on Figure 2. A subsidiary delta produced during the lowstand of ~1000 BP can be identified on that same photo.

The delta trench exerts a profound influence on deltaic sedimentation during a lake transgression. The rising lake first floods the subsidiary delta, then engulfs the trench, producing an elongate embayment. (A photograph of the Rush Creek delta illustrating the engulfment that resulted from the eight-foot lake rise of 1982-83 is shown on Figure 3.) Deepening water permits only progressively finer stream debris to reach the inundated trench floor. Both in the delta trench, and on the plain of the subsidiary delta, then, a lake transgression produces an upward fining sequence of sediments--from stream cobbles and gravels, to shallow water sands, to silts of deeper water.

By the time the rising lake reaches the plain of the parent delta, or the surface of a highstanding trench terrace, the stream mouth--and, correspondingly, the point at which the stream dumps all but the finest fraction of its load--has migrated far uptrench. Coarse stream debris is thus prevented from reaching these elevated surfaces. Very fine stream sediment, however, can be transported to these

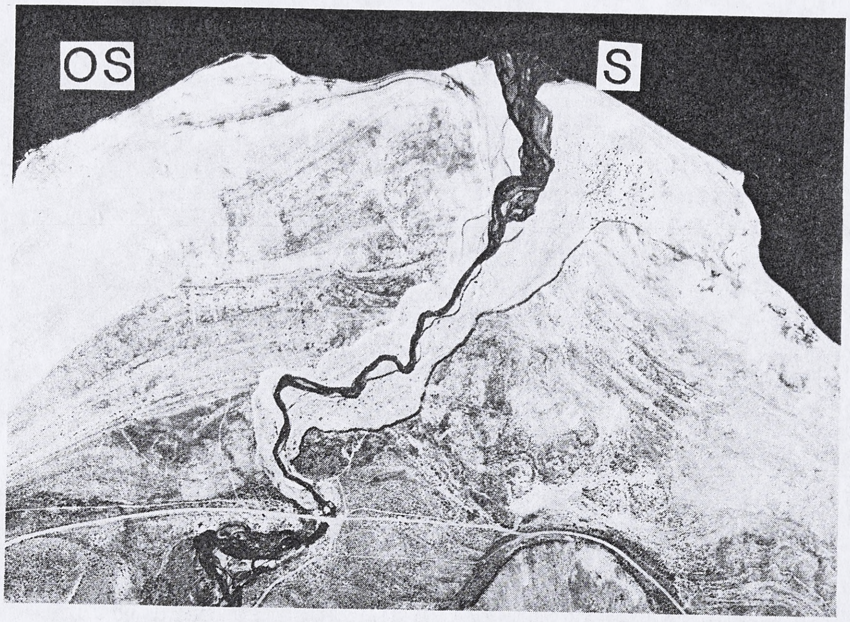

Figure 2a. Rush Creek delta ca. Oct. 1982. The Modern subsidiary delta is labeled "S". Note that it is composed of two identifiable stages--the broad feature associated with the period of high streamflow in 1967/69, and the smaller, arcuate form deposited during the past 4 years. An older subsidiary delta, presumably dating from the lowstand of about 950 yrs. BP, is identified at "OS".

Figure 2b. Detail of the 1980-83 portion of the subsidiary delta on Rush Creek.

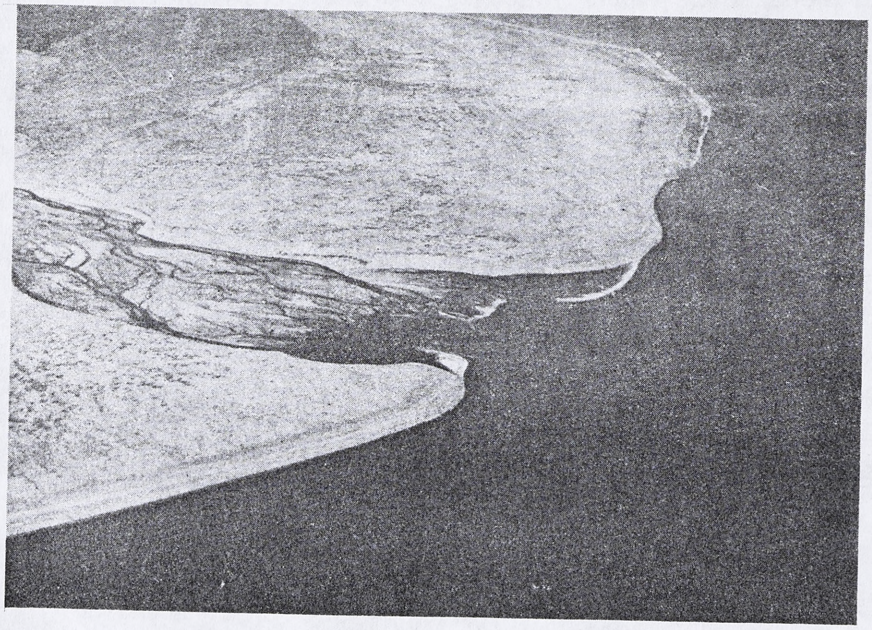

Figure 3. Rush Creek delta ca. May, 1984. The 7½ foot rise in lake level that occurred between the times when Figures 2 and 3 were photographed has resulted in the inundation of the 1980-83 portion of the subsidiary delta and the engulfment of the lower reaches of the delta trench.

surfaces by the hypopycnal stratum of stream water that flows lakeward over the heavy, saline water of the embayment. On the plain of the parent delta, and on the surfaces of trench terraces, then, the lake transgression does not produce a gradual upward-fining sequence of sediments, but rather an abrupt change--from fluvial cobbles and gravels to fine detritus transported by the hypopycnal stratum of stream water. At later stops we will examine lake transgressive deposits of the delta trench, delta plain, and trench terraces.

From here walk down into the delta trench, taking a position facing the right (south) trench wall near the upstream portion of the lakeward-most remnant of the 1967/69 stream terrace (Locality 1c, Map 1).

Walkstop 1c. Stratigraphy exposed in walls of the delta trench along lower Lee Vining Creek.

A generalized cross section of this exposure is shown on Figure 4 below. The section includes a basal unit of coarse beach sand that sandwiches the 1190±80 year-old Mono Craters ash of Spence Wood (1977). This coarse sand grades upward into a fluvial cobble gravel that is oxidized near its surface. Unconformably overlying the cobble unit are lake silts locally rich in pine cones and other plant detritus. The silts coarsen upward into a lake regressive sequence of coarse sand, gravel, and pebbles. This section was truncated by Lee Vining Creek during the high flows of 1967/69.

The abrupt transition from cobble gravel to lacustrine silts at this site is typical of many of the lake transgressive sedimentary sequences that we will see today. I elicit the combination of hypopycnal inflow and a terrace-lined delta trench to explain this relationship, though silts might also be expected to accumulate on a bed of coarse fluvial debris in an abandoned stream channel during a lake transgression.

Pinecones from the base of the silt deposit yielded a radiocarbon date of 890±50 years (USGS 1309); clearly, these silts were deposited during the lake transgression that killed the ~900 year old stumps discussed at walkstop 1a. The twelve-foot vertical difference between the surface on which the stumps are rooted and the terrace gravels on which the silts were deposited necessitates the existence of a delta trench ~900 years ago.

The 1190 year-old tephra exposed in this cut and at other sites along lower Lee Vining Creek is of interest because it can be used with some precision to determine the elevation of the lake surface at the time of the eruption. While the ash lies within coarse beach sands at the base of this cut (elev. = 6387.9 feet), it composes foreset beds at a slightly lower elevation (6387.2 feet). The lake surface thus stood very close to 6388 feet at the time of the eruption 1190±80 years BP.

From here, trace the contact between the oxidized cobble gravel and the overlying silt downstream about 30 M to the extensive exposure near the stream mouth (Locality 1d, Map 1). While much of this rather complicated section is covered by talus, it is still possible to see sedimentary evidence of the lake transgressions of ~950 BP, ~700 BP, and ~500 BP; soils and stumps associated with the lake regressions of ~1000 BP, ~800 BP, and ~550 BP; and the Mono Craters ashes of ~610 BP and 1190 BP.

This exposure has been generalized on Figure 5. Note that the silts of ~900 BP pinch out abruptly in mid-section. This is not only an erosional phenomenon related to truncation by the overlying sand and gravel, but a depositional one as

Figure 4. Stratigraphy exposed in the Lee Vining Creek cut, Locality 1c, Map 1.

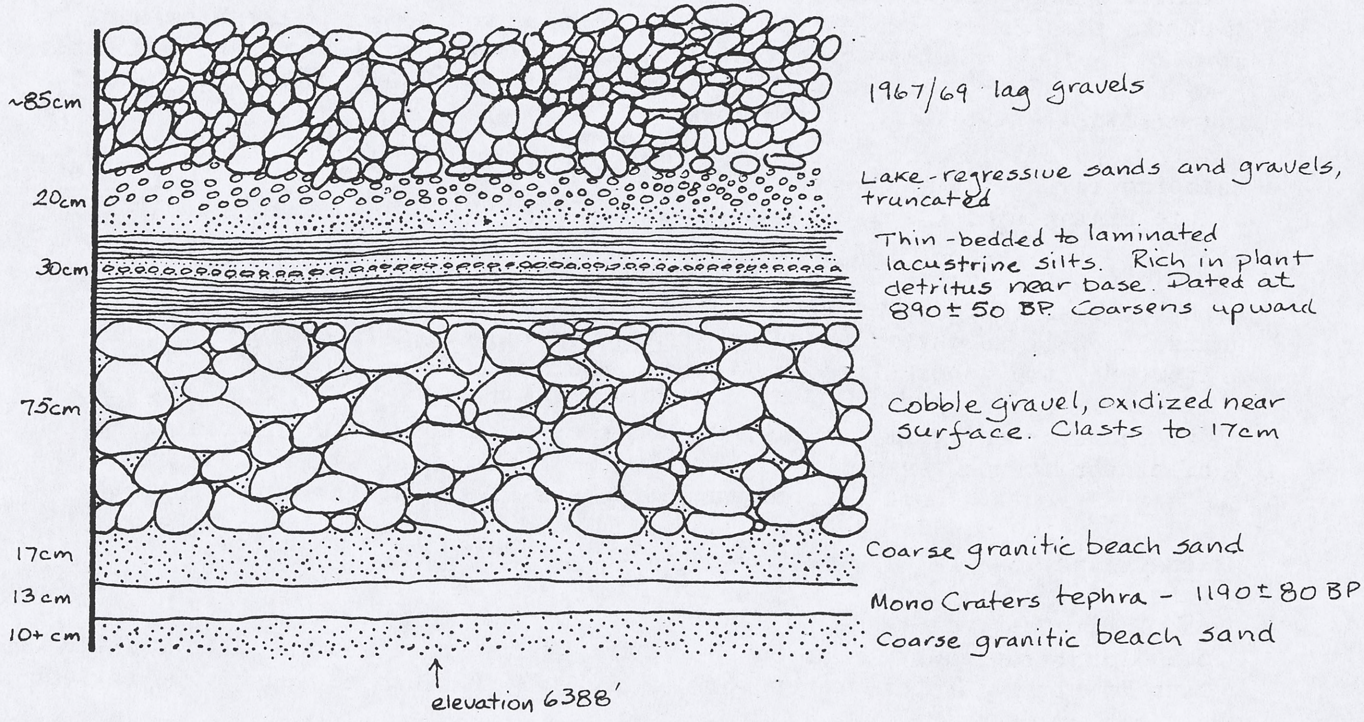

well, in that the silts were deposited behind (upslope of) a berm; lakeward of the berm no silts associated with the lake rise of ~900 BP can be found.

Several horizons that lie above the ~600 year-old Mono Craters ash in this section are composed of a very light brown to white, medium sand that crumbles easily to fine sand and silt when pinched between the fingers. Here and at other exposures around the lake this friable sediment is found in association with littoral sands. On several occasions during the past summer the writer observed extensive concentrations of dead brineshrimp that had blown to shore and become covered with a thin, discontinuous coat of tufa. It may well be that the light brown to white layers that overlie the 600 year-old tephra at this site are composed of partially calcified brineshrimp tests.

The upper ~1 M of sediment exposed here is too thoroughly bioturbated to permit easy interpretation. We will see a relatively undisturbed section of sediments at an analagous stratigraphic and elevational position at Stop 4b.

From here, regain the delta plain east of the channel, and walk upstream toward walkstop 1e (Locality 1e, Map 1). The vegetation on this lower part of the delta plain is dominated by rabbitbrush (Chrysothamnus nauseosus), sagebrush (Artemesia tridentata) and willow (Salix sp.) with an understory of rush (Scirpus sp.) and cheatgrass (Bromus tectorum). Note as you approach the prominent berm at 6428 feet near walkstop 1e that wild rose (Rosa woodsii) suddenly appears; wild rose is one of several plants that seldom grows below 6428 feet, the elevation of the historical highstand of the lake.

Walkstop 1e. Stratigraphy exposed in the walls of the delta trench, middle reaches of Lee Vining Creek.

This cut is notable for the five "A" horizons that overlie deposits associated with the lake regressions of ~2000 BP, ~800 BP, ~400 BP, ~200 BP, and 1919 AD. These units, as well as intervening lake-transgression deposits and the Mono Craters ash of ~600 BP, are generalized on Figure 6, below.

Return to the cars by walking down the delta trench to the shoreline. Before leaving the trench, note the curious pumice blocks that lie in mid-channel near the stream mouth. More will be said of these blocks at the next stop.

Mileage (cont.)

	Retrace your route to Hwy 395.
5.9	Junction county road and Hwy 395. In the roadcut immediately ahead of you two Mono Craters ashes (610 BP and 1190 BP) can be seen lying between mudflow deposits.
	TURN RIGHT onto Hwy 395.
6.15	TURN RIGHT into the old Mono County Marina. Park in the paved parking lot. Walk northeast along the small dirt path to the lake margin, Locality 2, Map 2.

STOP 2. Shoreline stratigraphy and pumice blocks at the Mono County Marina

In August of 1984, 10 M of core was extracted from this site (elevation 6381 feet) on the shore of Mono Lake. A preliminary log of the section is shown on figure 7a-b; note that the upper 900 mm of the log was drawn from a pit adjacent to the core site.

Figure 5. Stratigraphy exposed in the Lee Vining Creek cut, Locality 1d, Map 1.

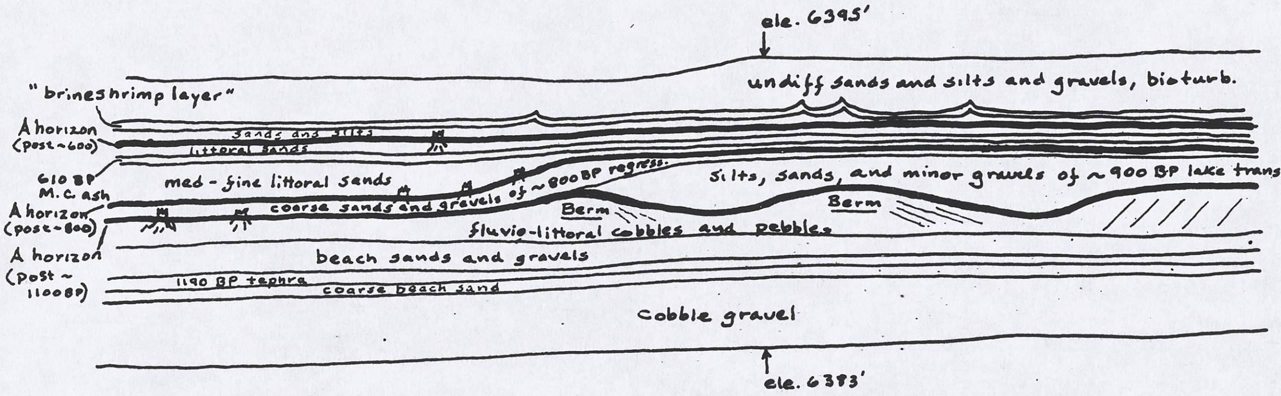

Figure 6. Stratigraphy exposed in the Lee Vining Creek cut, Locality 1e, Map 1.

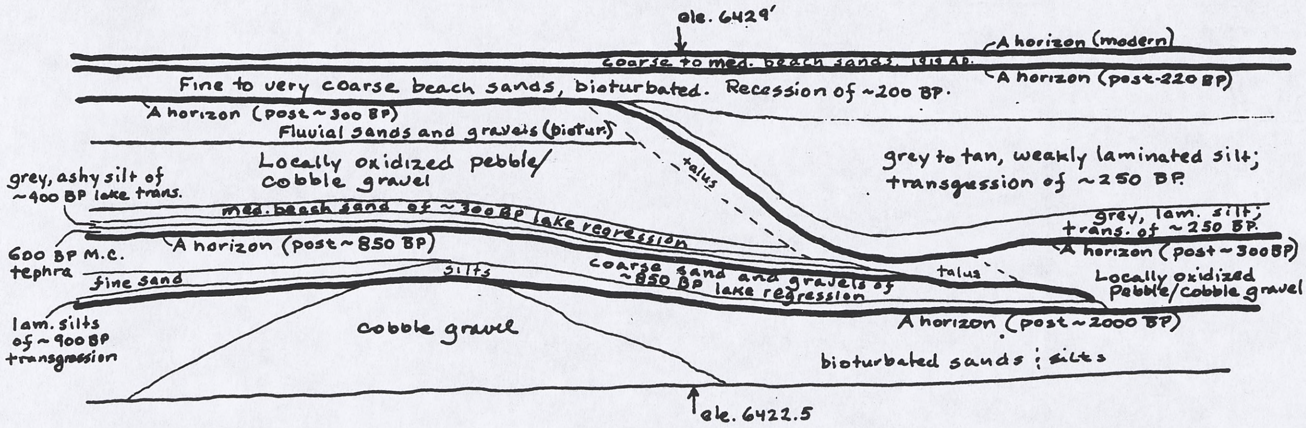

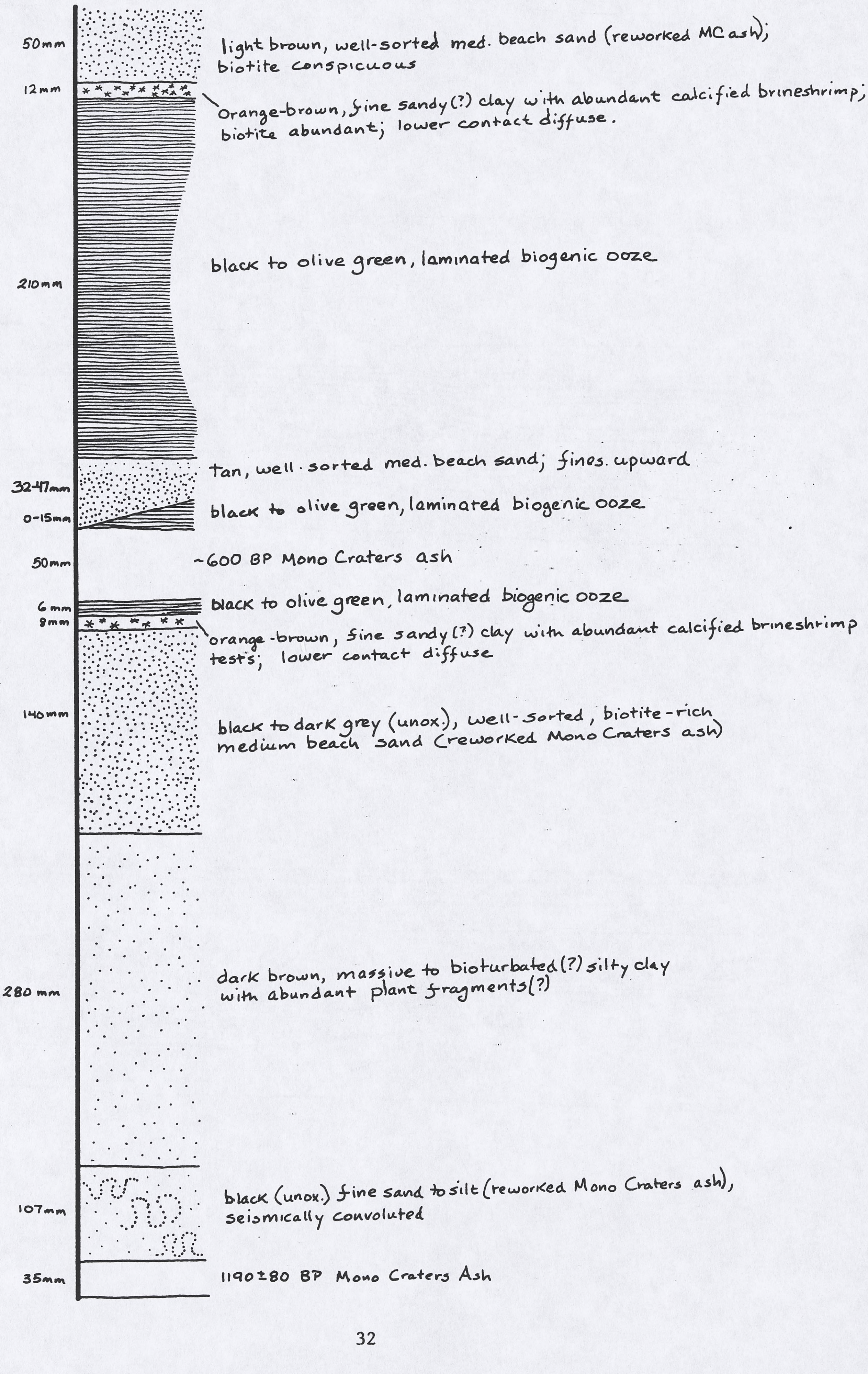

Figure 7. Preliminary log of a core extracted from Mono County Marina in August, 1984 (log continued on following page).

Figure 7b.

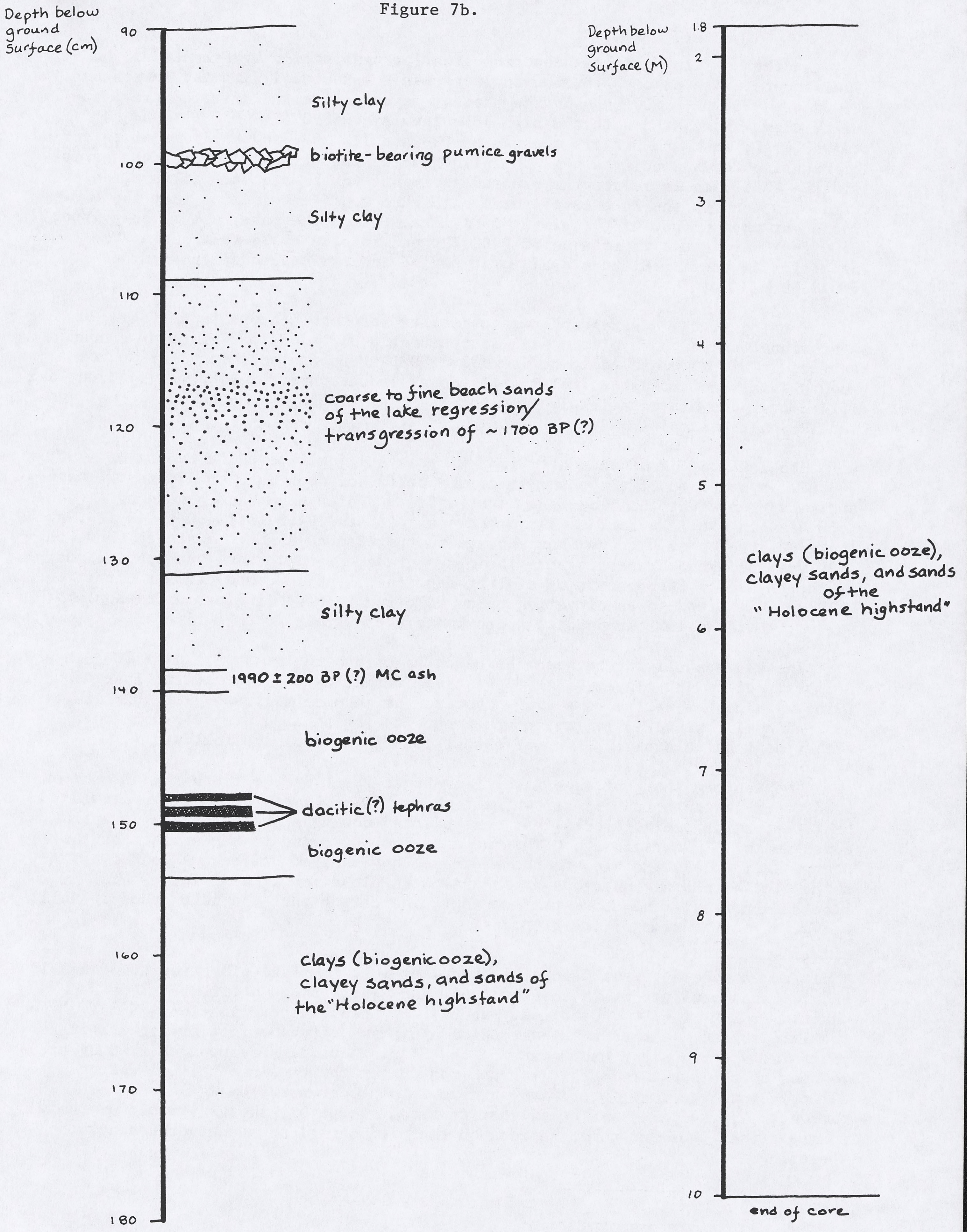

Depth below ground surface (cm)
90
100
110
120
130
140
150
160
170
180
Silty clay
biotite-bearing pumice gravels
Silty clay
coarse to fine beach sands of the lake regression/ transgression of ~1700 BP (?)
silty clay
1990 ± 200 BP (?) MC ash
biogenic ooze
dacitic (?) tephras
biogenic ooze
clays (biogenic ooze), clayey sands, and sands of the "Holocene highstand"
Depth below ground surface (M)
1.8
2
3
4
5
6
7
8
9
10
clays (biogenic ooze), clayey sands, and sands of the "Holocene highstand"
end of core

Another shallow pit has been excavated for examination by Friends of the Pleistocene. The exposed section includes sands associated with the lowstands of ~1000 BP, ~700 BP, ~500 BP, and the present day; massive to laminated clays and silty clays associated with the high lake levels of ~850 BP, ~600 BP, and ~400 BP to ~1970 AD; the Mono Craters tephras of 610 and 1190 BP; and horizons of calcified brineshrimp tests deposited near shoreline during lake transgressions and regressions. Take time to relate the exposed sediments to the sequence illustrated on Figure 7a, and to the lake level curve on Figure 1. (Keep in mind that the elevation at the surface of the pit is 6381 feet. Since the lake fell to only about 6390 feet during the regression of ~300 BP, and to only ~6395 feet during the recession of the immediate pre-historic period, no expression of those drops is found here.)

Turning to the stratigraphic record below the Mono Craters tephra of 1190 BP: A prominant aphyric, rhyolitic ash is found at a depth of 1380 mm below ground surface. This is presumed to be the 1990±200 BP Mono Craters tephra of Spence Wood. Thin, dacitic ashes lie slightly lower in the core, at 1480 mm, 1490 mm, and 1514 mm. These are most likely from the Negit archipelago, though I have not yet run XRF on the samples.

The lower 8.6 M of the core, from the base to just above the tephra of 1990± 200 BP, is composed of clays and sands indicative of deep lake conditions. These sediments represent the "Holocene highstand", a prolonged period beginning around 3600 BP when the lake surface stood between ~6485 and 6499 feet--30 to 45 feet above the flat stretch of highway that you see to the west.* A short distance above the 1990 year-old Mono Craters tephra the clays grade upward into coarse beach sands. By shortly after the deposition of that ash, then, the lake had declined from the Holocene highstand to an elevation below 6376 feet. Several lines of reasoning suggest that the lake dropped to approximately 6369 feet at this time.

The sediments lying between the beach sands and the MC tephra of 1190 BP are primarily silts and clayey silts suggestive of shallow to intermediate lake depths. Lying within these silts is a single horizon of angular to subangular, biotite-bearing pumice gravels similar in appearance to the shoaled pumice blocks that are evident at this site. A brief discussion of those blocks follows:

The western shore of Mano Lake, from Horse Creek in the south to near Cottonwood Creek in the north, is strewn with thousands of large (up to 2 M), angular, biotite-bearing pumice blocks that were ejected during a sublacustrine eruption approximately 1600 years ago. The buoyant blocks floated to the surface of the heavy, saline lake and blew to shore, where they shoaled and became coated with tufa. The blocks are numerous at and below an elevation of 6390 feet; the blocks are non-existant above that contour, indicating that the lake stood at this elevation at the time of the eruption.

---

*That clays here attributed to a highstanding lake (surface elevation ~6460-6499) should occasionally contain thin beds of sand, while those attributed to a somewhat lower lake (~6390- ~6460 feet) should not, requires explanation. Simply, when the lake surface reaches an elevation of approximately 6460 feet or higher, it abuts the steep eastern escarpment of the Sierra Nevada. Sediment carried by steep reaches of the small tributary streams that drain the escarpment is discharged directly into the lake, where it can move into deeper water by way of bottom currents. If the lake lies below that critical elevation, the great bulk of the coarse stream sediment comes to rest on the piedmont slope and never reaches the shoreline.

Color of the pumice ranges from very light grey to dark grey, with some of the clasts exhibiting alternating light and dark flow banding. Shape of the vesicles is variable, ranging from spherical to highly elongate. Large vesicles commonly contain delicate fibers of glass arranged in a complex web-like pattern.

The pumice blocks are most abundant along the lakeshore to the northwest of Negit Island, where they number in the hundreds per acre. Two of the islets northwest of Negit--Twain and Java (Figure 8)--are composed in part of large extruded masses of pumice similar in appearance and chemical composition to the shoaled blocks. (Results of XRF analyses on these and other samples of island volcanics are shown on Figures 8 and 9.) These islets, then, and perhaps other vents that are still submerged, are considered the likely sources of the pumice blocks.

In the lower reaches of the Lee Vining Creek cut that we visited earlier today the pumice blocks are overlain by a riverine cobble gravel. Sandwiched between this fluvial debris and one of the blocks was a deposit of pinecones that yielded a radiocarbon date of 1495±45 BP (USGS 1314). This provides a minimum date on the block eruption. The horizon of pumice gravels found here at the County Marina lies well above the Mono Craters ash of 1990 BP, and in fact above the beach sands that overlay that ash. For now, then, timing of the eruption that produced the pumice blocks is tentatively put at between 1495 BP and ~1700 BP.

Return to Hwy 395.

<u>Mileage</u> (cont.)

6.35	Junction Hwy 395 and entrance to Mono County Marina. Turn right on Hwy 395. For the next couple miles the highway hews closely to an elevation of 6456 feet--the surface elevation of the lake during the highstand of 220 BP.
9.25	TURN RIGHT off Hwy 395 onto Cemetery Road.
9.65	<u>STOP 3.</u> <u>Mono County Park</u>. Leave cars in the parking lot. Hike lakeward down the boardwalk to near the mouth of Dechambeau Creek, locality 3, on map 3.

<u>The role of hypopycnal inflow in the formation of tufa</u>.

Like other streams tributary to Mono Lake, Dechambeau Creek deepened its channel in response to the recent drop in base level, exposing sequences of sediments associated with lake fluctuations and Mono Craters eruptions. The rise in lake level that began in 1982 flooded the lower reaches of the channel, rendering many good exposures inaccessible, but creating an environment in which hypopycnal inflow and tufa precipitation are readily observed.

Note the concentrations of brineshrimp that occupy the quiet stratum of lake water near the channel bottom. Compare their movement to that of detritus entrained in the overriding layer of fresh water. The mixing of stream and lake water in zones of turbulence within the channel results in precipitation of tufa on channel walls and streamside vegetation. Notice the accumulation of newly-deposited tufa in the channel at this site.

The hypopycnal stratum of stream water from this and other tributaries persists beyond the mouths of the streams, diffusing outward over the open water of the lake. The two fluids mix in zones of wave agitation around the lake and island margins; this mixing, coupled with a loss of CO_2 during wave crash, instigates tufa precipitation. The horizontal "flanges" that protrude from tufa towers at this site, and the ubiquitous tufa rind that covers boulders on both the lakeshore and the islands, probably formed as a result of this mechanism.

Figure 8

Trace element chemistry and tephra stratigraphy of some of the Mono Islands.

(● = pit site)

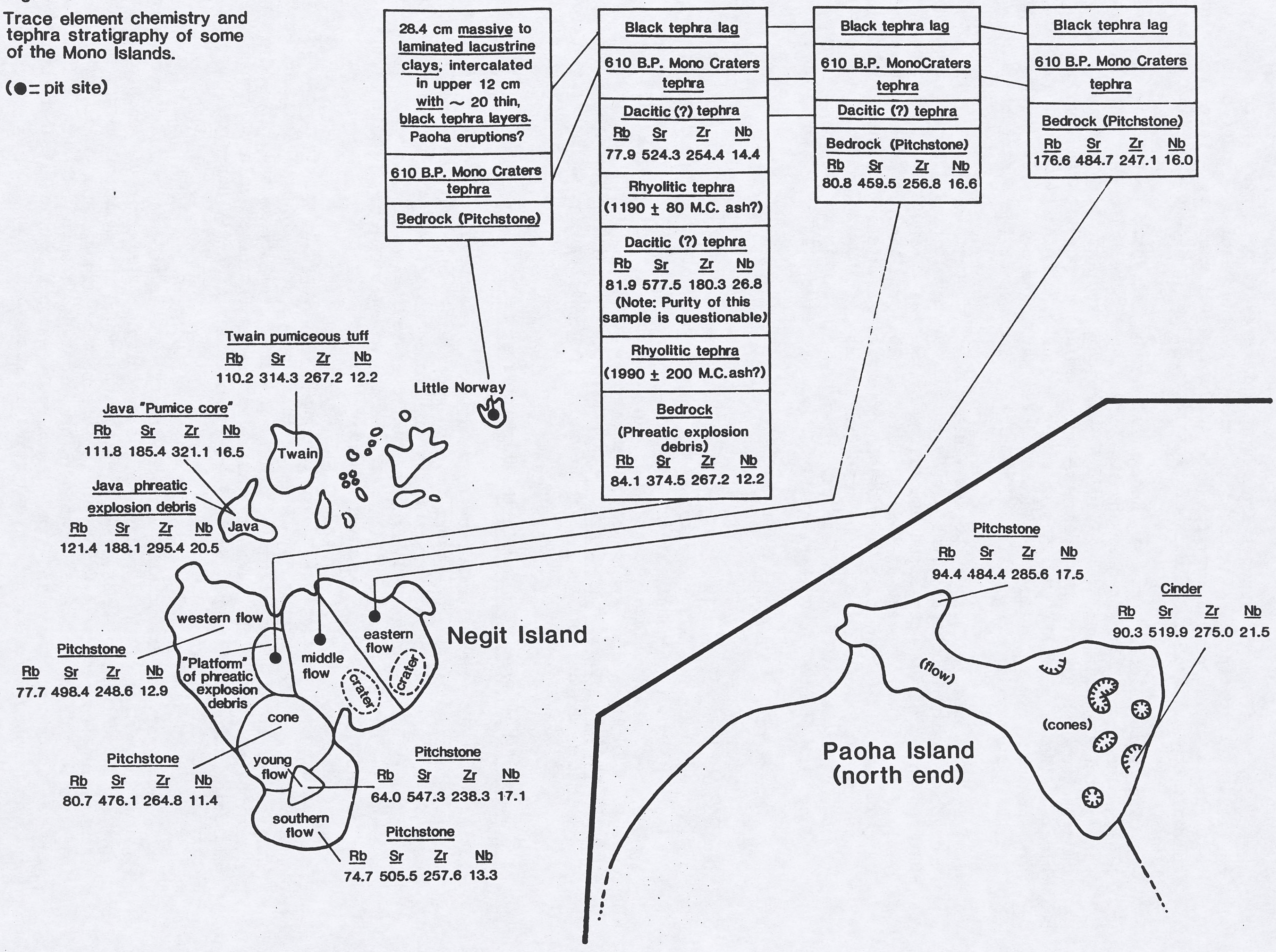

Figure 9

Triangle diagram (Rb - Sr - Zr) showing position of bedrock samples and ashes discussed in this guidebook

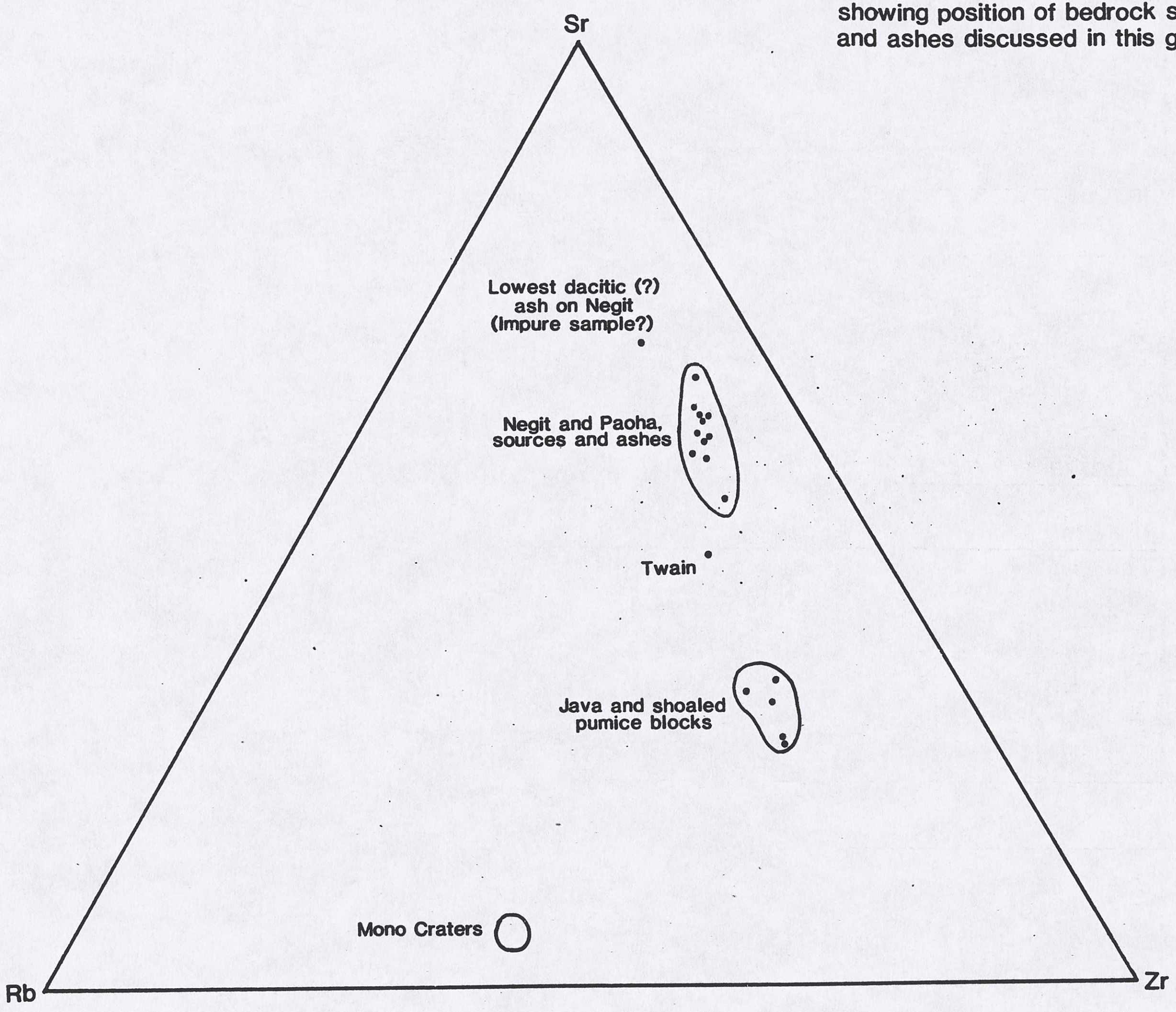

Results of XRF analyses (see also Figure 8):

Biotite - bearing pumice blocks (compare with "Java," Fig. 8)

	Rb	Sr	Zr	Nb
Sample 1	112.5	157.2	327.2	17.3
Sample 2	117.6	158.8	338.3	19.0
Sample 3	108.3	208.7	329.8	12.6
"Navy ash"	98.3	480.4	270.0	18.7

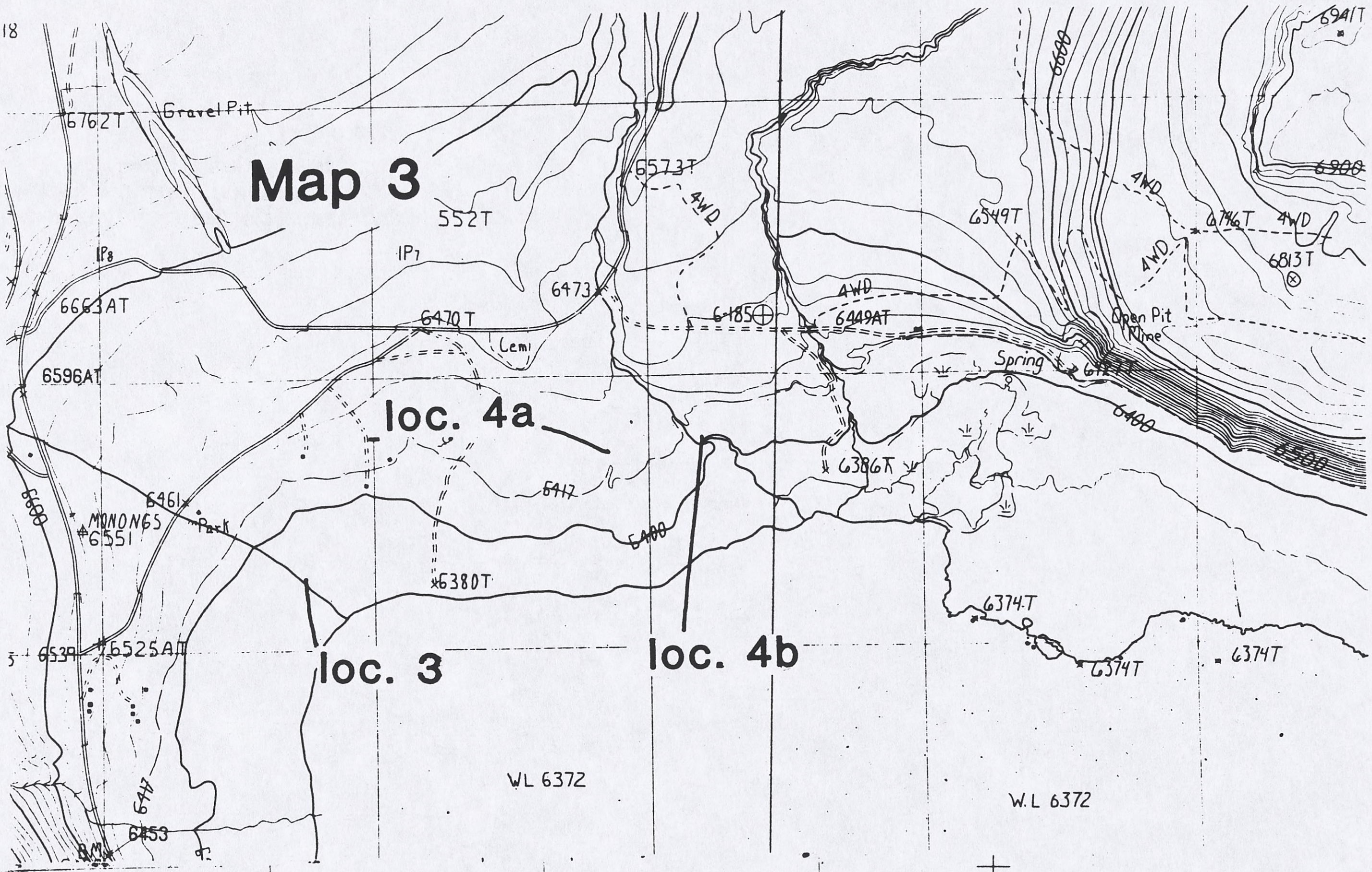

Map 3

6762T
Gravel Pit
552T
IP8
IP7
6663AT
6596AT
6470T
Cem
6473
6573T
4WD
6185
6449AT
6549T
4WD
6746T
6813T
6941T
6900
6600
Open Pit Mine
Spring
6427T
6400
6500
loc. 4a
loc. 4b
loc. 3
6417
6400
6386T
6461
MONONGS
Park
6551
6600
6380T
6374T
6374T
6374T
6537
6525AT
6447
6453
BM
WL 6372
W.L 6372

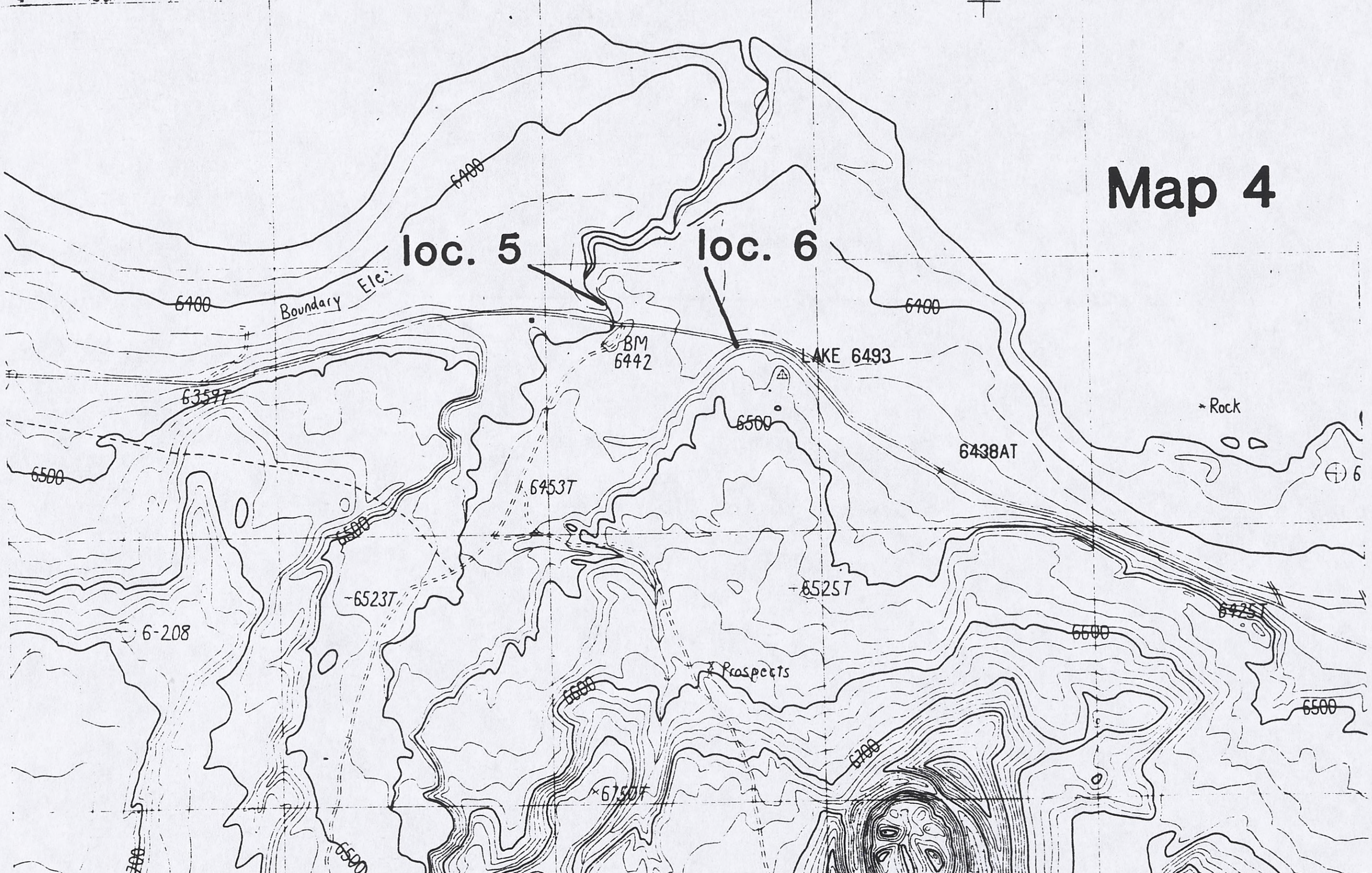

Map 4

6400
loc. 5
loc. 6
6400
Boundary Elec
6400
BM
6442
LAKE 6493
Rock
6359T
6500
6500
6438AT
6453T
6500
6523T
6525T
6425T
6-208
6600
Prospects
6600
6500
6700
6750T
6500
6700
Cem

Return to the cars and proceed east on Cemetery Road.

Mileage (cont.)

10.15	Older tufa (from lake transgression of ~3600 BP?) on right.
10.35	Rising onto the plain of an early stage of the Holocene delta of Mill Creek.
10.78	Crossing the westernmost of 2 Mill Creek channels. This channel was cut in 1967/69 during periods of high stream flow.
10.80	Crossing the eastern channel of Mill Creek.
10.82	STOP 4. Park cars along the roadside; please leave enough room to allow the passage of the large semi-trucks that use this road regularly.

Walk down the western channel of Mill Creek approximately 450 M to Locality 4a on Map 3.

Walkstop 4a. The post-600 BP record of lake fluctuations at ~6425 feet on Mill Creek (see Figure 10).

Just downstream from this exposure, a berm associated with the historical lake highstand of 6428' can be seen protruding from the surface of the delta plain. Stratigraphy exposed in this section, then, was unaffected by the historical lake rise. Just upstream from the exposure, the 600 year-old Mono Craters ash crops out; follow it downstream into the cut.

Between 600 years ago, when this ash was deposited, and the late nineteenth century, when the last major lake transgression began, Mono Lake rose to above the elevation of this exposure two different times. During the first of these transgressions (beginning ~500 years ago) the lake paused for a time at ~6425 feet and deposited the berm illustrated on the cross section. (A prominant berm can be seen in this same stratigraphic and elevational position in the Lee Vining Creek cut.) Lake silts from this and the subsequent transgression (beginning ~300 BP) built up behind the berm, providing a relatively thick and easily decipherable record of lake activity. Note that an "A" horizon overlies each of the two silt units.

From here walk east to Locality 4b on Map 3.

Walkstop 4b. Lake elevation at the time of the Mono Craters eruption ~600 years ago.

Convincing evidence that the lake surface stood at 6406 feet at the time of the Mono Craters eruption ~600 years ago can be seen in this section along the east bank of the eastern channel of Mill Creek. The relationship between the tephra of ~600 BP and adjacent units is illustrated on Figure 11. Below 6406 feet the ash appears as a white, medium sandy to silty laminated unit that is intercalated with laminae of fine, well sorted, light brown to grey sand derived from the Sierra Nevada. The ash overlies a wedge of this same sand that gradually thickens lakeward. The sand wedge, in turn, rests on an "A" horizon developed on a deposit of pebble gravel. Pebbles lying on the surface of this lower unit are coated with a very thin frosting of tufa indicative of a nearshore environment. This sequence can be traced lakeward for ~50 M.

At an elevation of 6406 feet the sand wedge pinches out, leaving the ash in direct contact with the "A" horizon. The pebbles on the surface of the soil upslope of this point are not coated with tufa, and the laminae of arkosic sand within the ash disappear. The ash assumes an appearance suggestive of aeolian reworking and plant turbation.

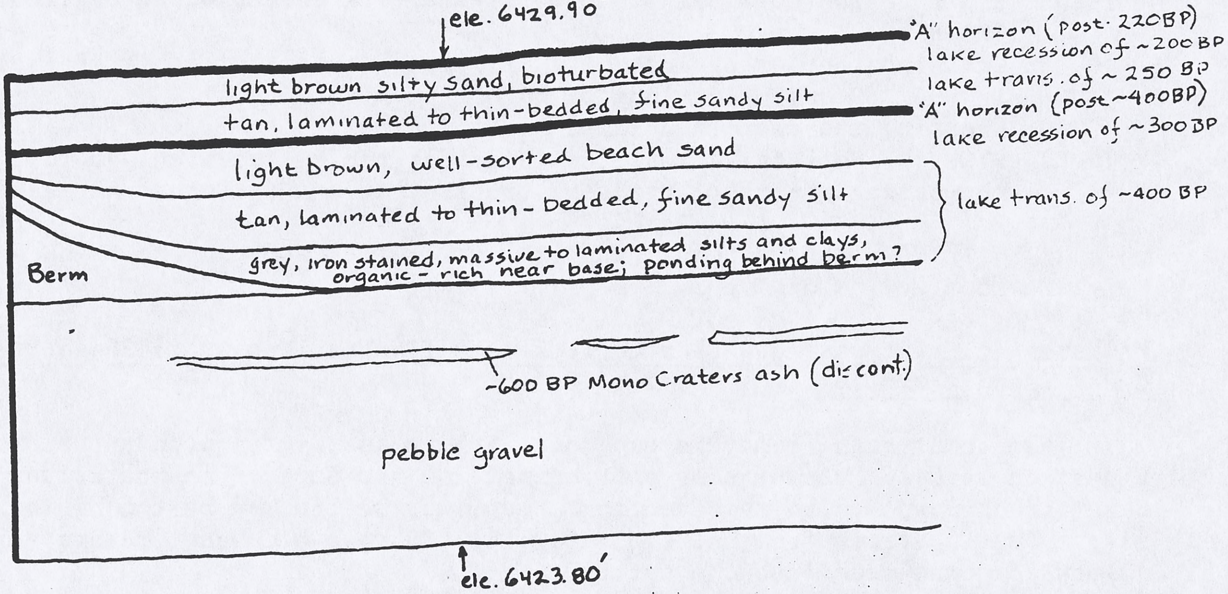

Figure 10. Stratigraphy exposed in the Mill Creek cut, Locality 4a on Map 3.

Figure 11. Stratigraphy exposed in the Mill Creek cut, Locality 4b on Map 3.

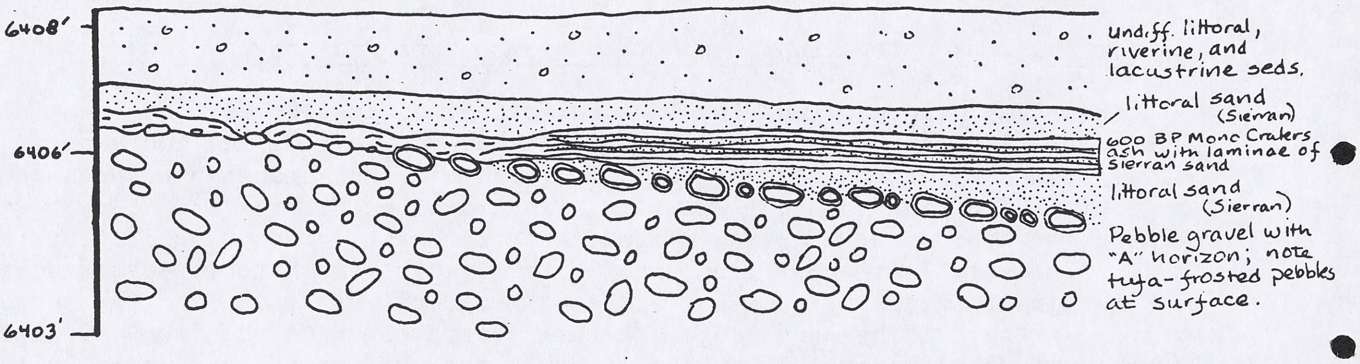

From this evidence it is concluded that above 6406 feet at this site the ash fell onto a vegetated, windblown surface; below that elevation it fell into a littoral environment characterized by the transport of fine sand and the precipitation of tufa. Exposures along Rush and Lee Vining Creeks corroborate a lake surface elevation of 6406 feet at the time of the eruption (see Figure 13).

Hikeback to the cars and return to the junction of Cemetery Road and Hwy 395.

Mileage (cont.)

12.35	Junction Cemetery Road and Hwy 395. TURN LEFT. Retrace route southward through Lee Vining.
18.85	Intersection Hwys 120 and 395. Continue south on Hwy 395.
19.65	TURN LEFT on county road.
20.20	The Holocene delta of Rush Creek, which we will visit momentarily, can be seen dead ahead protruding into Mono Lake.
20.45	Late Pleistocene tufa and Wilson Creek beds of Lajoie (1967) on left.
20.75	Road forks near Donderro Ranch. TURN RIGHT.
21.08	Crossing Horse Creek.
22.50	Crossing Rush Creek, largest of Mono Lake's tributary streams.
22.55	STOP 5. Rush Creek near Clover Ranch. Park cars to the sides of the road. Walk down the left side of the stream about 75 M and take a position facing the right wall of the stream cut, Locality 5, Map 4. A generalized cross section of this exposure is shown on Figure 12.

The chaotic jumble of volcanic debris visible in this stream cut is part of a block avalanche deposit emplaced during the eruption of Panum Crater about 600 years ago. At the time of the eruption the lake surface stood nine feet below the base of this exposure, at an elevation of 6406 feet (Figure 13). Deposition of the block avalanche created an irregular topography into which Rush Creek had to incise. Incision continued during the decades following the eruption, as the lake fell to the lowstand of ~500 years ago. Evidence of this incision is seen here in the form of a stream-cut bench capped with fluvial gravels that lies about ~2 M above the level of present-day Rush Creek.

The fluvial gravels are overlain by lacustrine silts deposited during the lake highstand of about 400 years ago. The subsequent decline in lake level (culminating in the lowstand of about 300 years ago) permitted vegetation to colonize the surface of the silt deposit, leading to the development of the conspicuous "A" horizon that lies about 1½ M below the top of the exposure. Note the remnants of tree stumps rooted in this soil.

By just before 220 years BP the lake again rose to the elevation of this exposure, where it flooded the soil and killed the vegetation. Lacustrine silts collected in the declivity overlying the soil. Since shortly after 220 BP, when the lake fell to below 6436 feet, "A" horizonation has proceeded on the surface of this younger silt unit.

Figure 12. Stratigraphy exposed in the Rush Creek cut, Locality 5 on Map 4.

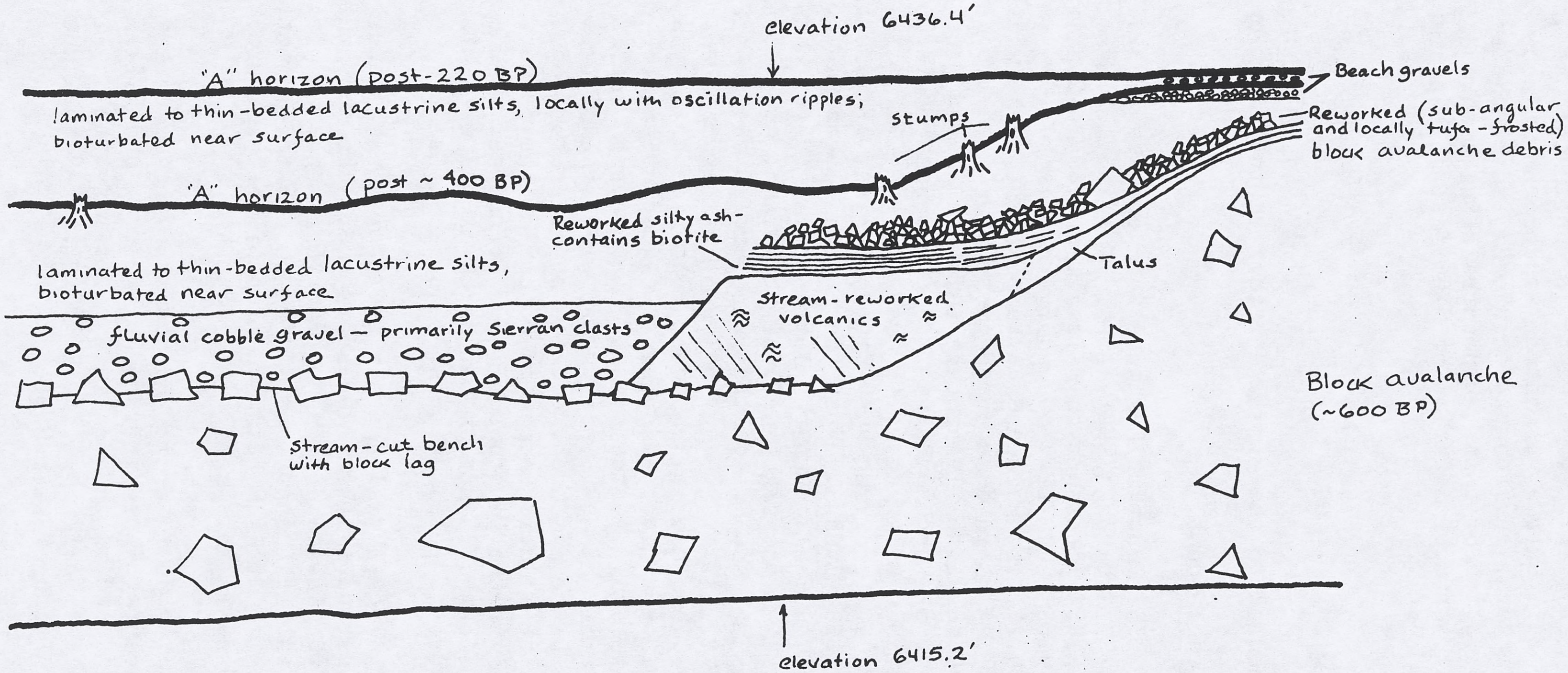

Figure 13. Rush Creek cut, ca. July, 1980. (Height of channel wall ~5 M) This small delta lies at an elevation of 6406 feet. It is composed of stream-laid silty tephra from the ~600 year old eruption, and overlies a surface of Sierran sand of the immediate pre-eruption period. Relationships such as this provide evidence that the lake stood at 6406 feet at the time of the Mono Craters eruption ~600 years ago. (Photo by Ted Oberlander.)

Return to the cars and drive east on the county road for a short distance.

Mileage (cont.)

22.80 STOP 6. Park near the toe of the Panum block avalanche of Spencer Wood (1977), Locality 6 on Map 4.

The lake highstand of 220 BP and its bearing on the ages of the Mono Islands.

Carved into this ~600 year old block avalanche at an elevation of 6456 feet is a prominant wave-cut bench capped by a deposit of beach cobbles and gravels. This feature is apparent both in the field and on aerial photographs (Figure 14). Importantly, no evidence of littoral deposition or erosion exists higher than 6456 feet on this ~600 year old feature. Other lines of evidence, in fact, indicate that this is the highest level to which the lake has risen in over 2000 years.

Radiocarbon dates on the three samples collected from sediments associated with this highstand are listed below:

Sample #	Locality and elevation	Date
USGS 1317	Lake sediments at 6433' on L.V. Creek	220±65 years BP
USGS 1320	Delta foreset beds at 6450.5' on L.V. Creek	220±60 years BP
USGS 1312	Palludal(?) sediments at 6412' on L.V. Creek	220±50 years BP

Note that all three of these samples yielded dates of 220 years BP. Thus, there is not only a high degree of surety in the level to which the lake rose during this transgression, but in the timing of the lake rise as well. This well-dated shoreline at 6456 feet, in combination with tephichronological data, can be used to shed light on the ages of the Mono Islands.

Negit Island is composed of a cinder cone, two shallow craters, at least five blocky lava flows, and a "platform" of older phreatic explosion debris (Figure 8). According to Lajoie (1968) the island is dacitic in composition.

A conspicuous, undeformed, wave-cut notch encircles almost the entire island at 6456 feet--the elevation of the lake highstand of 220 BP. No evidence of wave activity can be found higher on the island. One flow--the stubby feature that emanates from the south side of the cinder cone (designated "young flow" on Figure 8) lacks a shoreline at 6456 feet. The highest evidence of wave erosion on this flow lies twelve feet lower, at an elevation of 6444 feet. Eruption of this flow, then, post-dates--perhaps by only two decades or less--the lake highstand of 220 years BP.

Negit was thoroughly searched for evidence of tephra layers that might further clarify the ages of different parts of the island. 10 pits were excavated at various sites; logs of three of the Negit pits are included on Figure 9. Clearly, neither the "young flow" discussed above nor the large "western flow" are overlain by the ~600 year-old Mono Craters ash. The western flow, then, may well be the second youngest part of the island. The "eastern flow" is mantled by the 600 year-old ash, but not by older tephra units, making it the third youngest feature on Negit. Overlying the "middle flow" is the Mono Craters ash of ~600 BP and a somewhat older dacitic(?) ash. This feature, then, is intermediate in age. The "platform" area near the center of Negit is mantled with the

Figure 14. Panum Crater, Pumice Pit Crater, and the Panum block avalance of Wood (1977) ca. 1930 (lake elevation ~6421 feet). Note the shorelines carved into the block avalance at and below 6456 feet.

~600 and ~1200 year old Mono Craters ashes, two dacitic(?) ashes, and the 1990±200(?) BP ash of Spence Wood. This, then, may well be the oldest part of Negit Island; the complex history of the Negit cone, however, has yet to be deciphered.

The Negit islets. Some eighteen small, rhyodacitic islets (Lajoie, 1968) lie to the north and east of Negit Island. The ages of two of these features--Twain and Java--were discussed at Stop 2. Only one of the other islets--"Little Norway"--is of a configuration that prevents wave erosion of overlying tephra layers during fluctuations in lake level. This islet (Figure 9) is mantled by the 600 year old Mono Craters tephra, as well as by approximately twenty younger dacitic ashes. Little Norway, then, is somewhat older than 600 years. (The significance of the younger ashes will be discussed at Stop 7).

Paoha Island is a block of lake bottom sediments that was uplifted to its present position by the shallow intrusion of magma. Rhyolitic spires protrude through the lake sediments over the northern third of Paoha, while at least 7 dacitic cinder cones and a lava flow compose the island's northeastern corner (Lajoie, 1968).

Huge blocks of sediment have been shed from the flanks of Paoha, creating a chaotic topography along the island's western periphery. Scholl et al. (1967) argue that sliding most likely took place during the upheaval that created the island. Today, portions of the slide debris protrude above the lake surface west of Paoha as small islets.

Many scientists have noted the youthful appearance of Paoha. Scholl and his co-workers, for instance, pointed out the lack of an integrated drainage network on the island surface, while Russell contended that the lava flow on the northeastern corner of the island was the youngest volcanic rock in the Mono Basin. Quantitative assessments, however, have been limited to that of Scholl et al., who believed the island to be post-Altithermal in age, and to that of Lajoie, who considered it to be less than 3000 years old.

Encircling the island between 6372 feet (the elevation of the lake in 1982) and 6428 feet (the elevation of the historical highstand of 1919) is a prominent wave-cut bench. This feature is conspicuous on the resistant volcanic outcrops around the island as well as on the softer lake sediments. No evidence of littoral erosion exists above that level.

The lack of a shoreline at 6456 feet on Paoha provides strong evidence that the island did not exist 220 years BP. Maps of Mono Lake drawn in 1853 leave no doubt that Paoha Island did exist by that time. As a first approximation, then, the island can be said to have emerged sometime between 220 years BP and about 130 years ago.

At this point in the discussion it is advantageous to consider the age of Paoha Island in terms of sidereal years rather than radiocarbon years. Using the curve developed by Stuiver (1982), and relating all dates to the 1950 AD datum, the age of the shoreline at 6456 feet becomes about 1660 AD. To restate our "first approximation", then, the island emerged sometime between 1660 AD and 1853 AD.

This interval can be narrowed considerably by taking several factors into account. First, in 1883, when Israel Russell visited the island, he could find no evidence of a former shoreline above the lake elevation of that day. (This

elevation was later determined to be 6410 feet.) This means that the portion of the wave-cut platform lying between 6410 and 6428 feet on Paoha must have been cut historically, and, most importantly, that the lake has to have dropped from the highstand of 1660 AD to below 6410 feet before the island emerged.

Secondly, it must be assumed that the the displacement of water caused by the emergence of the island forced a rise in lake level. Depending on where the lake stood at the time of island emergence, and on what assumptions are made concerning the configuration of the lake bottom in pre-Paoha time, I derive a displacement equivalent to 4 to 6 feet of lake rise. Taking this displacement factor into consideration, then, it is reasonable to assume that by the time Paoha Island emerged, the lake had dropped from 6456 feet to or below about 6405 feet.

This amount of lake drop does not occur in a short period of time. Even under the strident and persistent climatic conditions of the Dust Bowl Period of 1924-34 (inflow ~70% of long term normal) the lake dropped less than one foot per year on average. Even if it is assumed that the climatic conditions during the decades following 1660 AD were similar to those of 1924-34 it would have required more than a half-century for the lake to drop from 6456 feet to 6405 feet. As a conservative estimate, then, the island emerged sometime between 1720 AD and 1850 AD.

Return to the cars and proceed eastward on the county road.

Mileage (cont.)

25.10 Road forks; turn hard left.
26.20 Road forks; turn right.
26.35 STOP. WARNING: SOFT SAND! Do not proceed beyond this point without 4-wheel drive. Walk lakeward across the band of relatively dense vegetation, then proceed eastward along the exposed lake bed until you reach the old Navy Pier, Locality 7, Map 5.

As you walk toward Stop 7 note the delicate, castellated sand tufa, or "calcite impregnated defluidization structures" (Cloud and Lajoie, 1980) along the exposed lake bed. These are thoroughly modern features, having formed from sand deposited during the lake recession of the past two decades. Proof of this can be seen in the form of cables that underlie the sand tufas. These cables were laid out by the U.S. Navy in the early 1960's.

STOP 7. Dacitic(?) ashes from Paoha Island. Figure 15 illustrates the stratigraphy found in the upper 10 cm of sediments at this site near Navy Beach. The units of particular interest in this section include a very thin horizon of reworked, fine pumice sand deposited during the lake regression of ~300 BP(?) and at least 11 dacitic ashes that lie above that sand. XRF analysis was undertaken on the highest of these ashes; results are listed on Figure 9 (see "Navy ash").

That these ashes are from Paoha Island is suggested not only by the trace element chemistry of the highest member, but by stratigraphic and geomorphic considerations as well: Paoha has a large number of potential sources of ash, while only one likely source--the cinder cone--exists on Negit; much of Paoha is mantled with a relatively thick layer of blank tephra, while on Negit Island the layer of blank tephra is relatively thin. (Indeed, in the vent of the Negit cinder cone the layer of blank tephra is very thin to non-existent.)

At Stop 6, it was noted that at least 20 dacitic ashes lie high above the 600 year-old Mono Craters tephra. The sequences of ash exposed here and

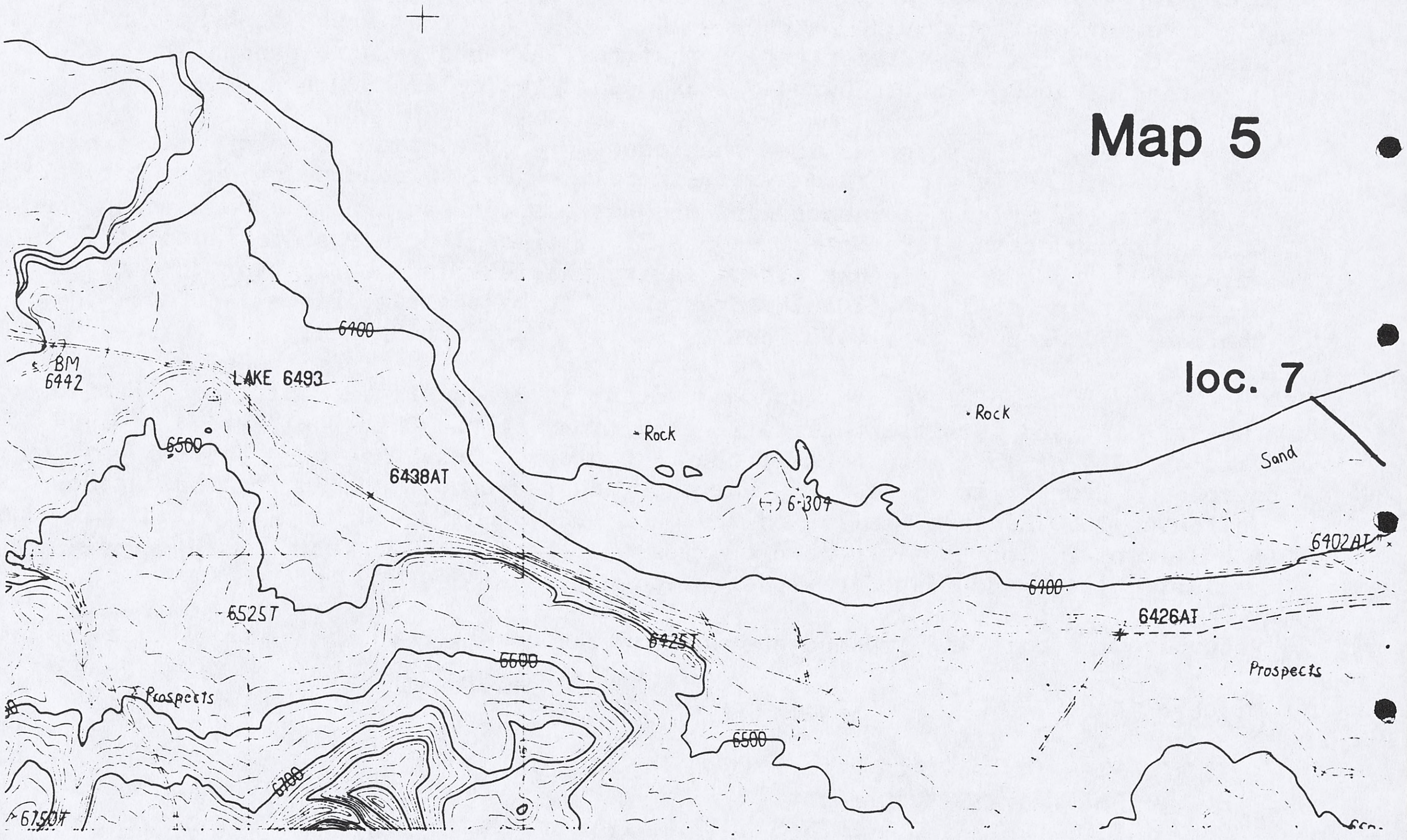

Figure 15. Stratigraphy exposed in the shallow pit at Navy Beach, Locality 1, Map 5.

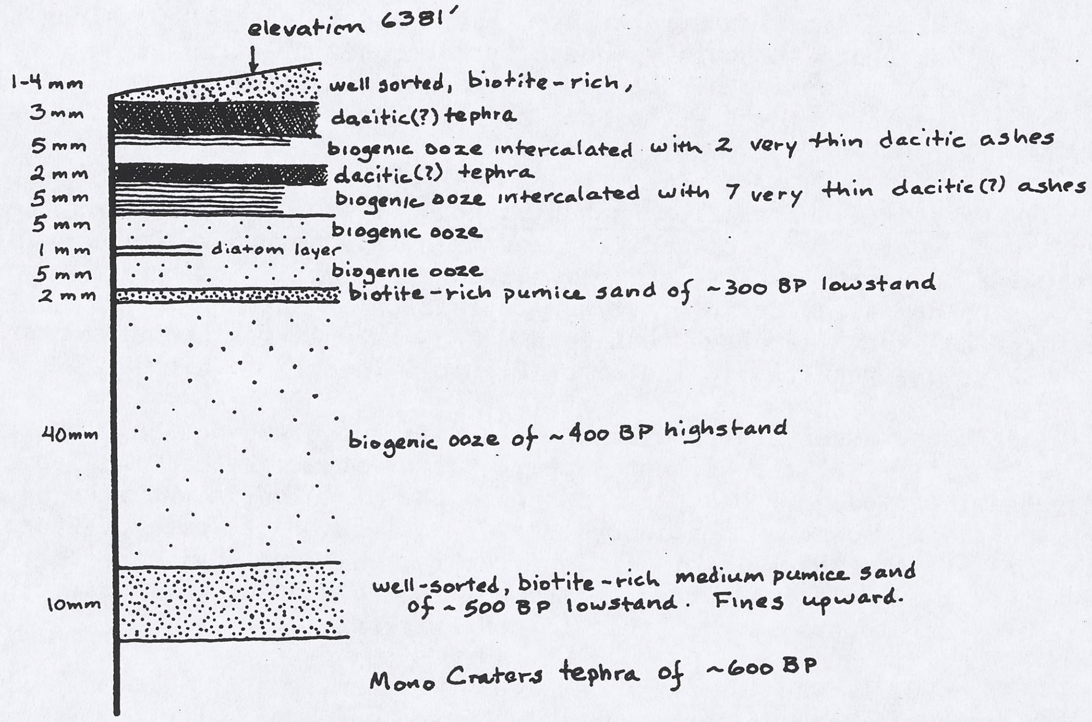

on Little Norway, then, indicate that over a period of perhaps a century vents on Paoha erupted no fewer than 20 times.

This concludes Day 2 of the FOP field trip. Retrace the route to Hwy 395.

Bibliography

Cloud, Preston, and Kenneth Lajoie, 1980. Calcite-impregnated defluidization structures in Littoral Sands of Mono Lake, California. Science, Vol. 210, pp. 1009-1012.

Dunn, J.R., 1953. The origin of the deposits of tufa in Mono Lake, California. Jour. Sed. Petrology, Vol. 23, No. 1, pp. 18-23.

Fletcher, Thomas Christopher, 1982. The Mono Basin in the Nineteenth Century: Discovery, Settlement, Land Use. Unpublished MA thesis in Geography, University of California, Berkeley.

Lajoie, Kenneth Robert, 1967. Quaternary Stratigraphy and Geologic History of Mono Basin, Eastern California. Unpublished Ph.D. dissertation in Geology, University of California, Berkeley.

Russell, Israel Cook, 1889. Quaternary History of Mono Valley, California. U.S.G.S. Eighth Annual Report, Part 1, pp. 261-394.

Scholl, D.W., Von Huene, R., St.-Amand, P., and Ridlon, J.B., 1967. Age and origin of topography beneath Mono Lake, a remnant Pleistocene lake, California. Geol. Soc. America Bull., Vol. 78, pp. 583-600.

Scholl, D.W., and Taft, W.H., 1964. Algae, contributors to the formation of calcareous tufa, Mono Lake, California. Jour. Sed. Petrology, Vol. 34, No. 2, pp. 309-319.

Stuiver, Minze, 1982. A high precision calibration of the AD radiocarbon time scale. Radiocarbon, Vol. 24, No. 1, pp. 1-26.

Wood, Spencer, 1977. Distribution, correlation, and radiocarbon dating of late Holocene tephra, Mono and Inyo Craters, eastern California. GSA Bull. Vol. 88, pp. 89-95.

Mono Lake County Park at Dechambeau Creek (Wood and Stine)

Late Holocene sediments, volcanic ash layers, structures of liquefied sediment.

In the summer of 1983 the lower reach of Dechambeau Creek had incised and exposed an informative stratigraphic section in which the latest volcanic events of the Mono Craters are recorded as volcanic ash layers (Fig.2-1). This locality may have been submerged in the 1984 rise of the lake level. A variety of sedimentary structures have developed in the ash deposits, some of which may be a record of liquefaction during earthquakes. This locality clearly shows evidence of the overlapping tephra lobes of the 1190 yr B.P. and the 640 yr B.P. Mono Craters eruptions (see Fig. 2-2). This overlap relationship is best displayed at localities along the west side of Mono Lake because the 1190 B.P. ash lobes were transported mostly west and south (Wood, 1977) whereas the 640 B.P. ash lobes are mostly to the north-northeast (Sieh and others, 1983). These localities along the west shore of the lake have cleared up confusion between these two very similar appearing Mono Craters ash layers that were suspected, but not clearly distinguished to be separate by Wood (1977).

The 1190 yr B.P. ash appears as a thin disrupted, convoluted , white layer in the lake sediments that was liquefied. At this locality the upper surface is eroded and truncated (Fig. 2-1) The overlying material is a thick grey ash that is thought to represent water-transported ash from the 1190 B.P. eruption that was deposited on the delta of Dechambeau Creek. This overlying layer of silt-sized ash contains a sand layer which is spectacularly disrupted and convoluted. The silt-sized ash apparently liquefied and disrupted the sand layer. The upper liquefied layer is about 0.6 m thick at this locality. The well-sorted silt and fine-sand-sized ash layers appear to be quite susceptable to liquefaction, whereas the clayey organic sediment that makes up most of the lacustrine deposit did not liquefy. The sediments of Mono Lake may contain a sequence of liquefied lake sediment and volcanic ashes that may ultimately yeild a history of seismicity associated with volcanism. At this locality there is evidence for at least two liquefaction events after the eruption and deposition of 1190 B.P. ash and before the 640 yr B.P. eruption. Liquefaction features are known to occur within several kilometers of the epicenter of magnitude 5.5 to 6 earthquakes (Kuribayashi and Tatsuoka, 1975; Youd and Perkins, 1978), but areally widespread liquefaction would indicate a larger event. This locality and others around the basin invite a more detailed study.

REFERENCES CITED

Sieh, K., Wood, S.H., and Stine S., 1983, Most recent eruption of the Mono Craters, eastern California (abs): EOS, v. 64, p. 889.

Kuribayashi, E., and Tatsuoka, F., 1975, Brief review of liquefaction during earthquakes in Japan: Soils and Foundations, v. 15, no. 4, p.81-92.

Wood, S. H., 1977, Distribution, correlation, and radiocarbon dating of late Holocene tephra, Mono and Inyo craters, eastern California: Geological Society of America Bulletin, v. 88, p. 89-95.

Wood, S.H., and Brooks,R., 1979, Panum Crater dated 640 + 40 radiocarbon years B.P., Mono Craters, California: Geological Society of America Abstracts with Programs, v. 11, no.7, p. 543.

Youd, T.L., and Perkins, D.M., 1978, Mapping liquefaction-induced ground failure potential: American Society of Civil Engineers Proceedings, Journal of the Geotechnical Division, v. 104, no GT4, p. 433-466.

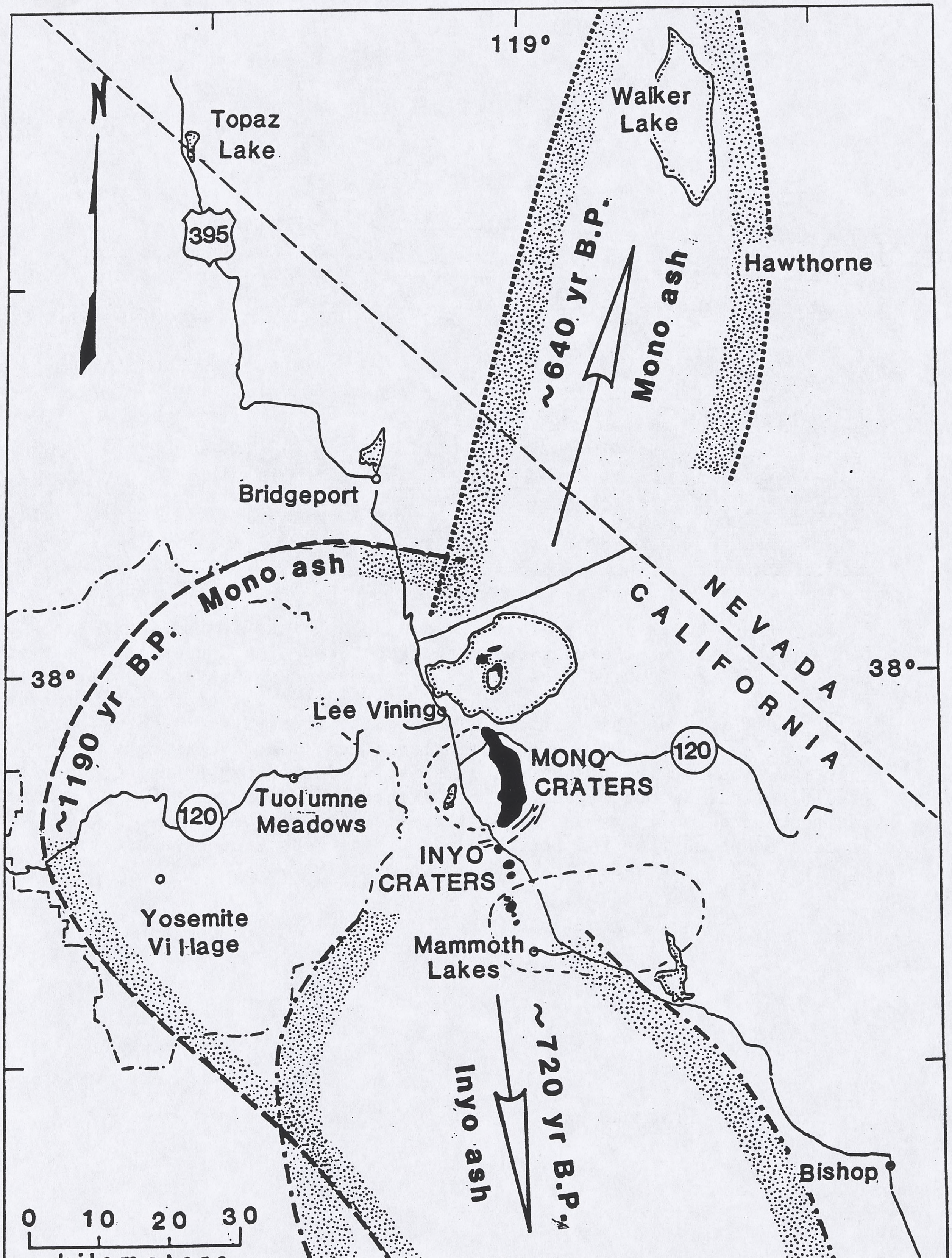

Fig. 2-2. Map showing the limits of known occurrences of three recent ash layers erupted from the Mono and Inyo Craters. The 1190 yr BP Mono Craters ash is "tephra 2 of Wood (1977)". The 720 yr BP Inyo Craters ash is "tephra 1 of Wood (1977)". The 640 yr BP Mono Craters ash is from the most recent eruptive episode of the Mono Craters reported by Sieh and others (1983).

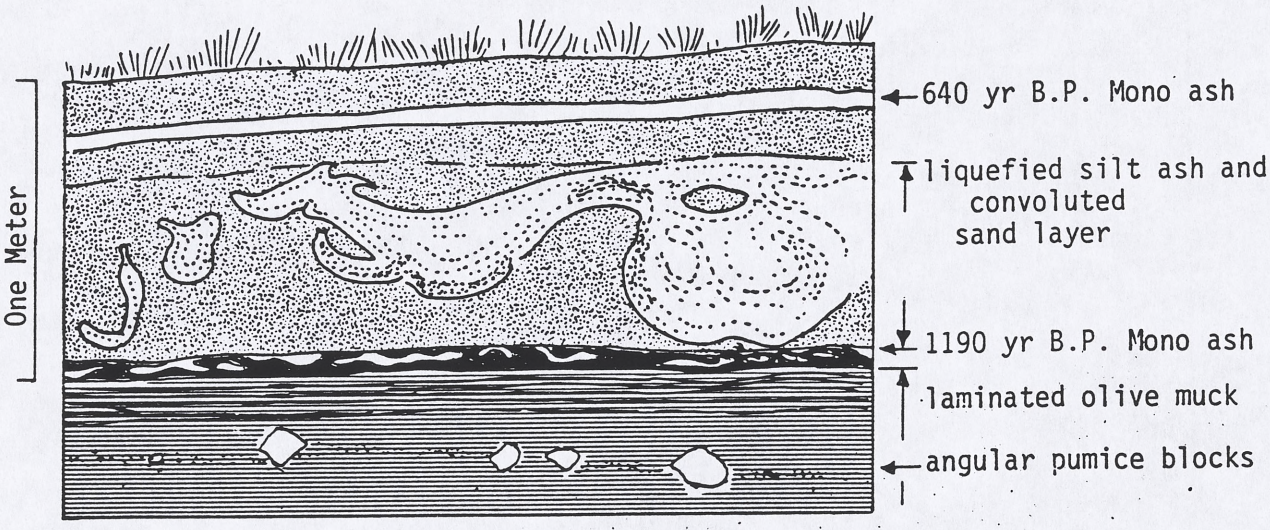

Fig. 2-1. Stratigraphy of volcanic ash and liquefied sediment exposed in the banks of lower Dechambeau Creek at Mono Lake. The angular pumice blocks near the base of the exposed section are shoaled blocks that apparently came from an eruption near Negit Island, where a similar pumiceous, biotite-bearing, rhyolite forms small islands that will be discussed by Scott Stine at STOP 3. The 1190 B.P. yr layer of white ash has been liquefied. The overlying 60-cm thick layer contains massive silt ash and a convoluted sand layer that appears to be the result of a second liquefaction event. The uppermost 0.3 to 0.5 meters of sediment and soil is not liquified, and it contains the 640 yr. B.P. Mono ash from an eruption from the northern end of the Mono Craters described by Sieh and others (1983) and dated by Wood and Brooks (1979).

MOST RECENT ERUPTIONS OF THE MONO CRATERS, EASTERN CENTRAL CALIFORNIA

by

Kerry Sieh

Division of Geological & Planetary Sciences
California Institute of Technology
Pasadena, California 91125

ABSTRACT

The Mono Craters in eastern central California constitute an arcuate 17-km-long edifice of late Pleistocene and Holocene rhyolitic domes and flows. Radiocarbon analyses indicate that the latest subplinian to plinian eruptive episodes within this chain of volcanoes occurred in about 705 ± 55 A.D. and 1395 ± 50 A.D. Stratigraphic and sedimentologic studies reveal that the products of the most recent episode emanated from several aligned vents along the crest of the northernmost 5 km of the chain. The oldest products of this eruption are several plinian to subplinian tephras. These are overlain locally by pyroclastic flow and surge deposits. Tephra rings, domes and coulees were constructed near the vents during the waning stages of the eruption.

The eruption was preceded by formation of a 1-2 km-long graben along the range crest. Isopach and other data demonstrate that the basal tephra layer was erupted from aligned vents within this graben. This white pumiceous layer has a maximum measured thickness of 56 cm and a dispersal index of several hundred square kilometers. The dispersal axis trends NNE from the vents and across Mono Lake. Subsequent pyroclastic fall deposits are similar to the basal layer in extent and thickness and have dispersal axes trending NNW to NE. At least two of the these beds originated from a vent about 1 km north of the initial vents and graben. Pyroclastic flow deposits rest upon the fall deposits at distances up to about 4 km from the vents. One blocky pyroclastic flow emanated from the site of Panum Dome and flowed NW into Rush Creek and Mono Lake, causing spectacular liquefaction and decollement within the substrate. The final stages of the eruption involved relatively passive but complex construction of several tephra rings and the extrusion of Panum dome, Cratered dome, North Coulee, and two other unnamed intervening domes.

INTRODUCTION

The Mono and Inyo craters and the volcanoes of Mono Lake (all shown in black in Fig. 1) constitute a chain of late Quaternary silicic volcanic edifices that extends 40 km northward from the Long Valley Caldera to Mono Lake, along the eastern frontal faults of the Sierra Nevada (Russell, 1889, Putnam, 1949; Mayo et al., 1936; Kistler, 1966; Huber and Rinehart, 1967; Bailey et al., 1976). Most of all of these volcanic domes, flows and craters appear to be less than about 40,000 years old (LaJoie, 1968; Wood, 1977, as modified by Wood and Brooks, 1979). These and associated pyroclastic flow and fall deposits that blanket the region represent more than two dozen major silicic eruptive episodes. Hence, the chain is one of the most active volcanic sources in the western U.S.

I am interested in helping to characterize that hazard, and have begun by studying the nature and distribution of the products of the most recent eruptive episode of the Mono Craters.

The abutting and overlapping domes, flows and craters of the Mono Craters (Fig. 2) constitute the largest part of the volcanic chain and appear to plug the vents of most of the latest Quaternary (40,000 years B.P.) eruptions (LaJoie, 1968). Most of these rocks are high-silica rhyolites with markedly similar bulk chemistry and trace-element chemistry (Carmichael, 1967, Table 5; LaJoie, 1968, Fig. 23, Table 4; Loney, 1968). Texturally, the rocks are much more variable. Those domes, flows and pyroclastic deposits erupted prior to about 2,000 years ago are porphyritic glassy rhyolites, whereas younger erupted products are aphyric or very sparsely porphyritic.

Most of the aphyric rhyolitic domes and flows (that is, Panum Dome, Cratered Dome, Upper Dome, North Coulee and South Coulee) are not mantled by pyroclastic flow or fall deposits. The other domes and flows are thickly mantled with pyroclastic debris.

In the region surrounding these unmantled edifices, the youngest volcanic deposit consists of the pyroclastic fall and flow beds illustrated and discussed below. This series of beds rests upon various older beds of lacustrine, marsh, aeolian and volcanic origin. In most cases, the older, underlying units exhibit bioturbation and higher organic content in their upper portions (see for example, the bed indicated by an arrow in the photo of site "BB" Fig. 3). This indicates that the pyroclastic deposits blanketed a ground surface which had undergone mild pedogenic processes and bioturbation between the two most recent eruptions.

The basal part of the youngest pyroclastic blanket consists of several well-sorted, widespread, distinctive beds which are illustrated in the seven photographs of Figure 3. The basal beds are composed of white lineated pumice (W), light gray non-vitreous glass (G), and black obsidian (B), in percentages that differ from bed-to-bed.

The basal bed (1) at all localities is about 80 to 95% white lineated pumice (W). In all exposures, the bed is normally graded in its upper portion. This indicates a gradual diminishing of the energy of this initial phase of the eruption. At sites where the bed is very thick (for example, see photos of site "BX" and "BB" Fig. 3), the lower part of the bed is rich in gray non-vitreous glassy clasts and accessory and accidental clasts that are commonly much larger than the white pumice clasts. This suggests that the initially erupted juvenile material (W) entrained materials from the walls of the volcanic conduit.

Figures 4a and 4b show the distribution and thickness of bed "1" in the area. Figure 4b is a blow-up of the near-source portion of 4a. Sites at which data were collected are shown as black dots. Those localities illustrated by the photos of Fig. 3 are also labelled. Bed "1" is the most broadly distributed of the products of this latest eruption. It covers more than

500 square km and its dispersal index is several hundred square kilometers, which puts it in the plinian category of Walker. The thickest (and coarsest) portions of bed "1" are near North Coulee; this indicates a source or sources under and immediately northwest of the southwest portion of North Coulee. The next bed in the series is labelled bed "2" and is composed of W, G and B clasts typically in the ratio of about 4:3:3. The black obsidian clasts (B) are concentrated in the lower 40% of the bed (for example, see the photos of sites "AX" and "BX" Fig. 3). The NNW trend of the dispersal axis (Figs. 5a and 5b) indicates that the plume from which the pyroclasts of this bed fell was blown NNW, over Mono Lake. The thickest and coarsest part of this bed is immediately NW of Upper Dome. This indicates that the pyroclasts composing this bed were ejected from a vent under Upper Dome, not from the same vent or vents of bed "1".

The third eruptive pulse of the latest eruption is represented by bed "3" (Fig. 3). It is also composed of nearly equal amounts of W, G, and B pyroclasts. Concentrations of W occur at the base of the bed at near-source sites. The dispersal axis of bed "3" trends NNW near the source (Figs. 6a and 6b) but bends to the NNE about 10 km from the vents. This probably indicates that low level winds were blowing NNW at the time of the eruption and higher level winds were blowing NNE.

The sources of bed "3" are vents now filled by Upper Dome <u>and</u> North Coulee judging from the isopach countours.

Younger pyroclastic fall beds composed principally of W, G, and B clasts overlie beds 1, 2 and 3, but these are not yet well correlated between sites. In general, however, it is clear that the dispersal axes of most of these beds trend northerly to northeasterly and originated from vents in the vicinity of Upper Dome and North Coulee.

Following the initial outbursts that resulted in deposition of the W, G and B-rich pyroclastic fall deposits, a series of pyroclastic flows emanated from vents in the vicinity of Upper Dome and North Coulee. I have been able to map only three of the several individual flows (A, B, and C in Fig. 7). Figure 7 gives a crude picture of the distribution of these and the remaining undifferentiated pyroclastic flow deposits. The upper bed of site "bx" (Fig. 3) illustrates the poorly sorted, massive nature of these flow deposits.

The region labelled "A" on Fig. 7 encompasses a geomorphologically well-defined flow deposit that originated from vents now buried by North Coulee. The deposit extends about 4-1/2 km westward from its source. It is characterized by an abrupt, lobate flow front and distinct ridges and troughs aligned parallel to the direction of the flow.

The region labelled "D" includes a broad area extending up to 9 km from the North Coulee vents. Most excavated exposures within this region reveal one or more massive poorly sorted pale pink to pale orange pumiceous beds ranging in thickness from 70 mm at distal sites to more than 3 m at a site immediately south of North Coulee and 1.5 m at a site northeast of Upper Dome. In the region between North Coulee, Upper Dome and Cratered Dome and the 300-year-old shoreline of Mono Lake, these deposits exhibit ridges and swales that trend perpendicularly to topographic contour. The extent of the flow deposits north of the 300-year shoreline of the lake is unknown.

In the vicinity of Panum Dome, this unit consists of undifferentiated flow deposits from the vent underlying Panum Dome. These and the flows labelled "C" and "B" post-date the flows that emanated from the region of North Coulee and Upper Dome and are discussed below.

Vents for the various erupted products of the latest eruption of the Mono Craters are shown in Figure 8. Dots outline the several domes and coulees. Vents labelled "I" are based upon geomorphologic interpretation of the surface of North Coulee. Vents 2 and 4 are currently exposed craters. Vent 5 is based upon geomorphologic interpretation of the surface of Upper Dome and the existence of a small satellite dome and a tephra ring on its south flank. Vent 6 is Cratered Dome and vent 7 is the axial fissure through which Panum Dome was extruded.

The heavy hachured lines are normal faults with tens of meters of slip. These are cut by craters 2, 4 and 5 and appear to be draped by the basal pyroclastic fall deposits. These faults probably indicate that a 1 to 2 km-long "keystone" dropped down over the rising magma body prior to its initial eruption.

Exposures in the vicinity of Panum Dome are particularly good, due to quarrying of the Pumice Pit Dome and erosion by Rush Creek. Hence, the sequence of events has been studied more completely there than elsewhere. Figure 9 is a generalized, composite columnar section which displays the pyroclastic products emanating from the Panum vent in about 1400 A.D.

The basal airfall deposits of the 1400 A.D. eruption that emanated from vents near Upper Dome and North Coulee underlie all of the Panum deposits. There exists no evidence of a bioturbated or organic-accumulation layer between these airfall deposits and the deposits from Panum. Thus, the opening of the Panum vent must have followed the airfall deposition by no more than a few years or decades.

Within a half-kilometer radius of Panum, a "throat-clearing breccia" overlies the airfall tephra and ranges up to several meters in thickness. Overlying the breccia near the vent is a white to pale pink pumiceous pyroclastic flow bed of quite variable thickness. In excavations 1.1 and 1.7 km southwest of Panum, this pebbly, cobbly bed forms 500-mm-high pebbly dunes aligned northwest-southeast. On figure 10, the light lines in the quadrant southwest of Panum represent the crests of those dunes apparent on aerial photographs. In Figure 7, the dune field is labelled "B". Although white, pumiceous pyroclastic flow deposits are present in excavations in all quadrants from Panum, for some reason dunes are apparent only in the southwestern quadrant. Amplitude of the dunes ranges to about 1 m and wavelength varies from about 10 to about 100 m. Slope angles of 20-25, are common. The dunes appear to be concentric about a point about 1000 m south of the center of Panum Dome, but the Panum vent, beneath Panum Dome , is the only plausible source for the dunes, because Pumice Pit Dome is blanketed by the basal airfall beds, throat-clearing breccia and the flow deposit. The pyroclasts of the dune bed must have been "bed load" at the base of a very hot radially expanding, southwesterly moving cloud.

Charred twigs of chapparal are common within the dune bed and yield a reservoir-corrected ^{14}C age of 530 ± 60 years B.P. (± 2σ). This is indistinguishable from an age of 550 ± 80 years B.P. on charred twigs within and just below the basal airfall tephra at another locality and an age of 580 ± 60 years B.P. on charred twigs within a pyroclastic flow in Rush Creek, northwest of Panum. The averaged and dendrochronologically corrected age of these samples is 555 ± 50 years B.P. (or 1395 ± 50 A.D.).

Excavations within 1-1/2 km of the Panum vent expose cross-laminated silty beds overlying the white pyroclastic flow bed. These pyroclastic surge beds are about a meter thick and display several sets of planar- and cross-laminated beds in the Pumice Pit Dome Quarry. Ripples that climb away from the source are dominant and erosional contacts are rare. Bomb-sags are common at several horizons.

In the quadrant northwest of Panum a very coarse block breccia (labelled "C" in Fig. 7) overlies the surge and flow beds described above. At site "t" (Fig. 7), it is more than 6-1/2 m thick. Angular light-colored aphyric blocks up to several meters in diameter are common. These and smaller blocks show abundant white percussion marks that resulted from collisions with other blocks as the breccia was being emplaced. About 10% of the blocks are black, banded obsidian and pumice. Breadcrust texture is common and numerous light-colored clasts are pressed into the surface of the black obsidian and pumice. Apparently the light-colored clasts were relatively cool and brittle when the breccia was emplaced, but the black clasts were hot and ductile. The breccia may well represent a collapsed dome.

In Figure 7, the block breccia is shown in a paler pattern where it underlies younger lacustrine deposits of Mono Lake. Fluvial deposits of Rush Creek that post-date the emplacement of the breccia are labelled "E" in Fig. 7. In the walls of Rush Creek Gorge, one can see spectacular evidence that sudden emplacement of the breccia resulted in liquefaction of and decollement within the lacustrine substrate and basal airfall beds onto which it flowed. Space, however, does not allow illustration of this chaotic folded and faulted assemblage.

Panum Dome, itself, and its associated tephra ring are very late and relatively passively erupted products of the latest eruption of the Mono Craters. The tephra ring, which rises as much as 60 m above the surrounding plain, rests upon the latest pyroclastic flow deposits that emanated from the Panum vent. Panum Dome is composed of four structurally and texturally distinct domes, the largest and youngest of which is called North Dome (Fig. 11). It consists of a light gray banded rhyolite surrounded by a collar of breadcrusted light gray pumiceous rhyolite and bisected by a north-south fissure. A slightly older and much smaller feature, South Dome, lies south of and is intruded by North Dome. This dome is cored by banded rhyolite and has a 10 m thick carapace of concentrically foliated pumice topped by a discontinuous shell of black structureless obsidian.

Southwest and east domes are remnants of domes older than South and North Dome. East Dome rocks bear the closest resemblance to rocks of the block breccia.

The latest eruption of the Mono Craters appears to have resulted from the intrusion of a rhyolite dike along at least a 6-km length of the chain. Figure 12 depicts an eruptive sequence consistent with this hypothesis and the data outlined above.

REFERENCES

Bailey, R., Dalrymple, G., and Lanphere, M. (1976) Volcanism, structure, and geochronology of Long Valley caldera, Mono County, California: J. Geophys. Res., 81, 725-744.

Carmichael, I. (1967) The Iron-Titanium oxides of salic volcanic rocks and their associated ferromagnesian silicates: Contr. Mineral. and Petrol., 14, 36-64.

Huber, N., and Rinehart, C. (1967) Cenozoic volcanic rocks of the Devil's Postpile quadrangle, eastern Sierra Nevada, California: U.S. Geol. Survey Prof. Paper 554-D, 21 p.

Kistler, R. (1966) Structure and metamorphism in the Mono Craters quadrangle, Sierra Nevada, California: U.S. Geol. Survey Bull. 1221-E, 53 p.

Lajoie, K. (1968) Late Quaternary stratigraphy and geologic history of Mono Basin, eastern California: Ph.D. thesis, Univ. Cal., Berkeley, 271 p.

Loney, R. (1968) Flow structure and composition and the southern Coulee, Mono Craters, California -- a pumiceous rhyolite flow: Geol. Soc. America Memoir 116, 415-440.

Mayo, E., Conant, L., Chelikowsky, J. (1936) Southern extension of the Mono Craters, California: Amer. Jour. Sci., ser. 5, 32, 89-91.

Putnam, W. (1949) Quaternary geology of the June Lake District, California: Geol. Soc. America Bull., 60, 1281-1302.

Russell, I.C. (1889) Quaternary history at Mono Valley, California: U.S. Geol. Survey, Eighth Annual Report, 303-355.

Walker, G.P.L. (1973) Explosive volcanic eruptions -- a new classification scheme, Geologische Rundschau, 62, 431-446.

Wood, S. (1977) Chronology of late Pleistocene and Holocene and volcanics, Long Valley and Mono Basin geothermal areas, eastern California: Final Technical Report to U.S. Geol. Survey, Geothermal Research, Extramural Program, Contract No. 14-08-0001-15166.

Wood, S. and Brooks, R. (1979) Panum Crater dated 640 ± 40 years B.P., Mono Craters, California: in Abstracts with Programs, Geol. Soc. America, 11, no. 7, 543.

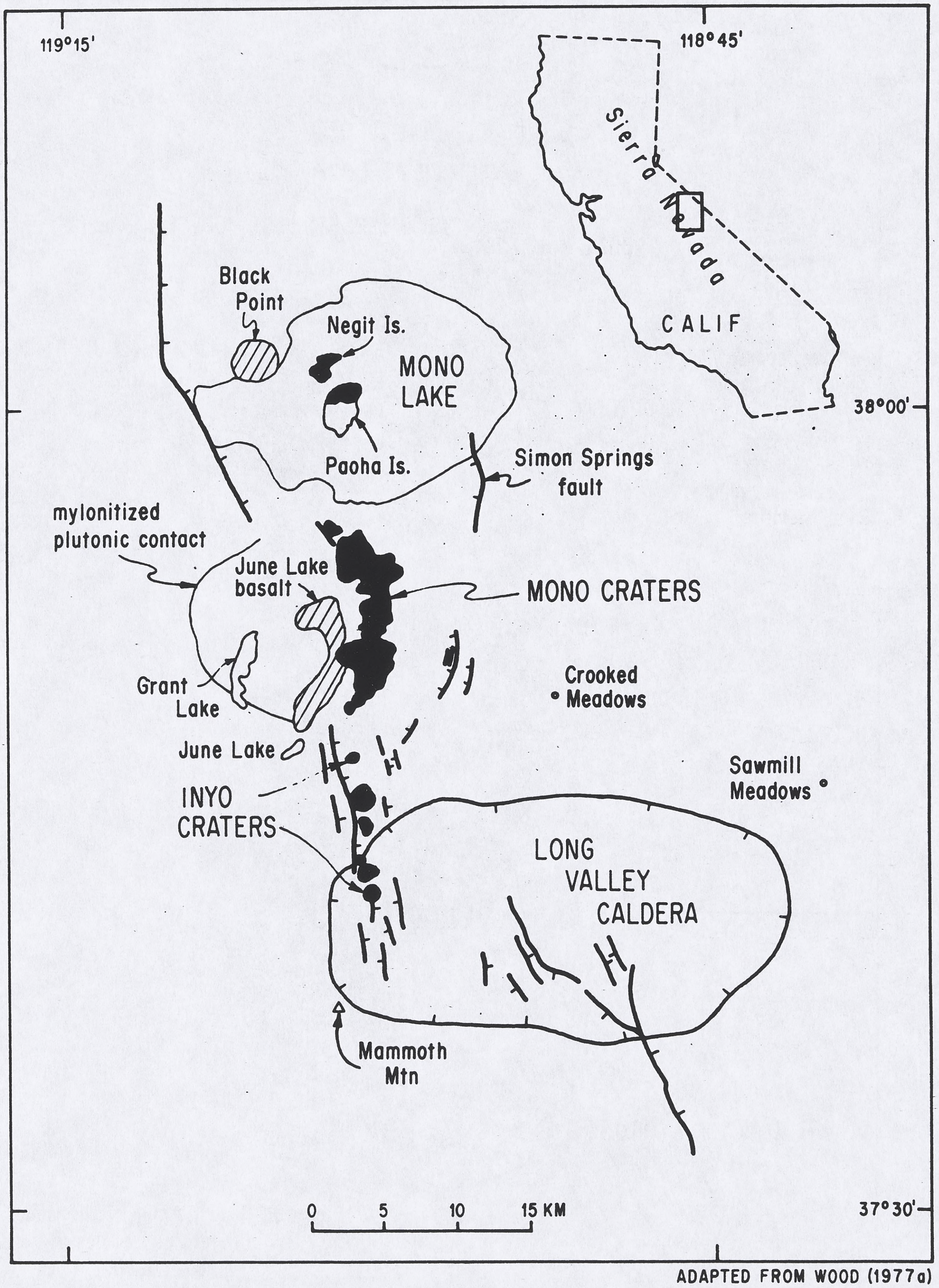

ADAPTED FROM WOOD (1977a)

Figure 1

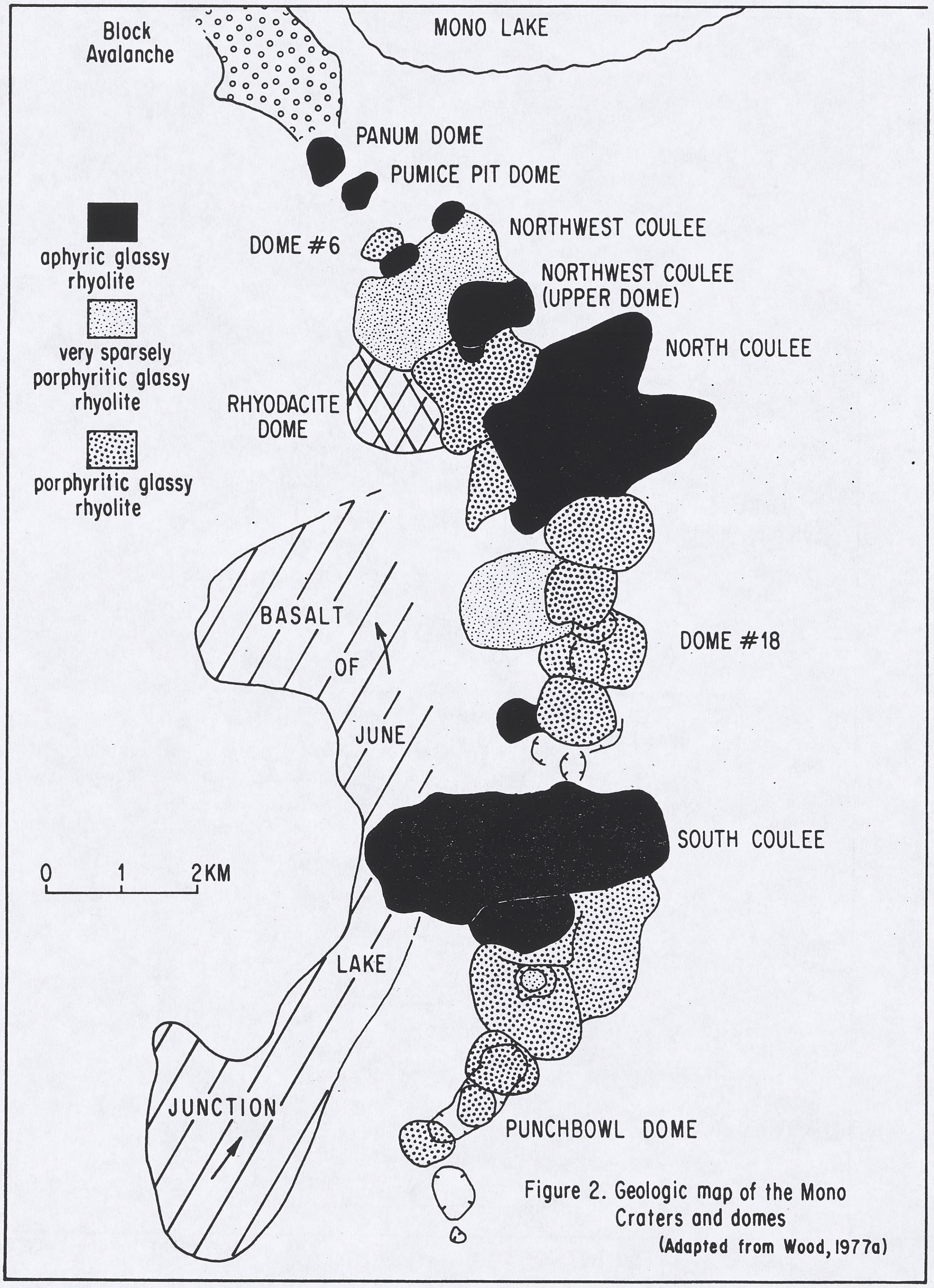

Figure 2. Geologic map of the Mono Craters and domes

(Adapted from Wood, 1977a)

Figure 2

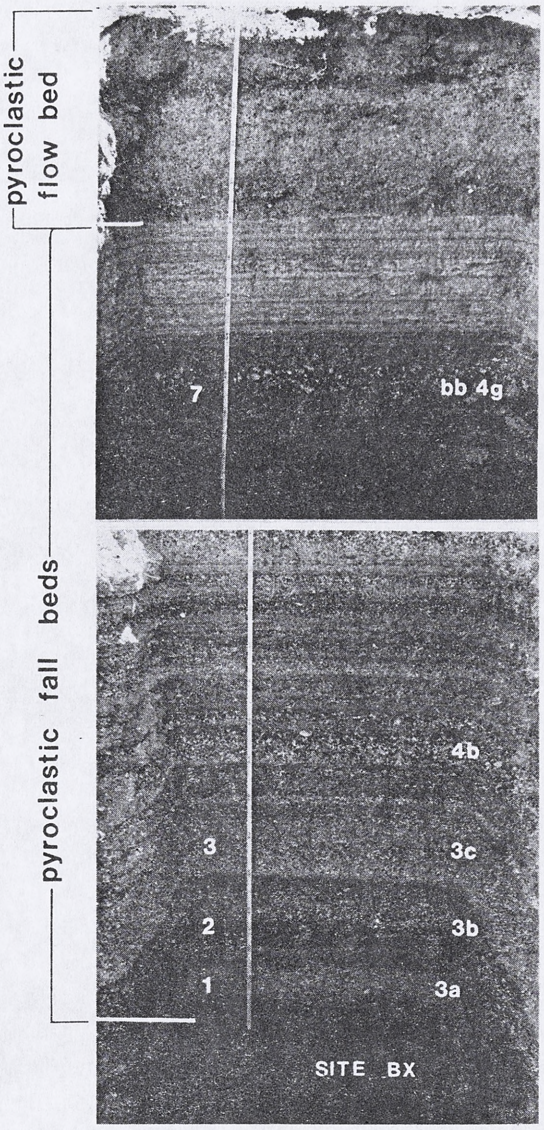
pyroclastic flow bed
pyroclastic fall beds
7
bb 4g
4b
3
3c
2
3b
1
3a
SITE BX

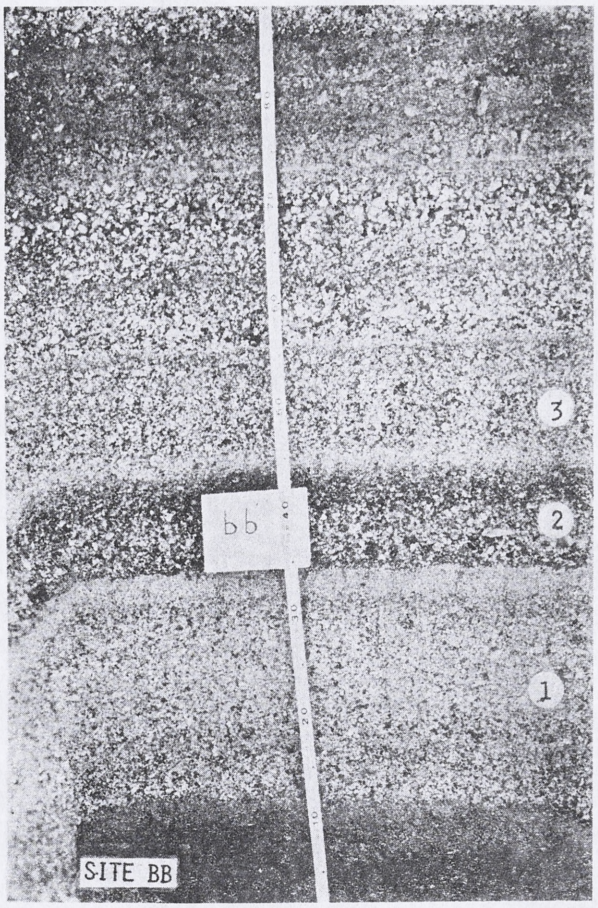
3
bb
2
1
SITE BB

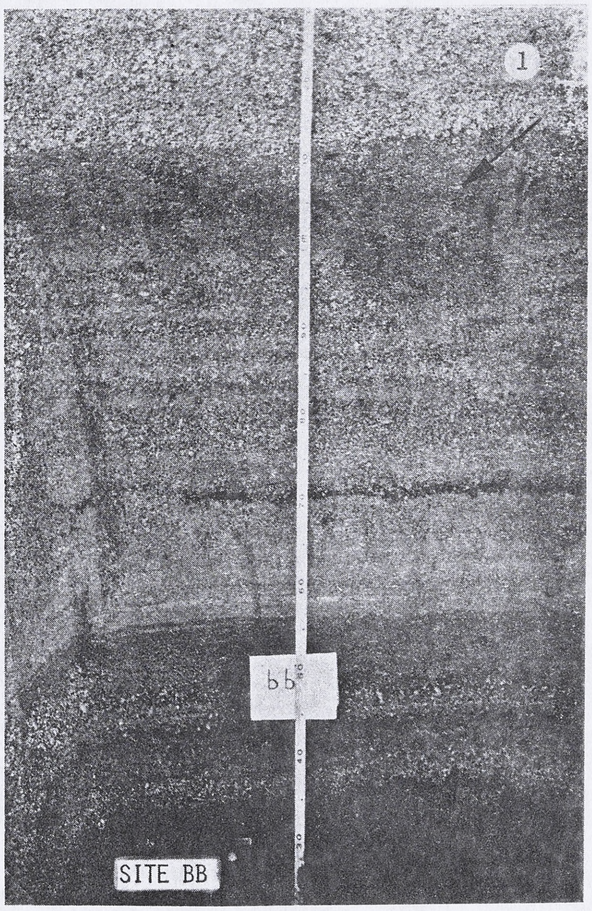
1
bb
SITE BB

Figure 3

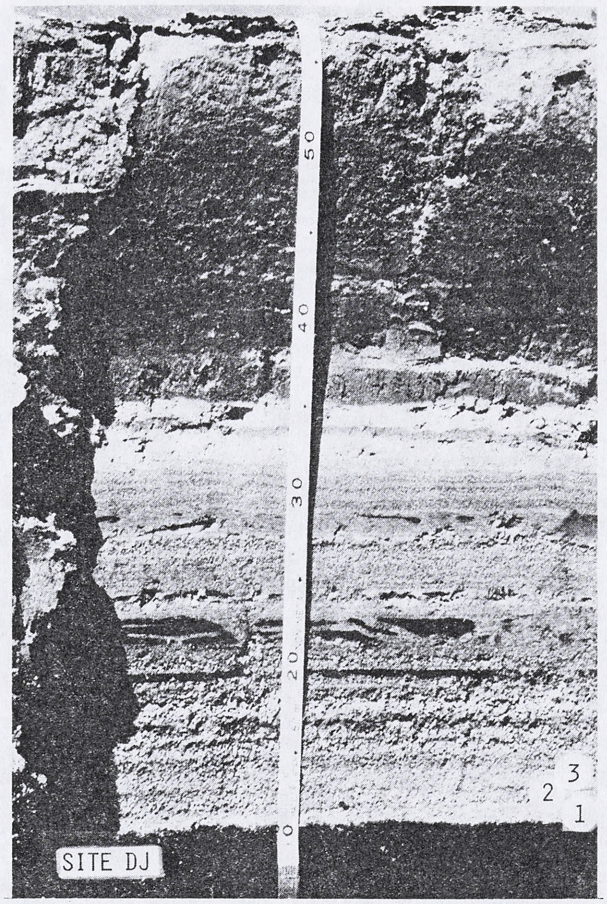
SITE DJ
1
2
3
0
20
30
40
50

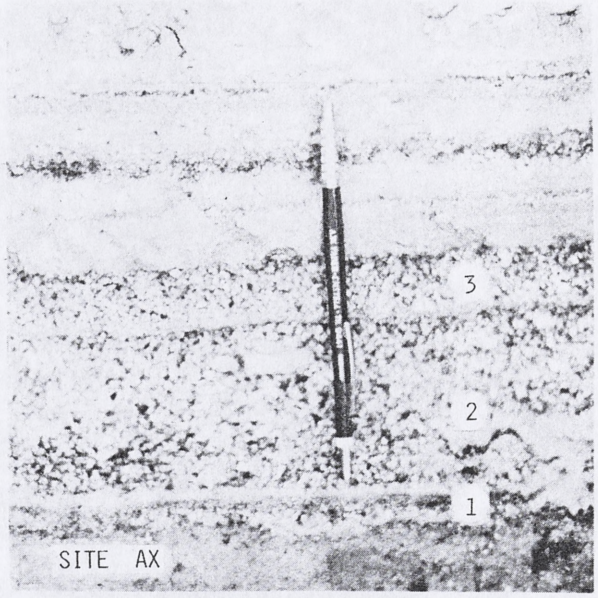
SITE AX
1
2
3

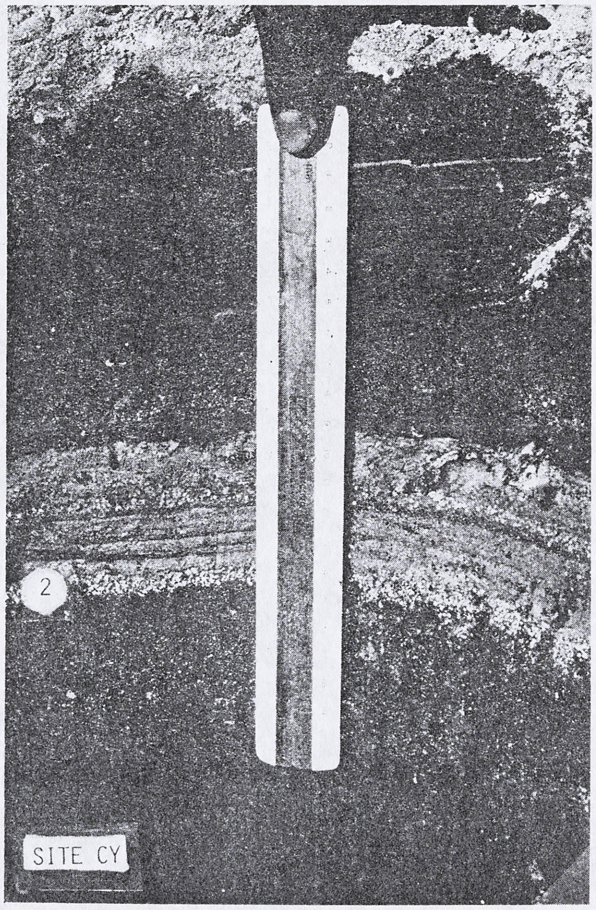
SITE CY
2

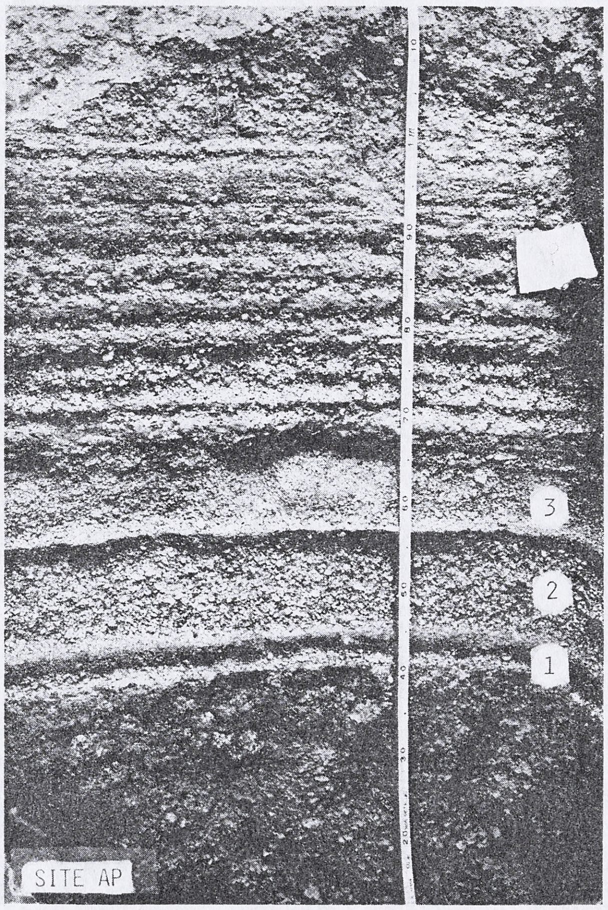
SITE AP
1
2
3

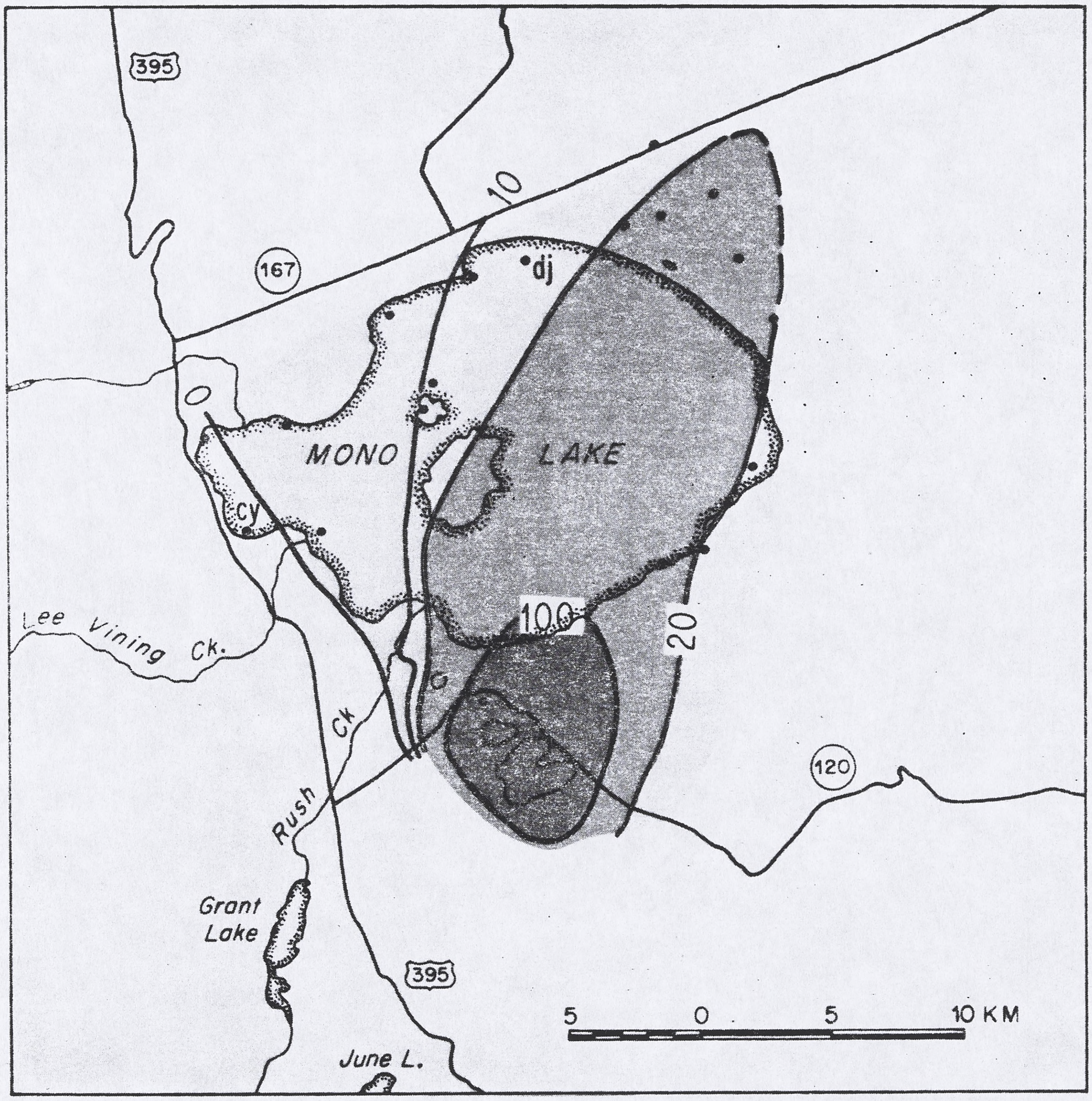
395
10
167
dj
0
MONO
LAKE
cy
Lee Vining Ck.
100
20
G
Rush Ck
120
Grant Lake
395
5 0 5 10 KM
June L.

Figure 4a

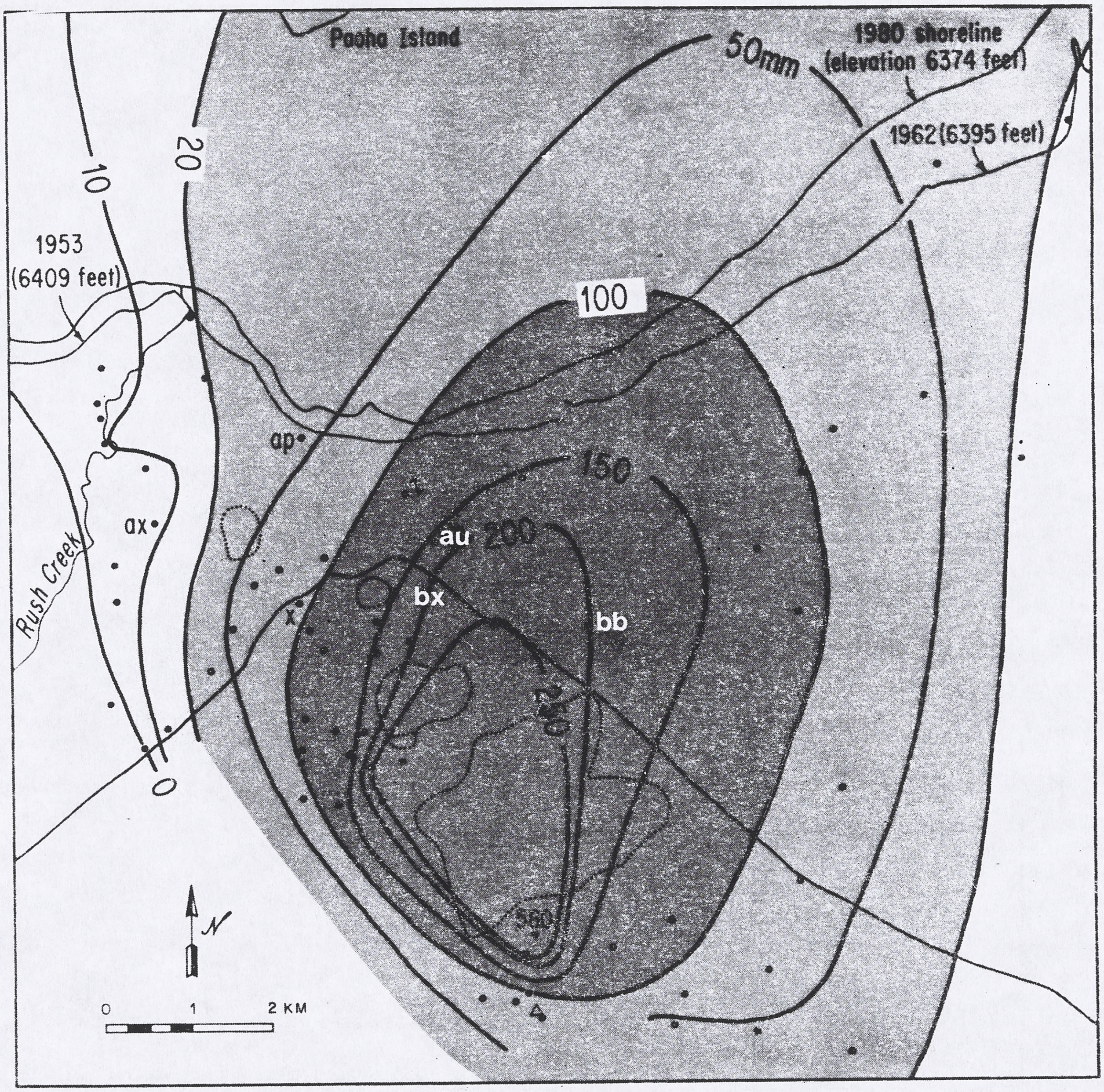
Paoha Island
50mm
1980 shoreline
(elevation 6374 feet)
1962 (6395 feet)
10
20
1953
(6409 feet)
100
Rush Creek
ap
ax
x
au
200
150
bx
bb
250
560
0
4
N
0 1 2 KM

Figure 4b

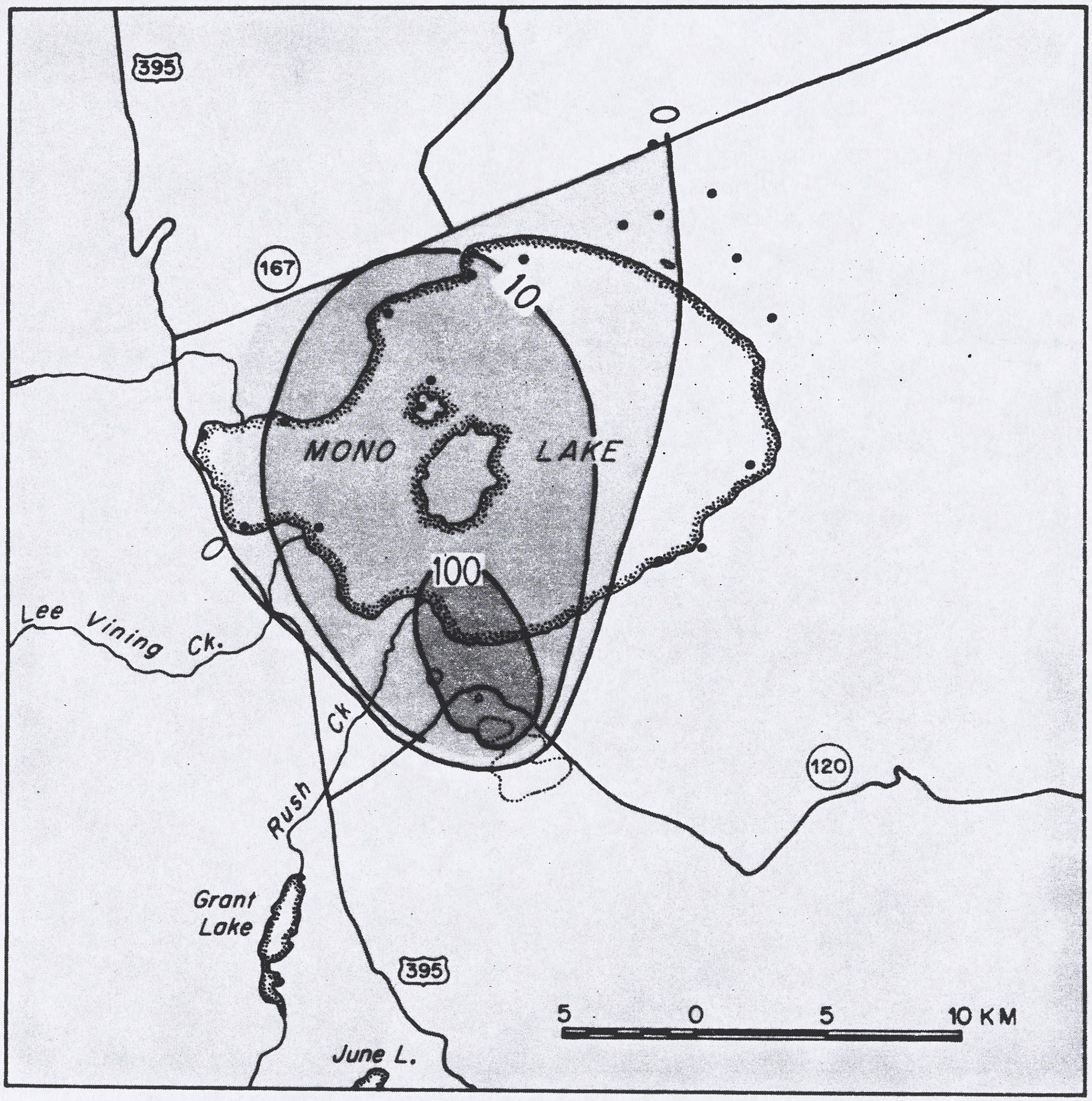
395
167
10
MONO
LAKE
100
Lee Vining Ck.
Rush Ck
120
Grant Lake
395
5 0 5 10 KM
June L.

Figure 5a

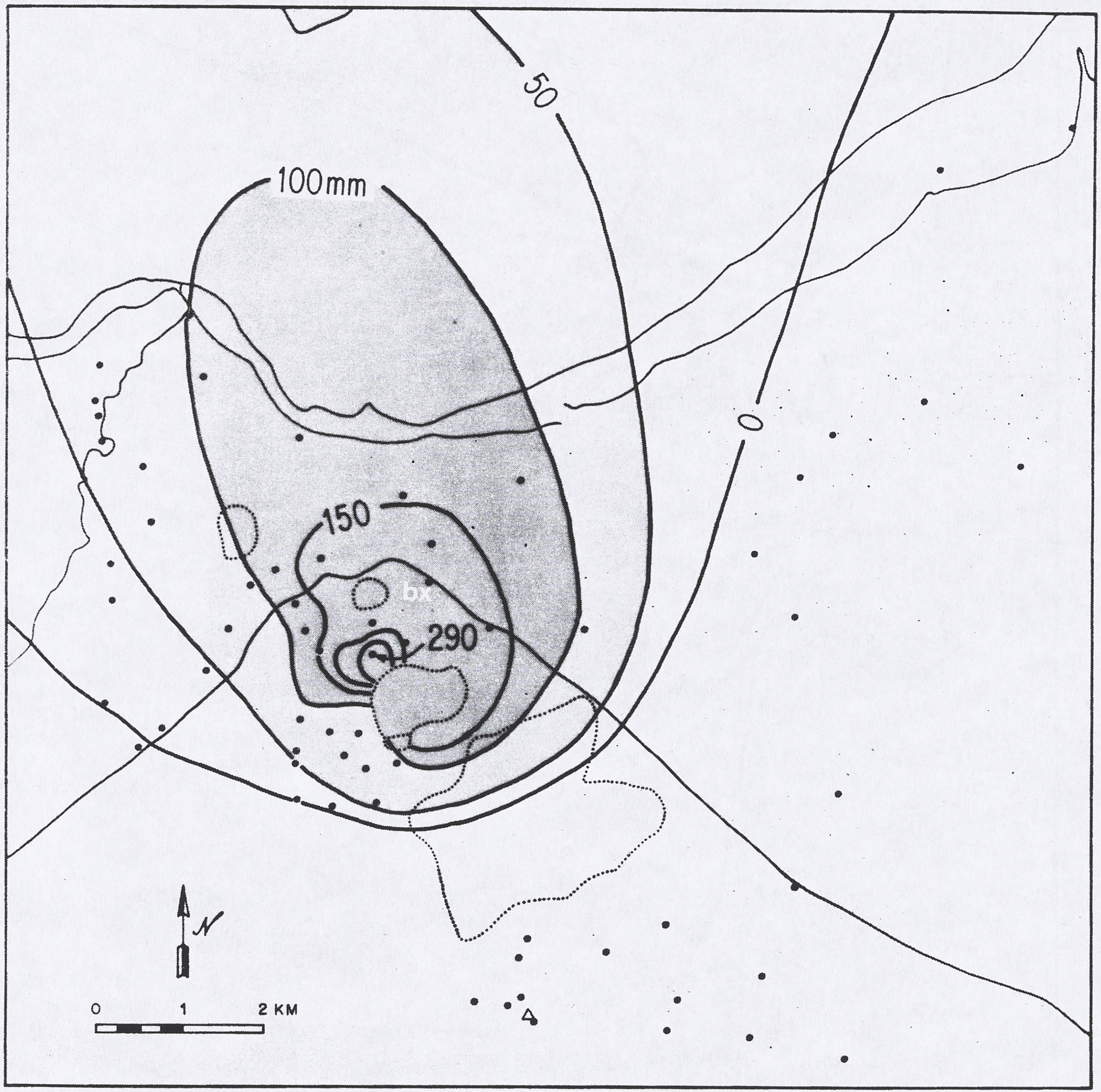

Figure 5b

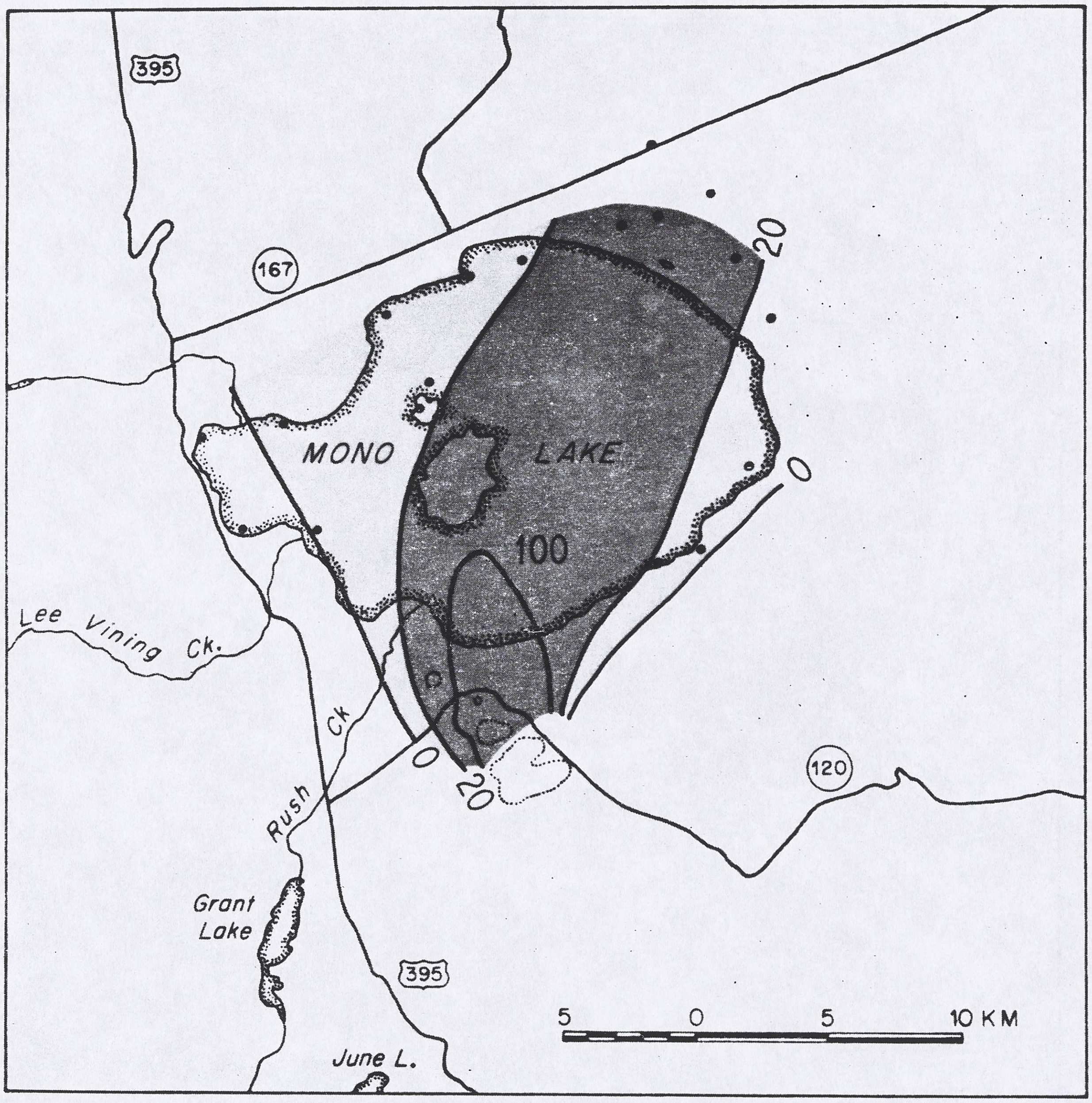
395
167
20
MONO
LAKE
0
100
Lee Vining Ck.
Rush Ck
0
20
120
Grant Lake
395
5
0
5
10 KM
June L.

Figure 6a

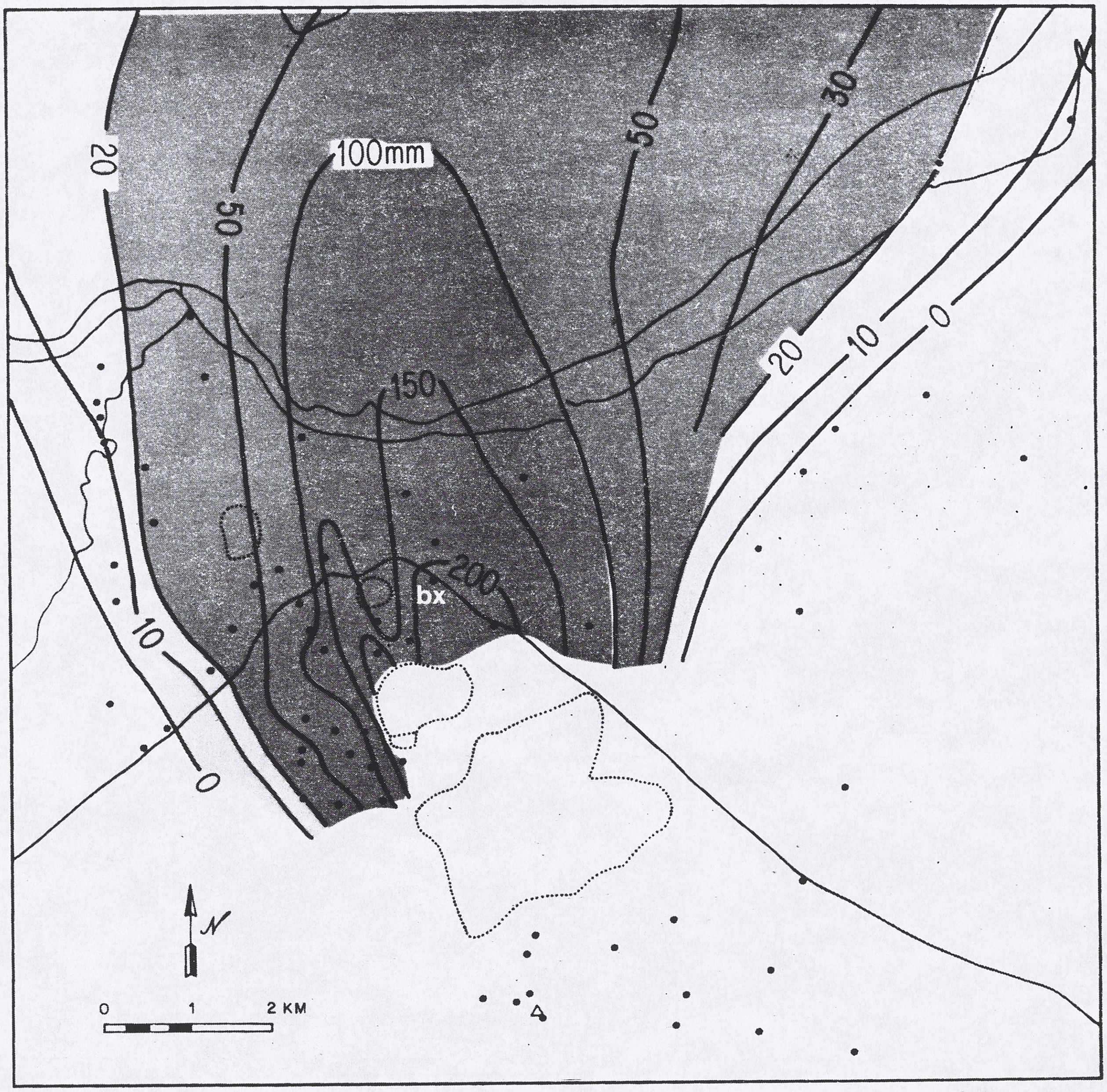

Figure 6b

Figure 7

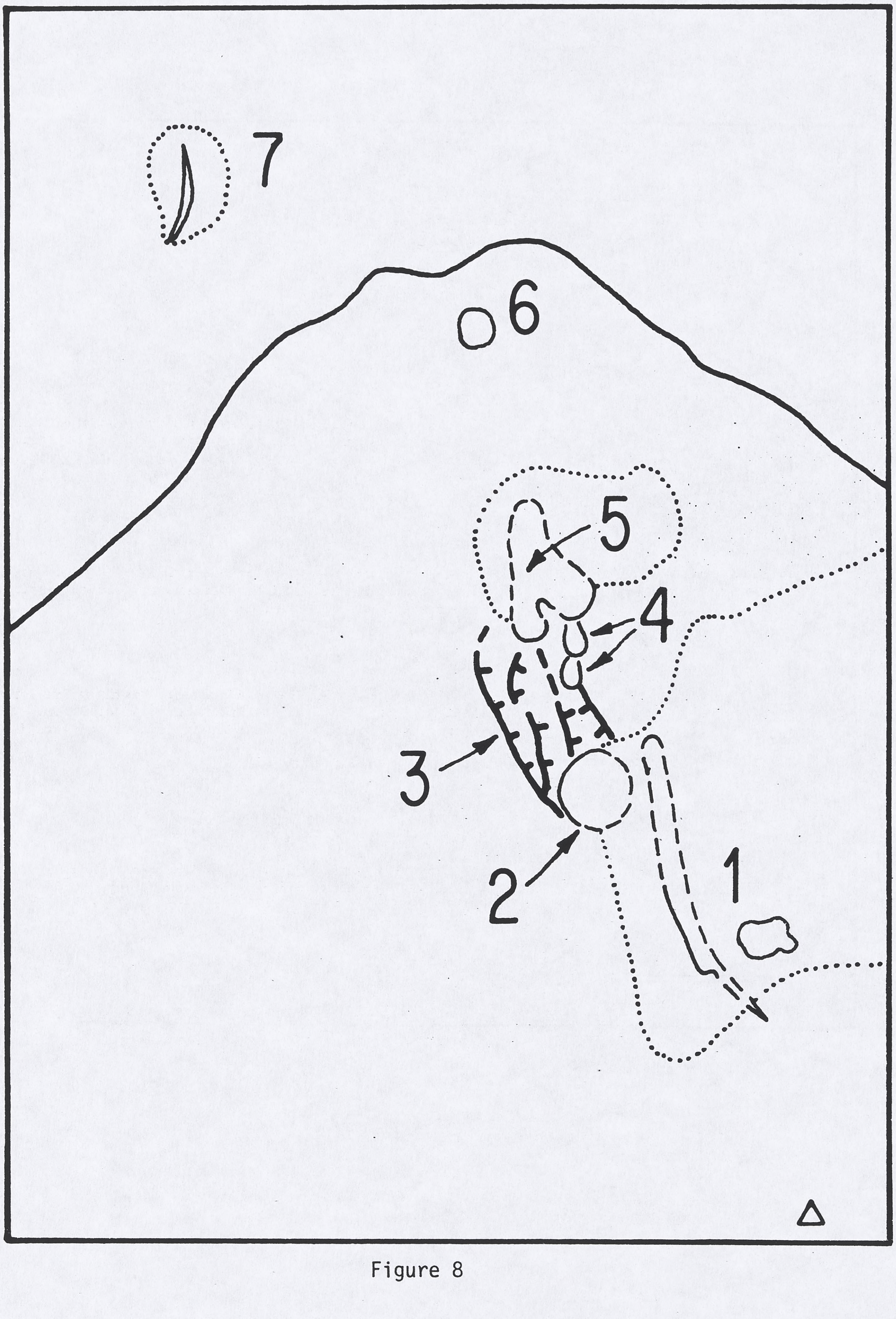

Figure 8

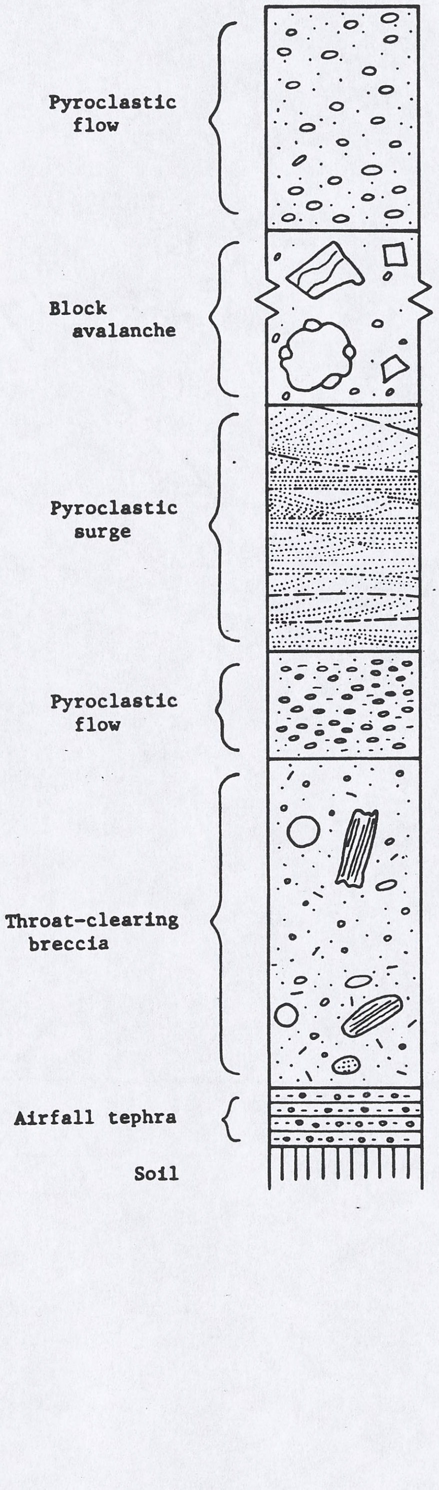

Massive, poorly sorted silty, sandy pebble gravel.

Massive, unsorted block breccia. Largest blocks several meters. Mostly angular rhyolite glassy blocks. Small % breadcrusted pumice with indentations holding adjacent pebbles. More than 10 m thick near Panum tephra ring.

Well-bedded cross- and planar-bedded silty sandy, mostly very fine and fine. Climbing crests of festooned antidunes migrate away from source.

Massive silty, sandy lapilli gravel. Mostly white lineated pumice. Forms 50 cm high dunes southwest of Panum. Abundant charcoal in lower parts of unit at greater distance from Panum.

Massive, unsorted heterogeneous breccia. Pebbles and cobbles are accidentals of lacustrine silt and rounded Sierran clasts. Loamy matrix contains juvenal pumice. More pumiceous toward top.

Well-sorted, well-bedded white lineated pumice, black obsidian and grey glass.

Figure 9

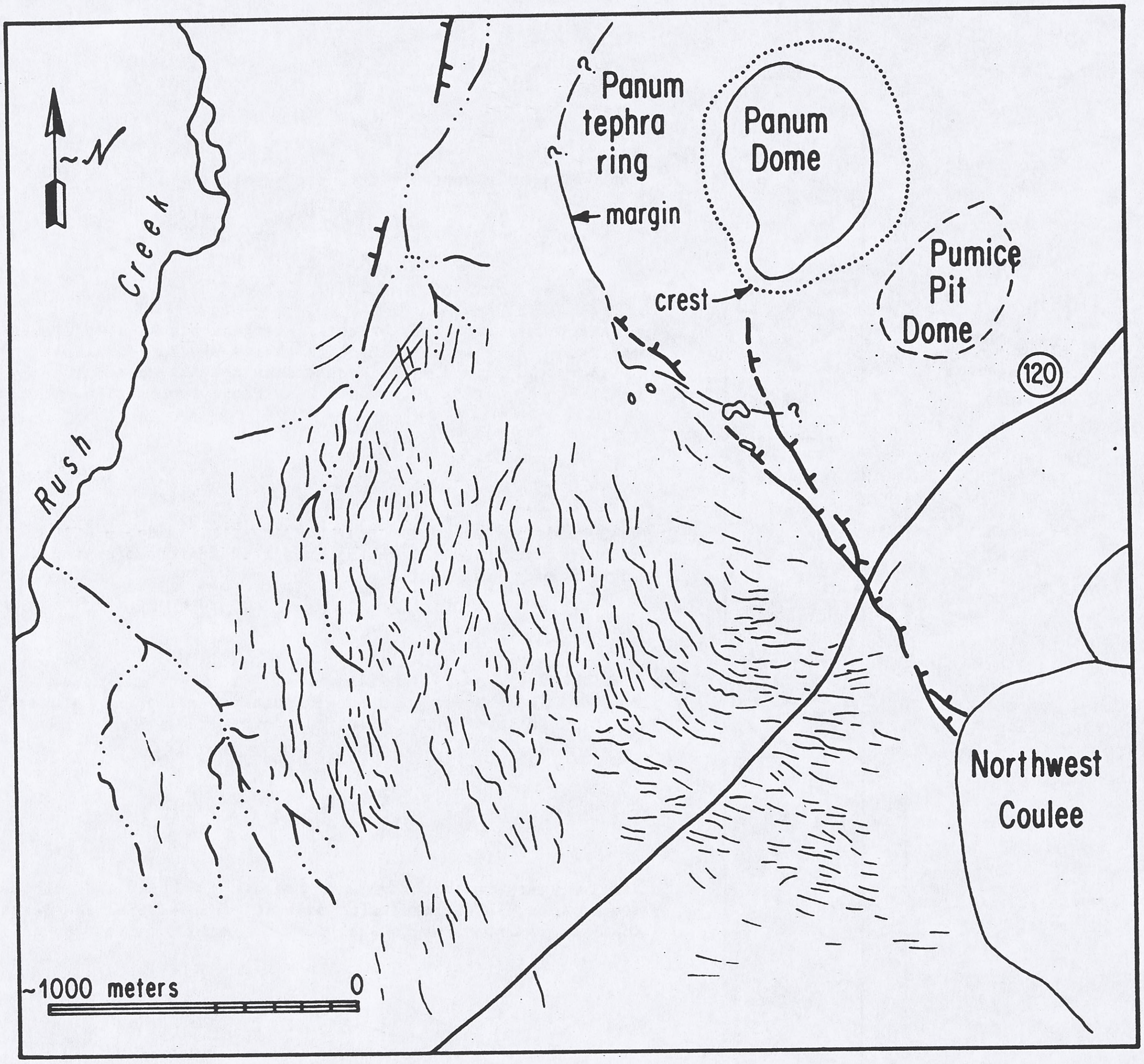
~N
Panum tephra ring
Panum Dome
margin
crest
Pumice Pit Dome
120
Rush Creek
Northwest Coulee
?
~1000 meters
0

Figure 10

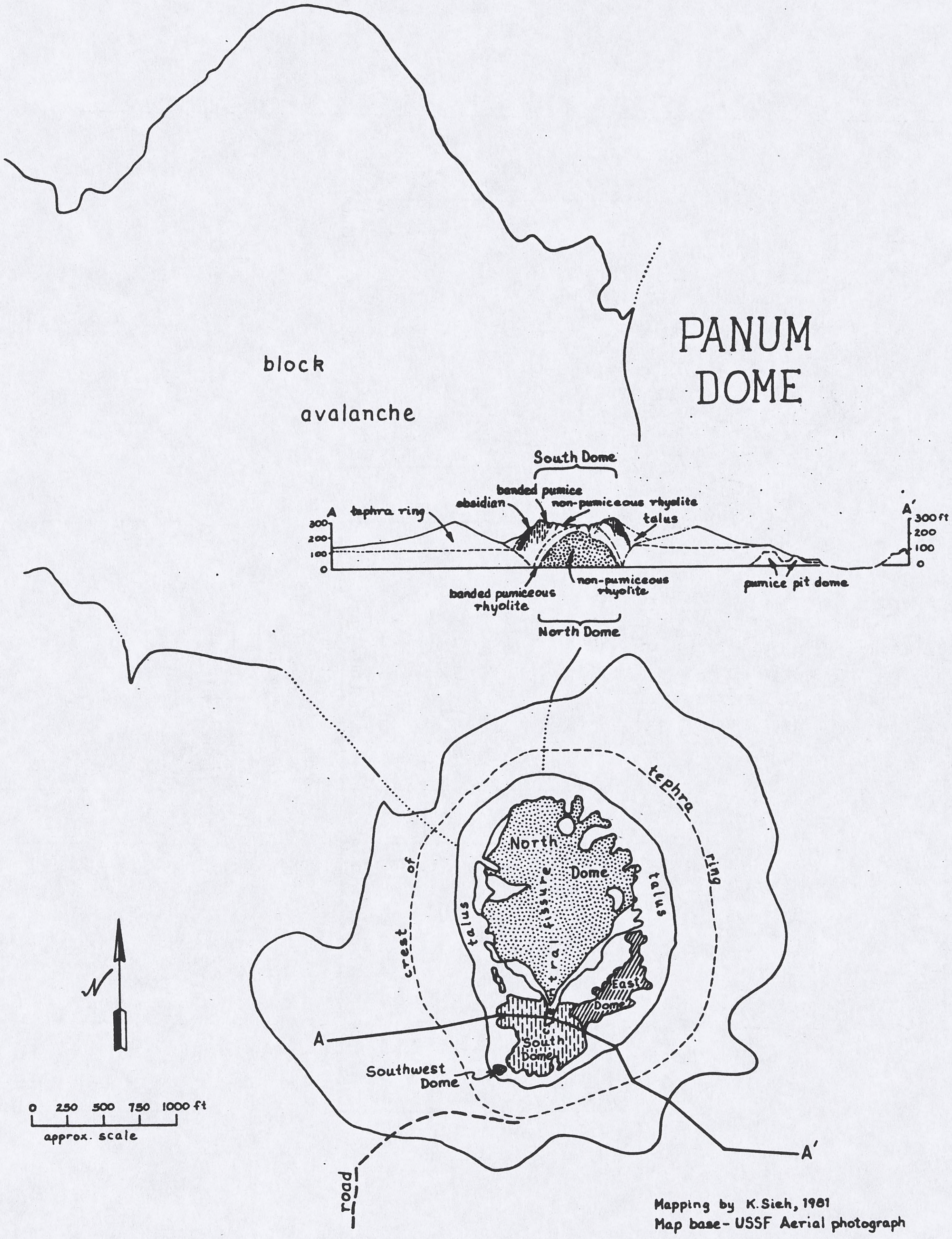

Mapping by K. Sieh, 1981
Map base - USSF Aerial photograph

Figure 11

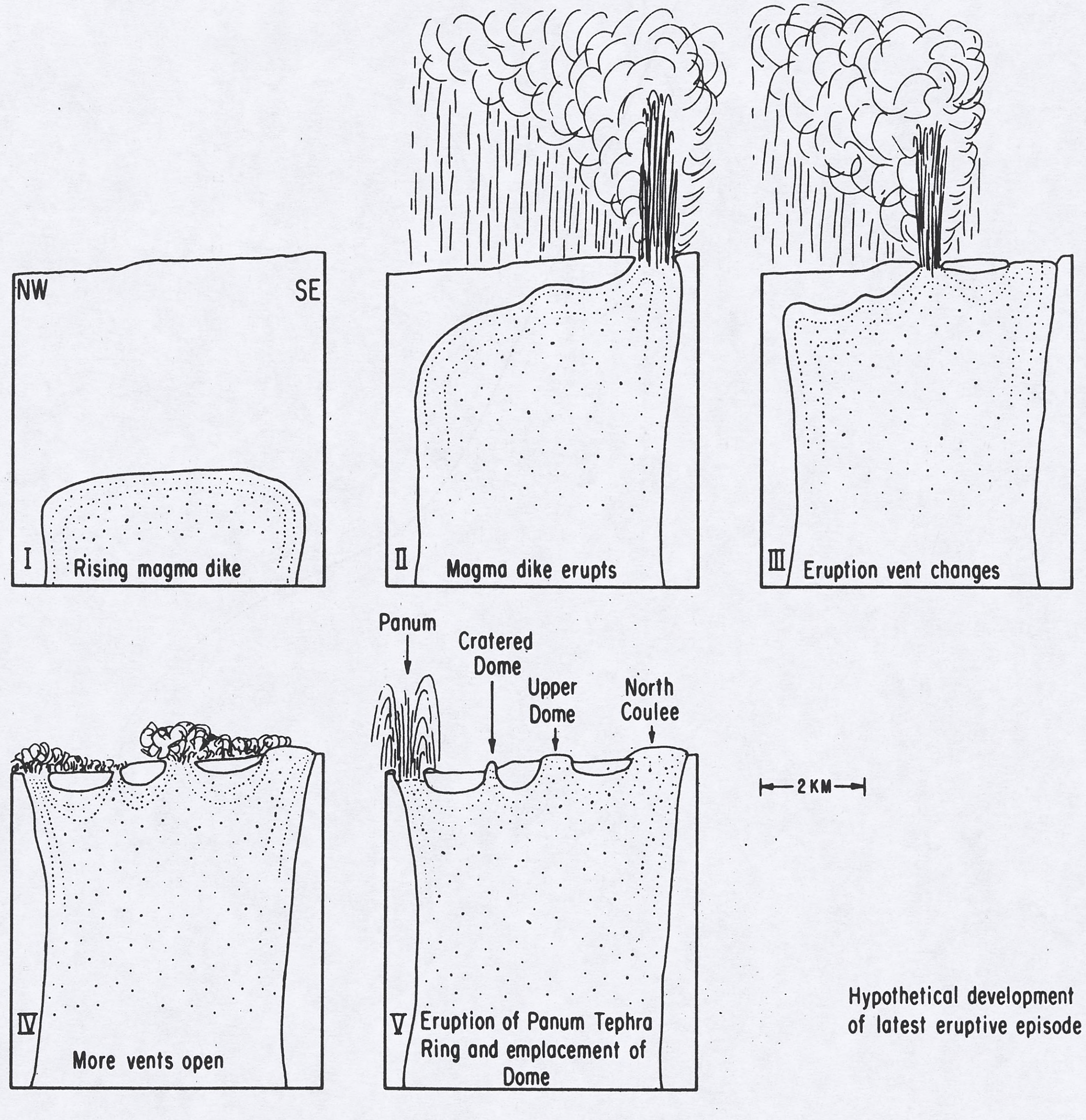

Hypothetical development of latest eruptive episode

Figure 12

Energetics of a Plinian Eruption at Mono Craters, East Central California

MARCUS I. BURSIK (Division of Geological and
Planetary Sciences, Caltech, Pasadena, CA 91125)
KERRY E. SIEH (Same)

A small plinian event initiated a volcanic eruption sequence at Mono Craters, California, approximately 600 years ago. Maximum pyroclast sizes were measured in the field. These data were extrapolated to obtain maximum pyroclast size at the source. Clast densities were measured in the laboratory. The volcanic gas was assumed to be steam at 873 K and 1 bar. Following the methods of Wilson, who utilizes the Bernoulli equation, Newton's second law, recent theoretical and experimental modelling of turbulent gravitational convection, and modern observations of plinian eruptions, we used these data to calculate the energetics.

Area of dispersal and degree of fragmentation of pyroclasts indicate this eruption was a small plinian event. Pyroclasts were expelled with velocities of 160 to 310 m/s from a 1500 m^2 vent underlying North Coulee. The resulting plinian column reached a height of 8 to 15 km. With a maximum mass eruption rate of 1.4 to 17 × 10^6 kg/s, 1.7 to 1.9 × 10^7 kg of juvenile pyroclastic debris were ejected in 2 to 30 seconds.

Comparison with published isopach maps of other events in the Mono-Inyo chain indicates that the eruptive sequence that began with this event is typical for the region. Such eruptions as Krakatau and Mount St. Helens were much larger.

Thermometry of Rhyolitic Obsidians Based on Water Speciation

DAVID A. PICKETT and EDWARD M. STOLPER (Both at: Div. Geol. Planet. Sci., Caltech, Pasadena, CA 91125)

We have studied the effects of temperature on the relative concentrations of molecular water and OH groups in three obsidians of differing total H_2O contents (0.96, 1.39, and 1.75 wt. %) from Mono Craters, CA. Glass samples were held in air at temperatures ranging from 400 to 660°C and then quenched. Concentrations of OH and H_2O in the quenched glasses were determined by near-IR spectroscopy. The ratio of molecular water to OH varies smoothly and reversibly with temperature in these samples, decreasing with increasing temperature.

Our results suggest that H_2O/OH ratios can be used for geothermometry of volcanic glasses with appreciable water contents. Most obsidian clasts from tephra deposits from recent Plinian eruptions at Mono Craters indicate temperatures of 450-600°C. Temperatures indicated for the higher water content glasses are typically at least 50°C cooler than the lower water content glasses. These could represent actual eruption temperatures or closure temperatures for the thermometer on cooling of the obsidians.

Several lines of evidence suggest that if the glasses record closure temperatures, actual eruption temperatures could not have been much higher than the closure temperatures. Our low water sample begins to vesiculate and flow at ~610°C and our high water sample does so at ~550°C. The unvesiculated and angular nature of the clasts we have studied thus suggests that eruption temperatures were not significantly higher than those recorded by the speciation of water.

If our results represent eruption temperatures, they are much cooler than expected magmatic temperatures and than temperatures recorded by other geothermometers in low water (<0.2%) dome obsidians. This could suggest cooling of the rhyolitic magma in the vent prior to eruption or thermal equilibration of the clasts with a gas cloud at 500-600°C during the eruption.

1. Fall Meeting
2. PICK209938
3. David Pickett
   170-25 Caltech
   Pasadena, CA 91125

   818-356-6238
4. V
5. none
6. O
7. 10% at 1983 AGU Spring
8. Student rate applicable
9. C

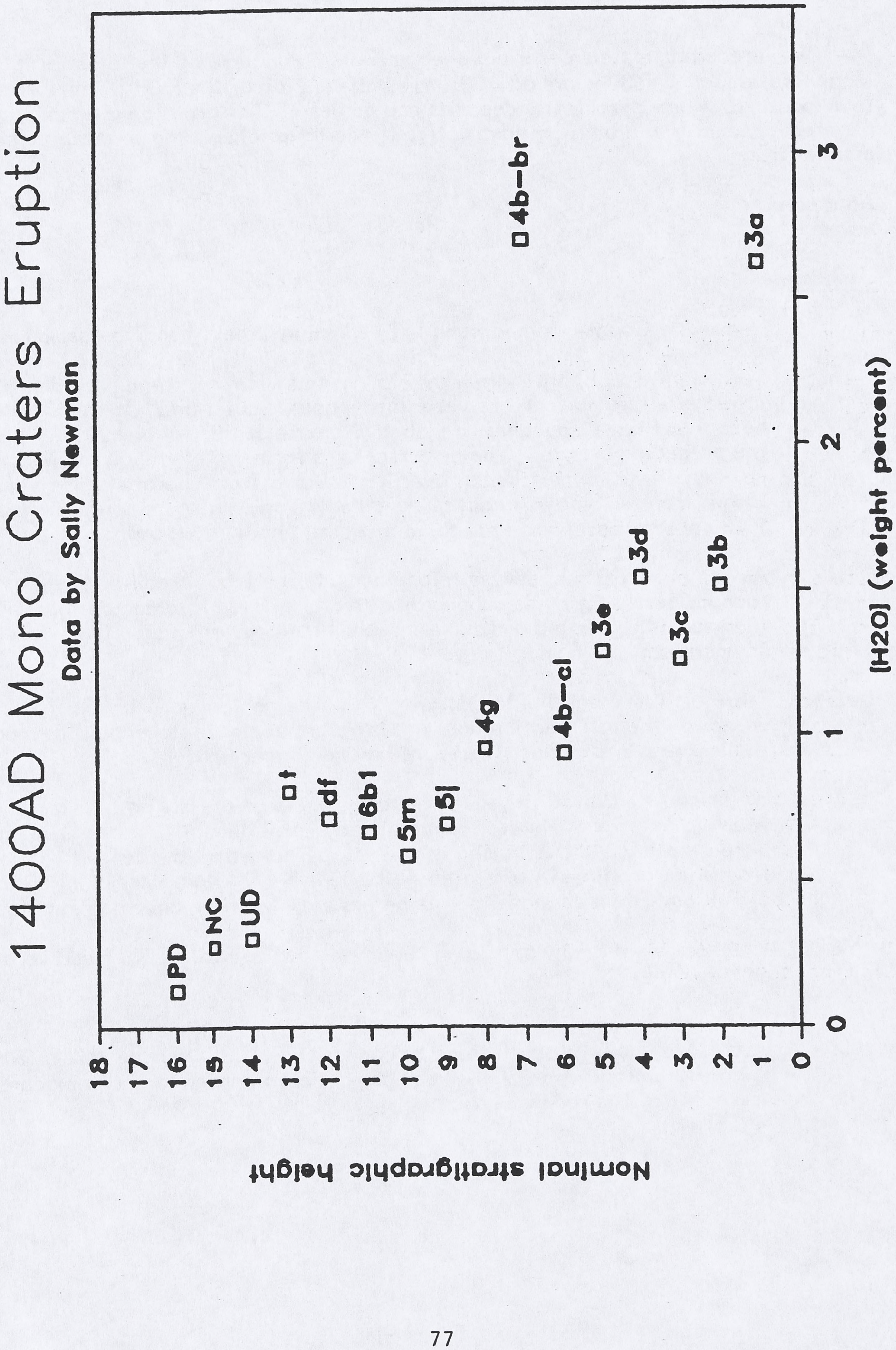
1400AD Mono Craters Eruption
Data by Sally Newman
Nominal stratigraphic height
[H2O] (weight percent)
0
1
2
3
4
5
6
7
8
9
10
11
12
13
14
15
16
17
18
0
1
2
3
PD
NC
UD
t
df
6b1
5m
5l
4g
4b-cl
4b-br
3e
3d
3c
3b
3a

ROADLOG AND DESCRIPTION OF STOPS TO VIEW PRODUCTS OF THE LATEST ERUPTION OF THE MONO CRATERS

The preceding article describes the products and nature of the latest eruption of the Mono Craters, about 600 years ago. On this half-day leg of the FOP fieldtrip, we will visit four localities where pyroclastic deposits and domes of that eruption are particularly well-exposed. The sites will be more instructive if you have taken time to read the short preceding article first.

Approximate Mileage Between Localities	
	Leave the County Campground in Lee Vining Creek, heading east on Highway 120.
2	Turn right (south) onto Highway 395. In this vicinity, the airfall deposits of the latest eruptive episode are very thin -- only about 2 cm. Of the individual airfall beds that I have isopached, only bed "2" extends this far west (See Figs. 3 and 5a in the preceding article). The dispersal axes for most of the airfall beds extend northnorthwest to northeast, over Mono Lake, from sources at the north end of the Mono Craters. As you begin to travel south on 395, these sources are about 9 kilometers distant and off to your left at about 10:30 o'clock.
2.3	As you cross Rush Creek, note on your left the fresh creek-bank exposure of well-rounded Sierran gravels capped by a thin gray bed of volcanic ash. This ash is older than the 600-year-old airfall series, the southwestern edge of which is about 2 miles downstream.
0.2	Turn left (northeast) onto Highway 120. The geologist buried on the southeast corner of the intersection does not have any of the Holocene ashes mantling his shallow grave, and must therefore have died quite recently.
2.0	We are now entering the southwestern margin of the airfall blanket from the 600-year old eruption. Thin remnants of the airfall blanket are preserved in this vicinity beneath a few hundred millimeter-thick pyroclastic flow deposit that emanated from the Panum vent, off to the left about 3-1/2 kilometers at 11:00 o'clock. The airfall beds thicken more than 2 meters between here and the next stop.
4.8	Intersection of Highway 120 and unpaved road to State Tufa Reserve. Continue east on Highway 120.
0.2	<u>Stop 1</u>. Roadcut on south side of Highway 120. Pull your vehicle as far forward on the north or south side of the road as possible in order to accommodate all vehicles safely off of the roadway.

This is site "bx" (Fig. 3), where a relatively complete section of the 600-year-old airfall beds can be viewed. Site "bx" is within 1 mile of the dispersal axis of all major beds within the airfall series. The airfall series is 2100 mm thick at this locality and rests upon a bioturbated, organic-rich surface that was developed upon an older, late Holocene pyroclastic deposit. The oldest bed (bed "1") is 200 mm thick, is composed predominately of white lineated pumice and fines upward in its uppermost few centimeters. Its source is the vent or vents at the crest of the range 1.7 to 2.0 km to the south, beneath North Coulee (Fig. 4b). We are standing about a mile west of the dispersal axis of bed 1. See pages 4 and 5 of the preceding article for additional discussion of this bed. Marcus Bursik, a graduate student at Caltech, has been using the methods of Wilson to calculate the physical nature of the eruption that produced this bed. A abstract of his findings is included on page 7.

The second bed of the 600-year-old series is about 180 mm thick and displays its characteristic obsidian-rich base here. The isopach map of bed "2" (Fig. 5a and 5b) indicates that its source was a vent now buried by Upper Dome, which is the highest, barren coulee visible on the southern horizon only 1.5 kilometers south of this roadcut.

The third bed of the airfall series is 200 mm thick in this exposure. It is labelled "bed 3" in Fig. 3 and its distribution is shown in Figs. 6a and 6b.

Bed 7 is the pebble gravel about 1 m above bed 3. It is quite distinctive -- everywhere dark in its lower half and light in its upper half, it extends northeastward from the Upper Dome vent well into Nevada. At this and other near-source sites, its lower half is unusually rich in accessory (non-juvenal) volcanic ejecta; perhaps this is because this eruption cleared out debris that had fallen into the vent produced during the eruption of beds 2 and 3.

Overlying bed 7 is a 400 mm-thick series of grey beds composed predominantly of vitreous glassy ash and lapilli. These beds are less extensive than the more pumiceous underlying airfall beds and represent the last major airfall deposits of the 600-year-old eruption. They too exited vents now buried beneath North Coulee and Upper Dome.

Overlying the well-sorted, well-bedded pyroclastic fall beds at site "bx" is a 600-mm-thick massive, poorly sorted bed. This is one of several pyroclastic flow deposits that were emplaced on the northeastern and western flanks of the North Coulee and Upper Dome vents (see page 3). Our next stop we will inspect one of these pyroclastic flows.

Leave Stop 1, heading west on Highway 120.

2.5 Turn left (south) onto unpaved road that runs along the western edge of the Mono Craters.

1.2 You are now driving on a pyroclastic flow deposit erupted from a vent now buried beneath North Coulee, most of which is hidden behind the 400-meter-high gray slope off to your left at about 9:30 o'clock, 2-1/2 kilometers distant. The flow (labelled "A" on Fig. 7) was emplaced prior to construction of the gray edifice, which is a late-stage construct similar to the Panum tephra ring.

Continue south along the unpaved road until you can bear left at a Y-intersection. Ridges parallel to the direction of flowage are quite apparent on the surface of this portion of the pyroclastic flow.

At the next Y-intersection bear to the right and continue to drive across the hummocky surface of the flow. Park off the road in the large grove of Jeffrey pines, a 100 meters or so beyond the area of recently burnt chapparal.

Stop 2. These Jeffrey pines are just beyond the southern margin of the pyroclastic flow. A range fire this summer conveniently removed the dense chaparral, exposing a sharp 1 meter-high edge of the flow. We will spend a few minutes exploring the flow margin in the burned-off area. Incidentally, the north-sloping plain upon which the flow was deposited is underlain by tephra that was ejected in about 700 A.D. from vents about 3 kilometers to the southeast, near South Coulee, the blocky, nearly barren coulee visible through the trees.

Depart Stop 2 along the same three unpaved roads you came in on. Upon reaching Highway 120, turn west onto the pavement.

0.3 Turn right (north) onto unpaved road leading toward Panum Dome.

0.2 As you begin to traverse the road toward Panum, you are passing over 1/2 to 1-1/2 meters of pyroclastic debris from the 600-year-old eruption. The airfall deposits are only about 100 mm thick here. They are overlain by charcoal-rich pyroclastic flow deposits that emanated from a vent now beneath Panum Dome. One of these beds was deposited as a series of concentric dunes (see Figures 7 and 10 and text on page 4). These 1/2-to 1-m-high dunes are readily apparent in this vicinity, and can be mapped up to 3 kilometers from Panum.

1.0 Stop 3. Panum Dome and Tephra Ring. Park in the designated parking area at the base of the Panum tephra ring and proceed on foot along the trail leading to the southern rim of the tephra ring. See page 5 and Fig. 11 for a brief discussion of Panum Dome and its associated tephra ring. We will clamber around on the dome in order to view the various structures and rock textures that constitute the dome.

Upon leaving the parking area on the south side of the Panum tephra ring, follow the unpaved road that leads north skirting the western fringe of the tephra ring.

1.0 Stop 4. Block avalanche deposit. Park single file on the unpaved road. The gully immediately west of the road exposes the upper 7 meters of a bouldery breccia that Wood (1977) first termed a "block avalanche". At other localities, this breccia can be seen to overlay the 600-year-old pyroclastic fall beds and the initial deposits associated with the opening of the Panum vent (See Fig. 9). This blocky breccia is described briefly on page 5. Continue northwest on unpaved road.

0.3 Turn right onto another unpaved road.

0.5 Turn left onto another unpaved road that crosses Rush Creek. Note the chaotic outcrops of the block breccia in the banks of Rush Creek. Here the breccia is overlain by young lake deposits. Continue westward along this well-maintained unpaved road.

2.0 Turn left and uphill at intersection near ranch buildings. You are now driving up onto the Pleistocene delta of Lee Vining Creek.

1.3 Turn left (south) onto Highway 395, heading for the Inyo Craters, which will be described by Dan Miller.

OBSIDIAN HYDRATION-RIND DATING OF THE MONO CRATERS

Spencer H. Wood, Department of Geology and Geophysics, Boise State University, Boise, Idaho 83725.

The Mono Craters are a 17-km-long, north-south-trending, arcuate chain of rhyolite domes, flows, and tephra deposits. The rhyolites are remarkably uniform in chemical composition (Carmichael, 1967) except for an older rhyodacite dome on the northwest side (Lajoie, 1968). The chain is made up of several mappable petrographic variations (Fig. 1). The older lavas are porphyritic with sanidine, whereas the the youngest lavas are entirely aphyric rhyolite.

A variety of geochronologic methods have been applied to obtain dates on the Mono Crater eruptions. The most consistant ages have been radiocarbon dates on materials associated with the tephra. Ages on the various tephra layers range from 30,000 yrs to 640 yrs BP (Lajoie, 1968; Wood, 1977a, 1977b; Wood and Brooks, 1979; and Sieh and others, 1983). Direct dating of the domes by the obsidian hydration-rind method was first done by Friedman (1968) by methods developed by Friedman and Smith (1960). Friedman obtained late Holocene ages on several of the domes.

This study extends Friedman's (1968) work to the entire volcanic chain. Obsidian samples were systematically collected from every dome or flow. Because the hydration rate of obsidian is a strong function of temperature, care was taken to collect from north-facing, shaded outcrops. Direct sun exposure has been shown to significantly increase the hydration-rind thickness (Wood and Brooks, 1979). Thin sections were cut from several samples from each dome, and the hydration rind thicknesses were measured along suitably oriented micro-cracks in the obsidian (Fig. 2) using a standard petrographic microscope equiped with a filar micrometer eyepiece. Results are reported as histograms showing the scatter of measurements for any one dome or flow (Fig. 3). Conversion of hydration-rind thickness to an age uses the equation for the inward movement of hydration front derived by Friedman and Smith (1960) from diffusion theory and from experimental results.

$x^2 = k\,t$

x = hydration-rind thickness in micrometers after time t.

k = rate constant for the hydration reaction in units of micrometers^2/1000 yrs.

t = time in years.

The value of k varies with temperature of the microenvironment, and with the composition of the glass (Friedman and Long, 1976). In normal weathering environments, the value of k has been shown to be independent of humidity, because diffusion of water into the glass is the rate limiting process (Friedman and Long, 1976). It is thought that the ambient humidity of air always provides sufficient moisture even in dry climates such that diffusion rates are not affected, although this assumption is currently being checked by field experiments (Friedman, personal communication, 1984). Various considerations related to the age calculation have been most recently discussed by Friedman and Obradovich (1981). Comparison of hydration rind thickness with radiocarbon dates in this study suggests that young samples have either an initial hydration rind imposed during cooling of the lava or that young samples undergo a higher rate of hydration than older samples. A value of 12 micrometers^2/1000 yrs is obtained for the 640-yr-B.P. Panum Crater dome, whereas

the older domes can be reconciled with the radiocarbon chronology using the rate of 5 micrometers ^{2}/1000 years originally assumed by Friedman (1968). Problems with the discrepancies in hydration rates of the younger samples have not been resolved. Despite problems in deriving an absolute age, the relative ages of older samples (greater than 2000 yrs) appear to be correctly displayed if they are expressed in terms of the square of the hydration-rind thickness.

The relative ages of the domes and flows of the Mono Crater chain are plotted against cumulative volume of erupted rhyolite lava and estimated tephra volume in Figure 4. The radiocarbon chronology derived from stratigraphic occurrences of tephra reported by Lajoie (1968) and Wood (1977b) is summarized in Figure 5. Both chronologies show a major change in the nature of the eruptions about 3000 years ago. The erupted lavas changed over a period of less than 1000 years from porphyritic glassy rhyolite to aphyric glassy rhyolite. Samples analyzed by Carmichael (1967) show that this change in petrography is also reflected in the temperatures derived from Fe-Ti oxides. The porphyritic samples yeild a temperature of 800°C, and aphyric lavas are 910°C. The cumulative volume plot (Fig. 4) shows a dramatic increase in the average volumetric rate of eruption from the system accompanied the change in the lava character. The rate changes from about 0.2 km^3 /1000 yrs to 0.8 km^3 /1000 yrs, and individual eruptive events become more volumnous by reason of the decreased viscosity of the hotter, crystal-free magma. The latest eruptive episode (about 640 years B.P.) may have had a volume of about 0.1 km^3 of magma (calculated at a density of 2.2 g/cm^3), but considerable uncertainty exists until the distant tephra is surveyed.

REFERENCES CITED

Carmichael, I.S., 1967: The iron-titanium oxides of salic volcanic rocks and their associated ferromagnesian silicates: Contributions to Mineralogy and Petrology, v. 14, p. 31-64.

Denham, C.R., and Cox, A., 1971, Evidence that the Laschamp Polarity did not occur 13,300-30,400 years ago: Earth and Planetary Science Letters, v. 13, p. 181-190.

Friedman, I., and Smith, R.L., 1960, A new dating method using obsidian: Part 1, The development of the method: American Antiquity, 25, p. 476-537.

Friedman, I., 1968, Hydration rind dates lava flows: Science, v. 191,p.347-352.

Friedman, I., and Long, W., 1976, Hydration rate of obsidian: Science, v. 191, p. 347-352.

Friedman, I., and Obradovich, J., 1981, Obsidian hydration dating of volcanic events: Quaternary Research, v. 16, p. 37-47..

Lajoie, K. R., 1968, Late Quaternary stratigraphy and geologic history of Mono Basin, eastern California (PhD dissertation): Berkeley, University of California, 271 p.

Sieh, K., Wood, S. H., and Stine, S., 1983, Most recent eruption of the Mono Craters, eastern California (abs.) EOS, v. 64, p. 889.

Wood, S. H. , 1977a, Distribution, correlation, and radiocarbon dating of late Holocene tephra, Mono and Inyo craters, eastern California: Geological Society of America Bulletin, v. 88, p. 89 - 95.

Wood, S.H. , 1977b, Chronology of late Pleistocene and Holocene volcanics, Long Valley and Mono Basin geothermal areas, eastern California. Final technical report U.S. Geological Survey Geothermal Research Program Contract no.14-08-0001-15166, 55 p.

Wood, S. H., and Brooks, R., 1979, Panum Crater dated 640 + 40 radiocarbon years B.P., Mono Craters, California: Geological Society of America abstracts with Programs, v. 11, no.7, p. 543.

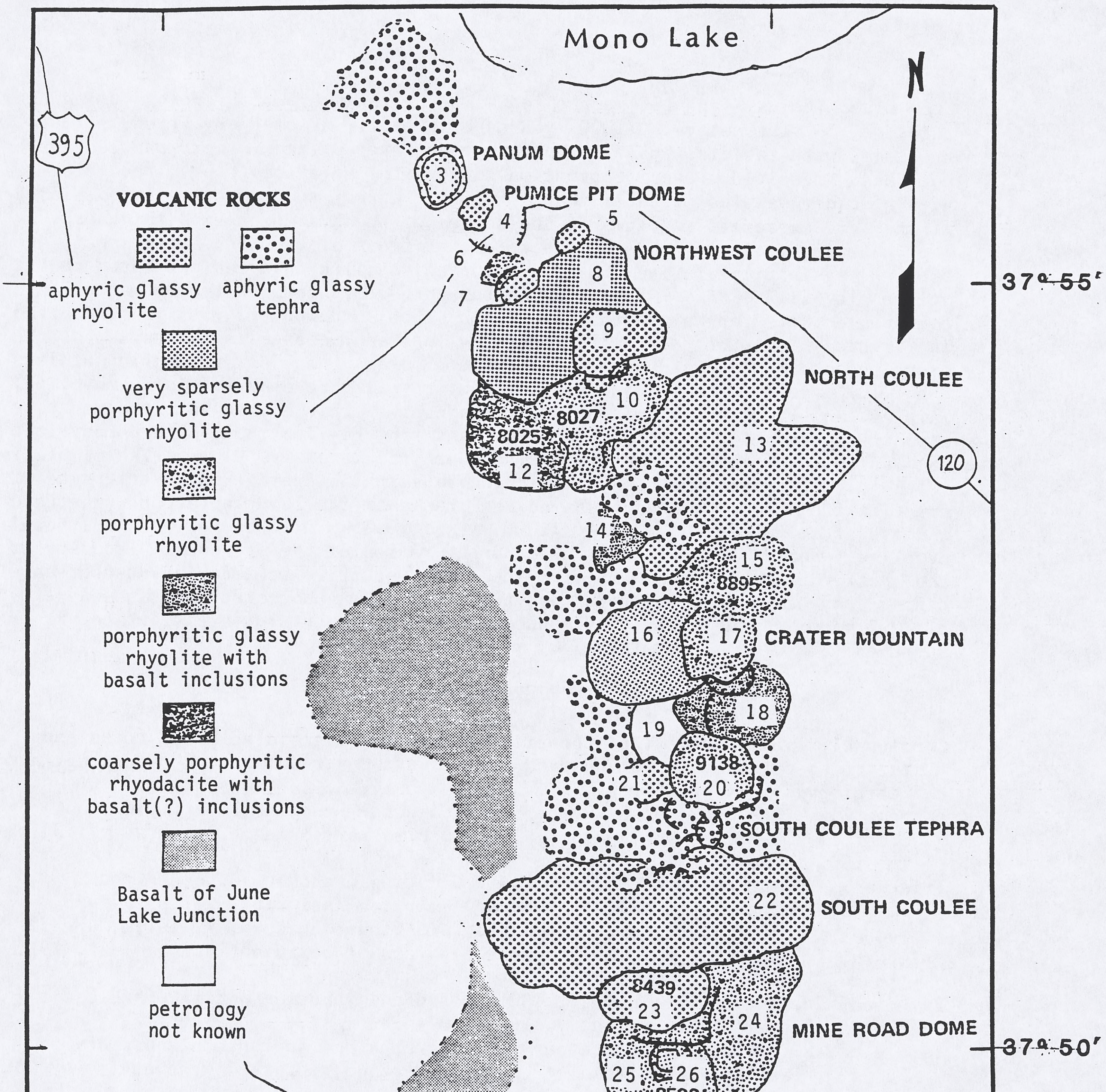

Fig. 1. Geologic map of the Mono Craters showing petrographic variations of the domes and flows. Numbers refer to histograms of hydration-rind measurements of Figure 3.

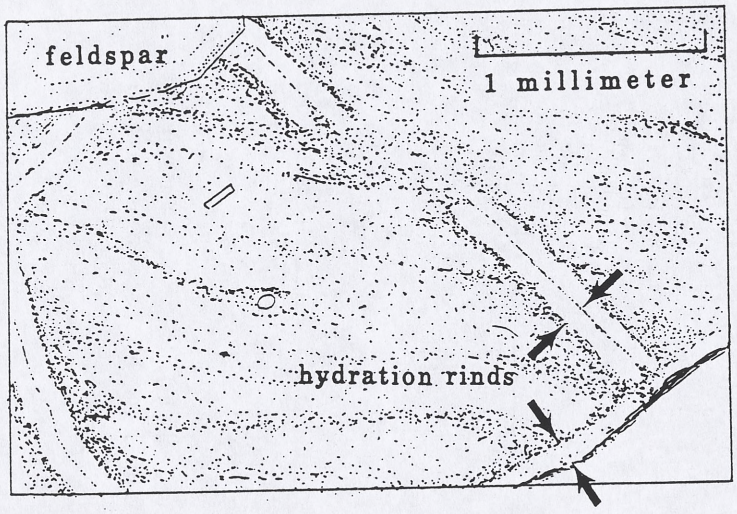

Fig. 2. Drawing of an obsidian thin section from dome no. 6, the oldest dome determined in this study. Hydration-rind thickness is measured from the microcrack to the edge of the birefringent rind. Lower left edge of the section is an exterior surface of the obsidian sample showing the same hydration rind thickness as the microcracks. Internal cracks give more consistant results because they are not chipped during lapping, and they are more abundant in a thin section than exterior surfaces.

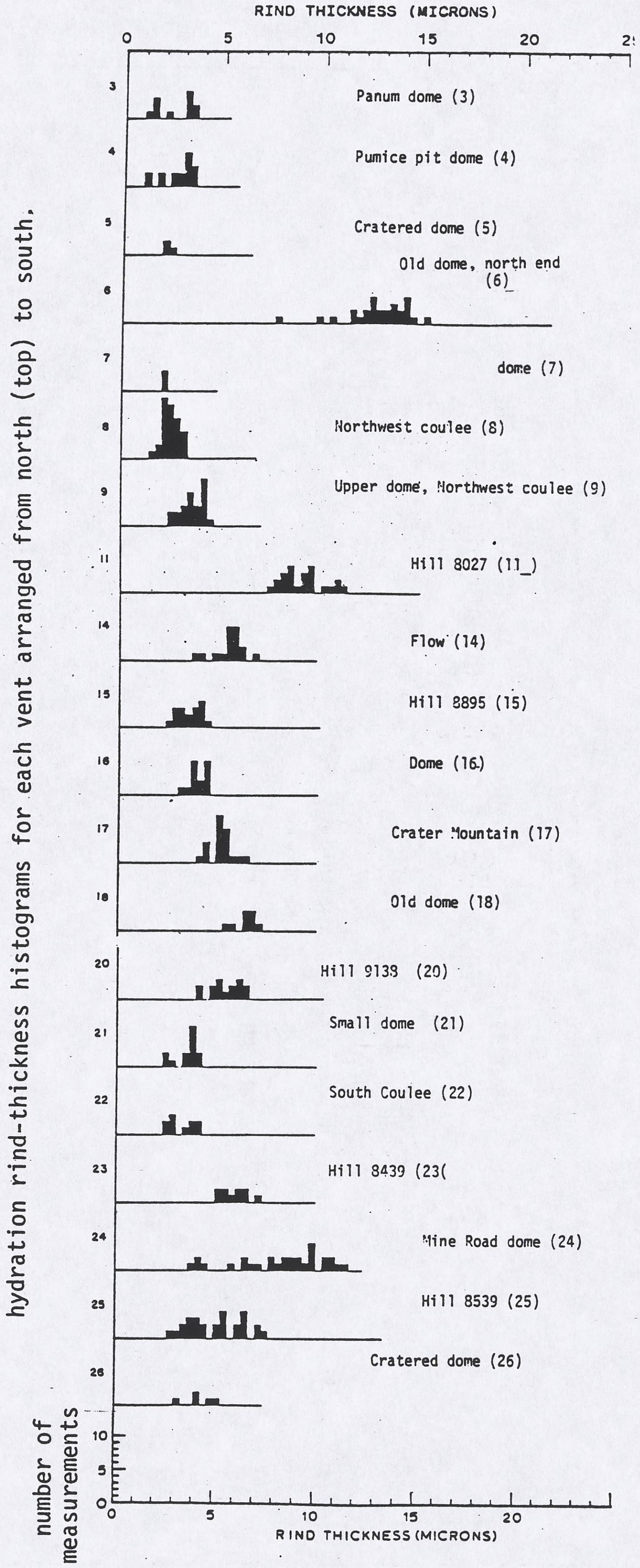

Fig. 3. Histograms of obsidian hydration rind measurements on each dome or flow. Numbers refer to location on Figure 1.

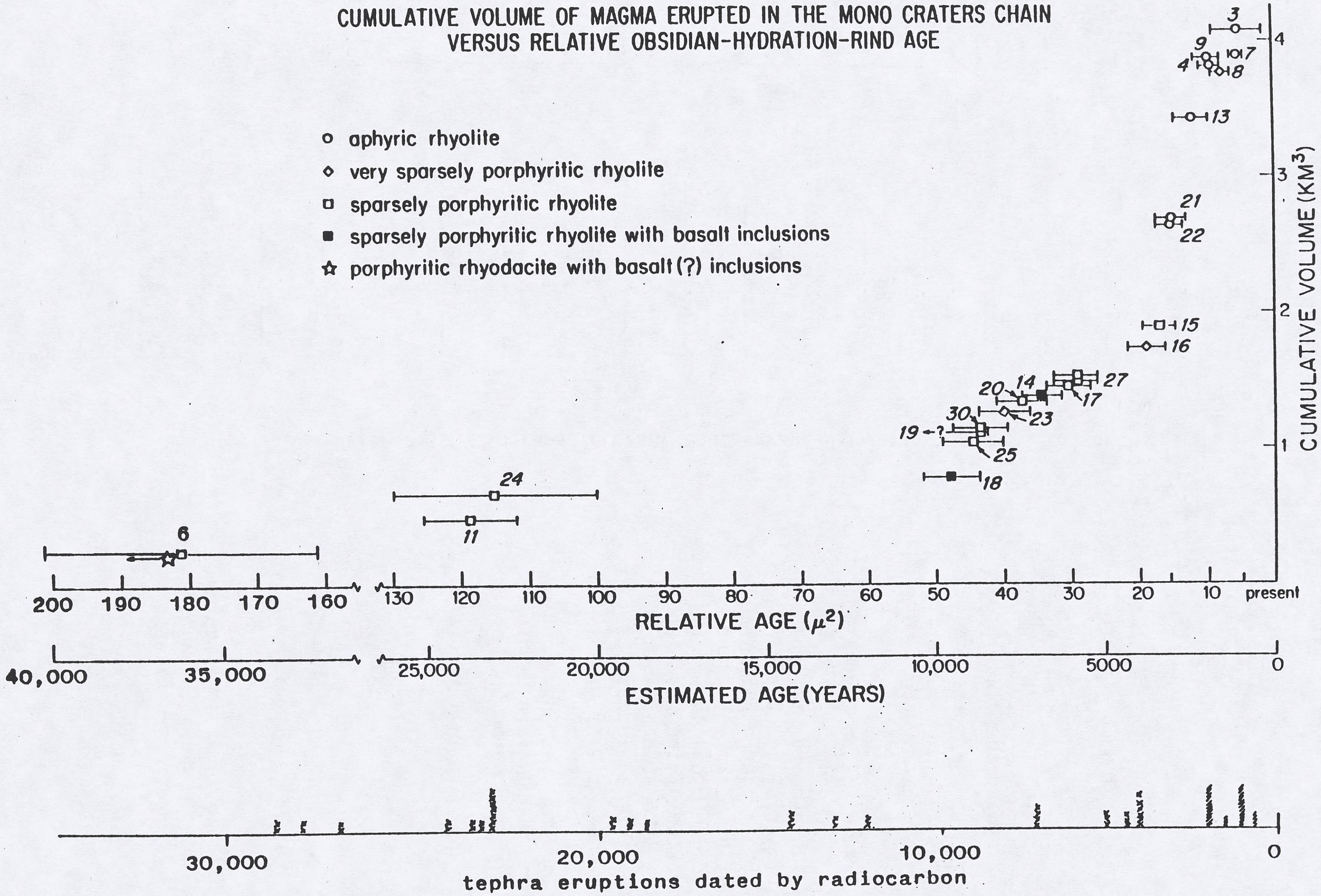

Fig. 4. Plot of age estimated from hydration rinds vs. cumulative volume of the Mono domes and craters. Volumes include only lavas and local tephra and should be adjusted as better knowledge is obtained of the tephra distribution. Volumes of local tephra are recalculated to a magma density of 2.2 g/cm^3. Average rates of magma eruption are derived from the slopes of a curve drawn through the points. Numbers on points refer to the dome numbering system of Figures 1 and 3.

Fig. 5 A summary of radiocarbon dating of Mono tephra as of 1977. Each square represents a radiocarbon date in a section containing tephra. Dates are summarized in Wood (1977b). The dates on the older porphyritic rhyolites are from ostracod tests sampled and dated by Lajoie (1968) and reported in Denham and Cox (1971). The critical dates for the change from porphyritic lavas to aphyric lavas are radiocarbon age determinations W-3471 (3300 ± 200 yrs B.P.) and W-3472 (1990 ± 200 yrs B.P.) on interbedded organic soils, logs, and tephra at Sawmill Meadow on Glass Mountain, about 30 km east-southeast of the Mono Craters. These latter two radiocarbon determinations were done at the U.S. Geological Survey laboratory by Meyer Rubin.

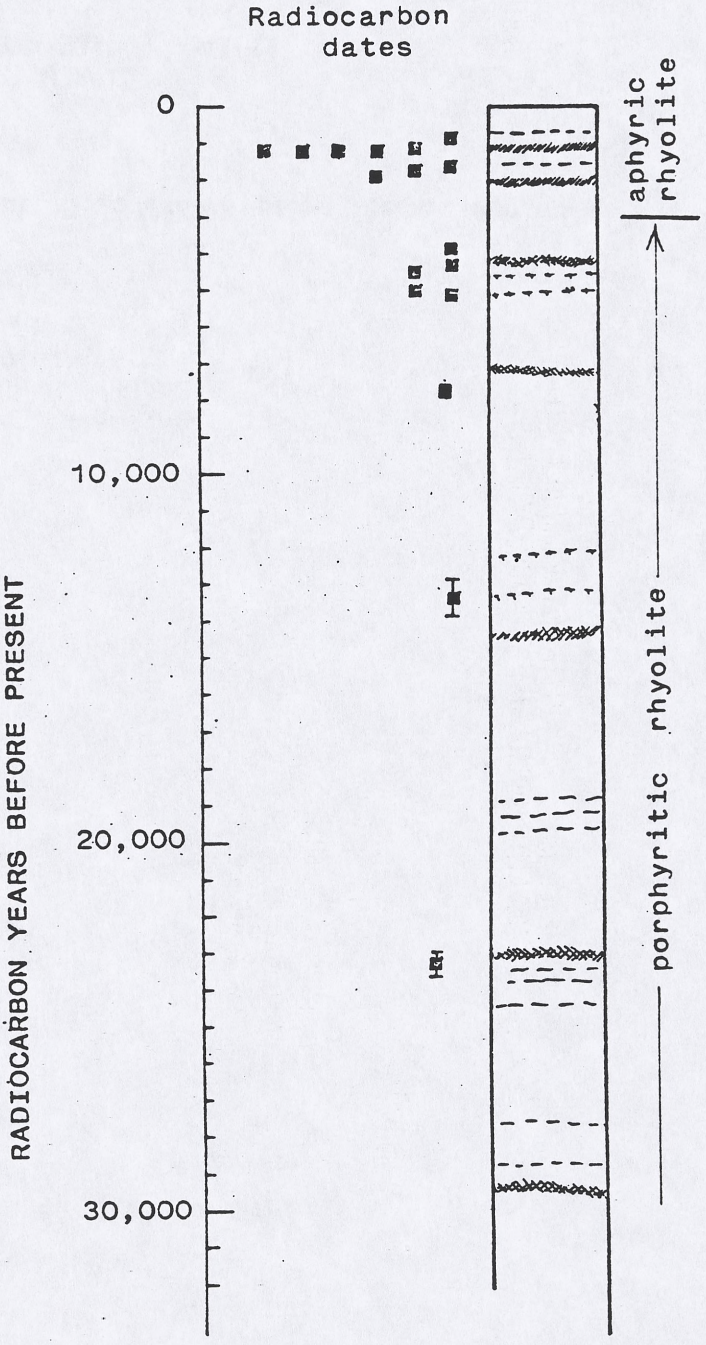

FRIENDS OF THE PLEISTOCENE FIELD TRIP
OCTOBER 12 - 14, 1984

Chronology and stratigraphy of recent eruptions at the Inyo volcanic chain

by

C. Dan Miller
U.S. Geological Survey
MS 903, Denver Federal Center
Denver, Colorado 80225

(Miller) Stop 1 Deadman Summit along Highway 395

Section of airfall tephras from Obsidian Flow vent, Tephra 2 of Wood, and older pyroclastic-flow deposit exposed in roadcut on the northeast side of Highway 395.

This 2.2-m-high roadcut is about 1.5 km northeast of the Obsidian Flow vent and exposes a series of airfall and pyroclastic-flow deposits erupted from at least three separate vents during about the last 1,200 yrs (fig. 1). At the base of the section is a lapilli and ash pyroclastic flow more than 25 cm thick whose base is not exposed. The deposit has a flat top, contains small pieces of charcoal, and shows no evidence of soil oxidation or erosion at its upper surface. The source vent for this unit is unknown at present, but one candidate is nearby Wilson Butte, about 2 km to the northwest. The age of the pyroclastic flow is unknown, but probably is close to 1,200 yrs B.P., based on lack of weathering and erosion between it and the overlying well-dated ash layer.

The pyroclastic-flow deposit is overlain by a 3-cm-thick silt-sized rhyolitic ash-fall deposit. This unit is the 1,190 B.P.-yr-old Tephra 2 of Wood (Wood, 1977). Tephra 2 erupted from the north end of the Mono chain and is a widespread marker bed in the Mono-Inyo region.

Tephra 2 is overlain by about 1.7 m of lapilli-fall beds erupted from the Obsidian Flow vent. This stratigraphic section is located on the axis of a lobe of tephra that can be traced more than 25 km to the northeast from the Obsidian Flow vent, covers an area of more than 140 km^2, and represents a magma volume of 0.02 km^3 (fig. 2). Individual tephra layers vary in thickness from a few centimeters to about 25 cm and consist of varying mixtures of juvenile pumice, lithics, and obsidian, and occasional accidental fragments.

No radiocarbon dates have been obtained on the upper series of fragmental deposits, but they overlie a tephra deposit from the South Deadman vent (Stop 2) that erupted about 600 yrs ago, and Jeffrey Pines growing on these deposits have as many as 525 rings; the age of the deposits is thus bracketed between about 600 and 525 yrs B.P.

The Obsidian Flow tephra lobe was deposited during early explosive eruptions at the source vent; later eruptions produced near-vent ballistic and pyroclastic-surge deposits. Activities at the Obsidian Flow vent culminated with emplacement of the Obsidian Flow rhyolite flow which has a volume of about 0.17 km^3. The Obsidian Flow is visible through the trees to the southwest of Stop 1.

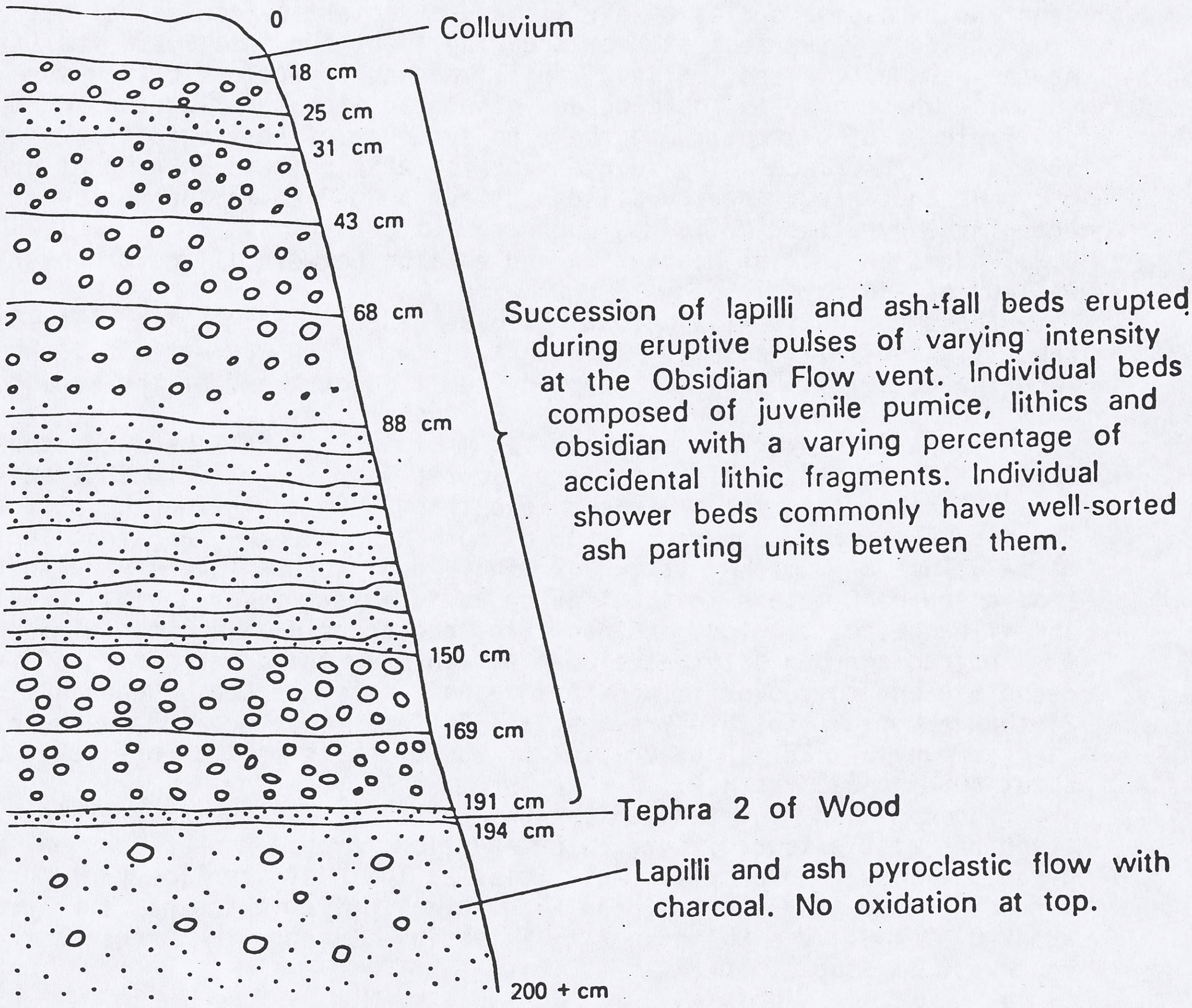

FIGURE 1.--Sketch of stratigraphic section exposed at Deadman Summit on northeast side of Highway 395. The section is about 2.2 m thick and exposes fragmental deposits erupted from three separate vents during about the last 1,200 yrs. At the base of the section is a single poorly sorted lapilli and ash pyroclastic-flow deposit. It is overlain by about 3 cm of air-fall tephra identified as Tephra 2 of Wood (Wood, 1977), dated at 1,190±80. The upper 1.7 m in the section is a series of lapilli-fall tephra beds erupted at the Obsidian Flow vent about 1.5 km to the southwest.

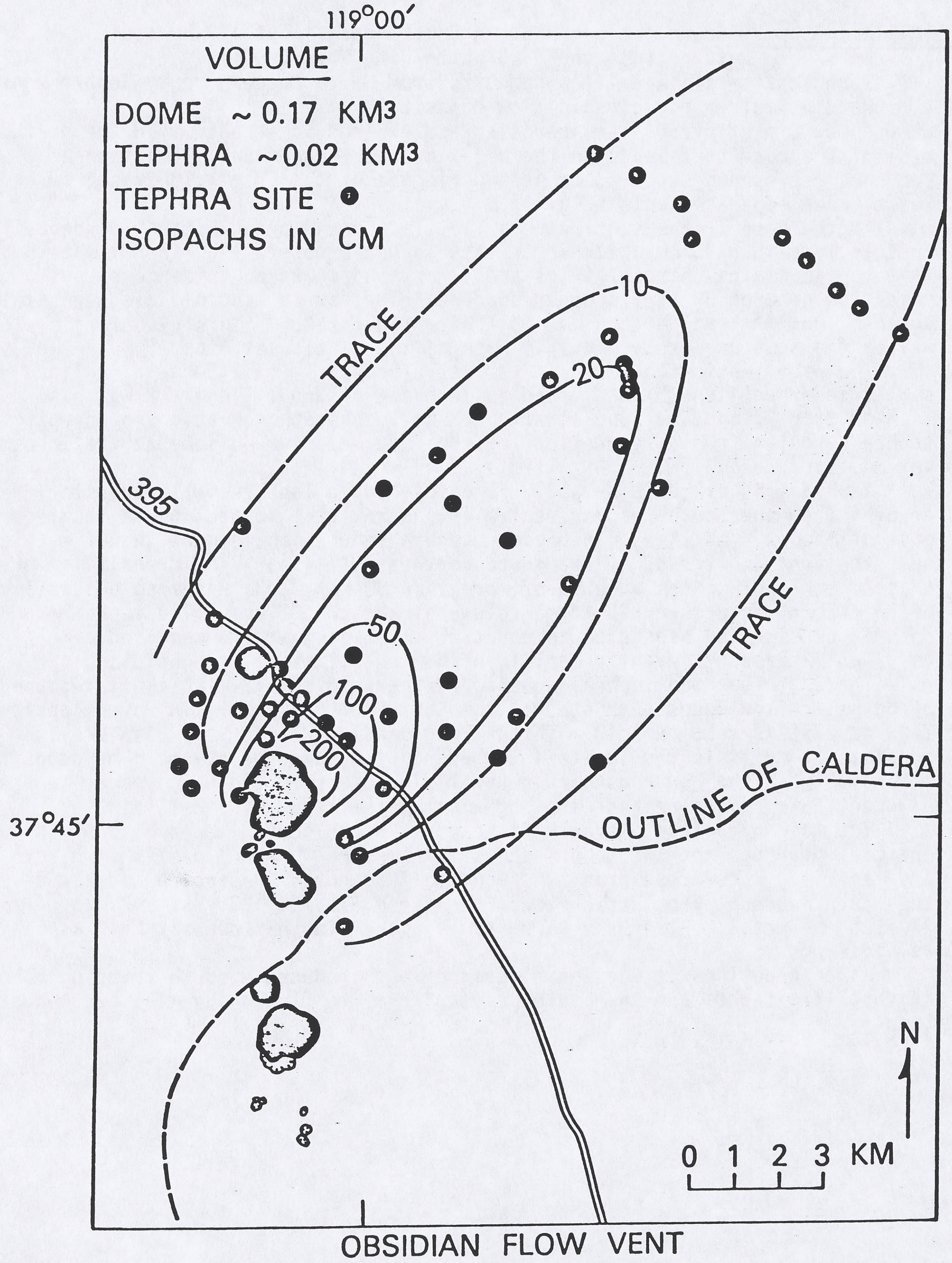

FIGURE 2.--Distribution and thickness of tephra from magmatic eruption at Obsidian Flow vent 650-550 yrs ago. Location of Stop 1 is along Highway 395 on the axis of the tephra lobe.

(Miller) Stop 2 Roadcut along Deadman Creek Road, about 1/2 km south of turnoff to the USFS White Wing Work Center

Pyroclastic-fall and -flow deposits from South Deadman vent, Tephra 2 of Wood and older pyroclastic-flow deposit.

About 3 m of pyroclastic deposits are exposed in a roadcut on the north side of the road that leads to the Deadman Creek campground. The tephra sequence represents deposits erupted during about the last 1,700 yrs from at least three separate vents (fig. 3).

At the base of the section is a lapilli and ash pyroclastic-flow deposit that is more than 25 cm thick whose base is not exposed. The deposit has a flat top, contains charcoal twigs and limbs, and shows no evidence of soil oxidation or erosion at its upper surface. The source vent of this deposit is unknown, but its radiocarbon age is 1660 ± 140 yrs B.P. This pyroclastic flow may be the same one exposed at the base of the section at Stop 1.

The pyroclastic-flow deposit is overlain by a 1- to 1.5-cm-thick fine silt-sized rhyolite ash identified as Tephra 2 of Wood. Tephra 2 was also seen at Stop 1, and is found stratigraphically beneath magmatic and phreatic tephra deposits from all eruptions of the last eruptive episode at the Inyo volcanoes.

Tephra 2 is overlain by about 55 cm of bedded lapilli-fall deposits erupted from the South Deadman vent. This stratigraphic section is located east of the axis of the South Deadman tephra lobe which is more than 2 m thick near the vent and trends to the north northeast (fig.4). The deposit is more than 20 km long, covers an area of more than 80 km^2, and, assuming a porosity of 35 percent, represents a magma volume of about 0.01 km^3. The tephra deposit consists of beds 3 cm to about 25 cm thick that are composed of varying mixtures of juvenile lapilli of pumice, lithics, and obsidian.

The South Deadman tephra sequence is overlain by a 2-m-thick flat-topped pyroclastic-flow deposit erupted at the South Deadman vent. The pyroclastic-flow deposit is more than 10 m thick along Deadman Creek (Stop 3) where it consists of multiple flow units interbedded with surge deposits. The deposits extend 6 km to the northeast and several kilometers to the west, cover an area of about 15 km^2, and represent a magma volume of about 0.05 km^3 (fig. 4).

The main pyroclastic-flow unit is pink in the center where it contains charcoal branches and twigs, and shows faint normal grading of lithic blocks and lapilli and reversed grading of pumice fragments. Radiocarbon dates on the South Deadman pyroclastic flows range from 510±100 ^{14}C yrs. B.P. to 770±120 ^{14}C yrs B.P. Jeffrey Pine stumps rooted in this deposit have as many as 615 rings.

Later eruptions at the South deadman vent produced a south-trending lobe of rhyolitic tephra and the South Deadman rhyolite flow which will be seen at Stop 3.

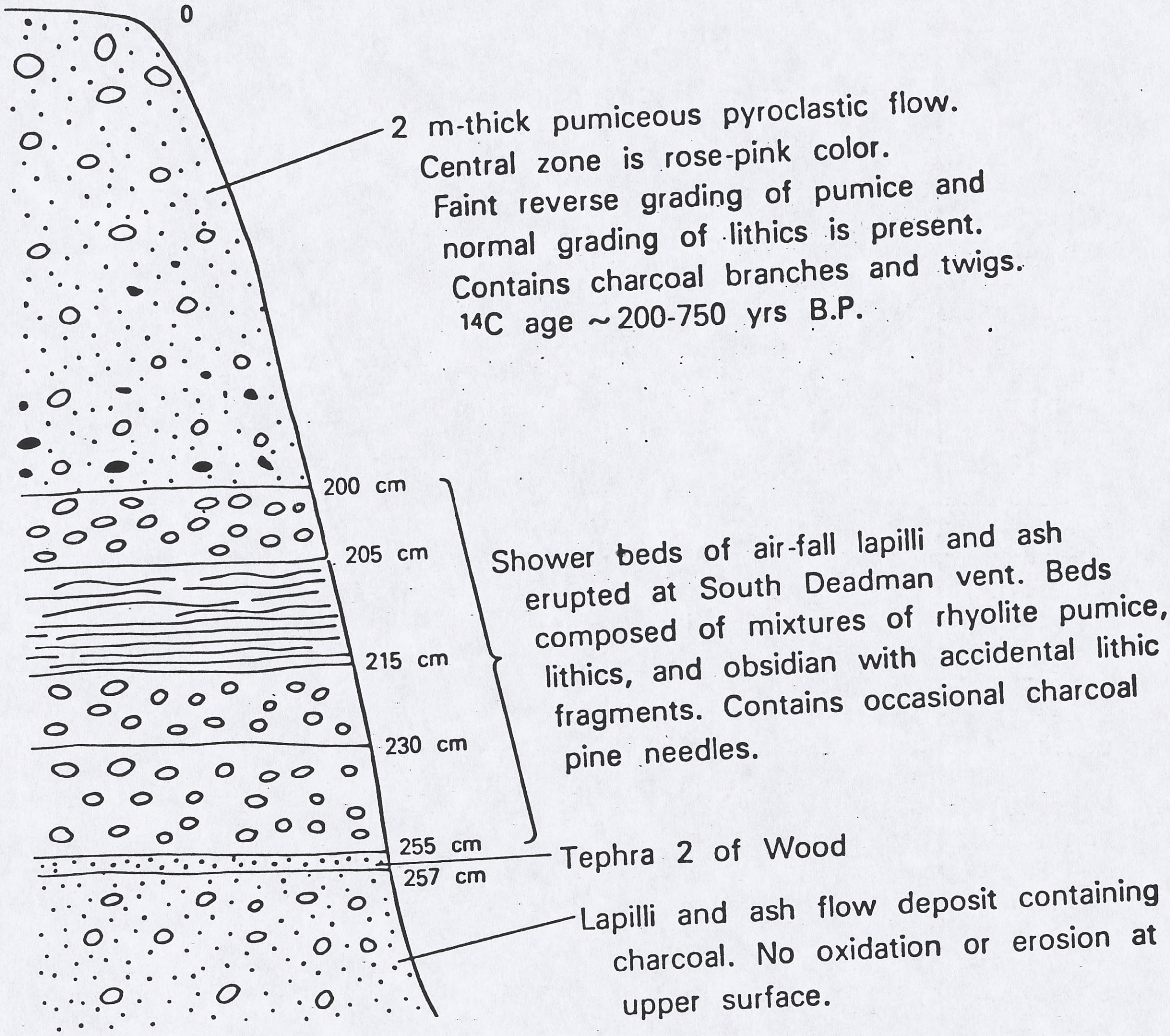

FIGURE 3.--Sketch of stratigraphic section exposed along Deadman Creek Road about 1/2 km south of turnoff to U.S. Forest Service White Wing Work Center. The section is about 3 m thick and contains fragmental deposits erupted at three separate vents during about the last 1,700 yrs. At the base of the section is a lapilli and ash pyroclastic-flow deposit. It is overlain by the 1,190±80-yr-old Tephra 2 of Wood. Above Tephra 2 is about 55 cm of bedded lapilli-fall deposits erupted at the South Deadman vent. Overlying the lapilli fall deposits is a 2-m-thick block, lapilli, and ash flow erupted at the South Deadman vent. The flow thickens and becomes coarser toward the vent (Stop 3).

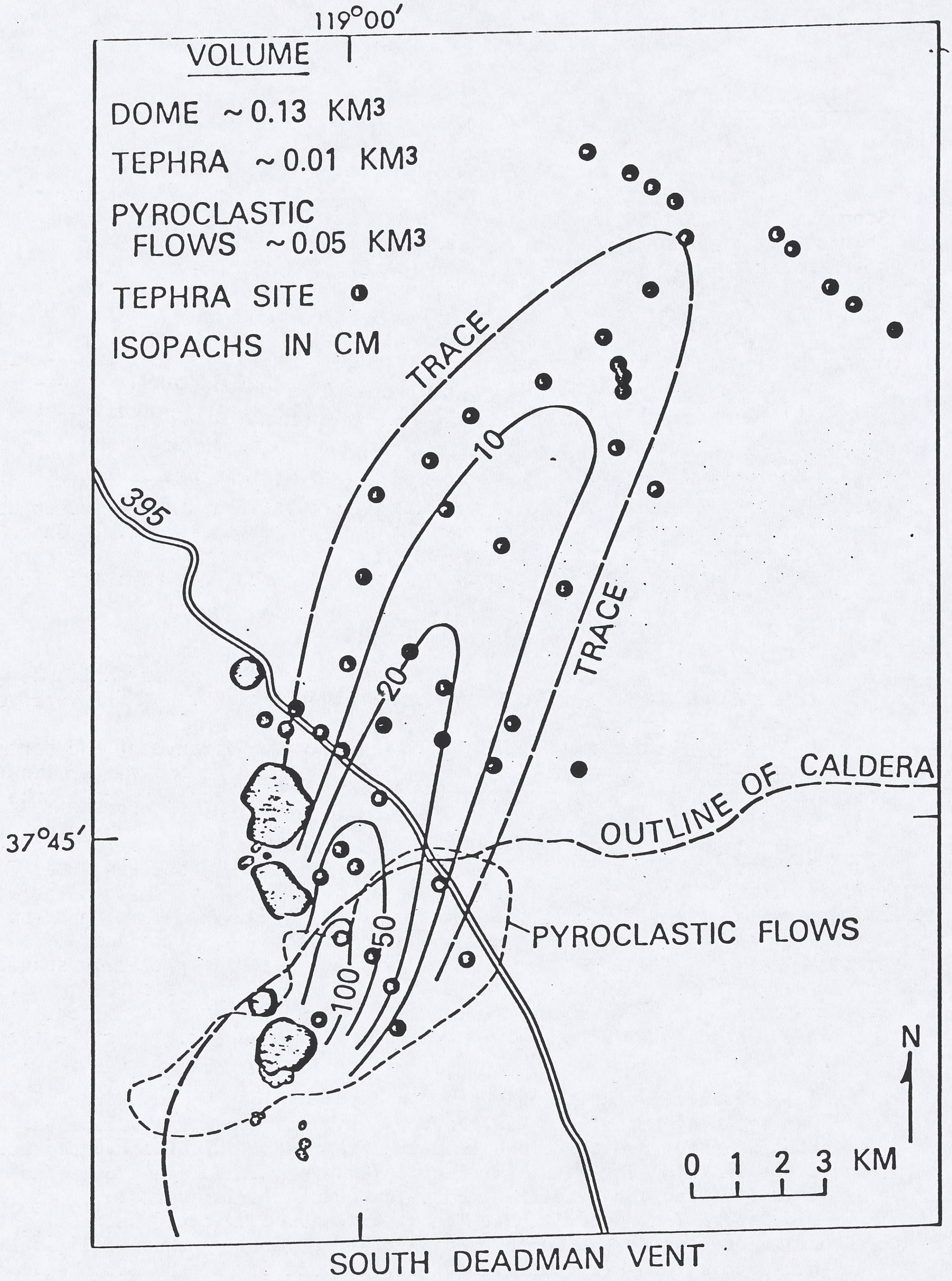

FIGURE 4.--Isopach map of tephra and distribution of pyroclastic flows from first eruption at South Deadman vent 650-550 yrs ago. Location of Stop 2 lies near the east side of the 50-cm contour. Location of Stop 3 is near the northeast edge of South Deadman rhyolite flow.

(Miller) Stop 3 Deadman Creek Campground, roadcut at entrance to south campground, 1/2 km north of South Deadman Dome

South Deadman pyroclastic-flow and -surge deposits, petrology and chemistry of South Deadman rhyolite dome.

At this locality, the pyroclastic flow that forms the ground surface at Stop 2 is more than 10 m thick, where it is exposed along the banks by downcutting of Deadman Creek. At this Stop, the main pyroclastic flow unit is coarser and thicker than at Stop 2, but it retains a pink-colored center, the same general appearance and composition, and it still has a broad flat upper surface.

At this location, and elsewhere near the vent, the pyroclastic-flow deposit is overlain by a series of lapilli and ash pyroclastic-flow and -surge deposits that vary in thickness from about 1 to 2.5 m and appear to form dunes, hills, or levees on top of the main pyroclastic-flow deposit (fig. 5). The upper sequence of pyroclastic deposits contains occasional bits of charcoal and shows considerable variation in bedding, grading, and sorting characteristics that apparently resulted from near-vent variations in the character and intensity of the eruption. Such variations have not been seen in deposits exposed several kilometers or more from the vent (e.g., Stop 2).

The final event in the eruptive sequence that occurred about 600 yrs ago at the South Deadman vent was eruption of the South Deadman rhyolite flow which has a volume of about 0.13 km^3.

(Miller) Stop 4 Highway 395 at turnoff to Arcularius Ranch.

Observation stop for view of northwest moat of Long Valley Caldera, north and west walls of caldera, Deer Mountain moat rhyolite, and Inyo rhyolite flows.

At this stop, spectacular views toward the west, northwest, and north reveal the walls and moat of Long Valley Caldera. Behind the viewer (to southeast) is the forested resurgent dome in the west-central part of the caldera.

From this location, three Inyo rhyolite flows can be seen: From north to south they are the Obsidian Flow (outside the caldera), the Glass Creek Flow (flowing down the caldera wall), and the South Deadman Flow (within the caldera and visited at Stop 3). All three vents are alined in a north-south direction and erupted during a short-time interval 650-550 yrs ago. The eruptive sequence during the most recent episode began with closely spaced explosive eruptions at South Deadman, Obsidian Flow, and Glass Creek vents, respectively, and was followed closely by multiple phreatic explosions along Glass Creek, south and west of Deer Mountain, and on the flanks of Mammoth Mountain. After explosive magmatic and phreatic activity stopped, rhyolite flows were extruded at the South Deadman, Glass Creek, and Obsidian Flow vents.

Alinement of magmatic and phreatic vents and their association with north-south grabens and ground-surface cracks, suggest that the Inyo eruptive episode 650-550 yrs ago resulted when an 8-km-long vertical dike was intruded into an elongate zone of crustal extension at the base of the Sierra Nevada escarpment. Rhyolite flows erupted from the three magmatic vents active during the most recent episode can be seen from this location along with debris from one of the Inyo crater explosions exposed at the top of Deer Mountain.

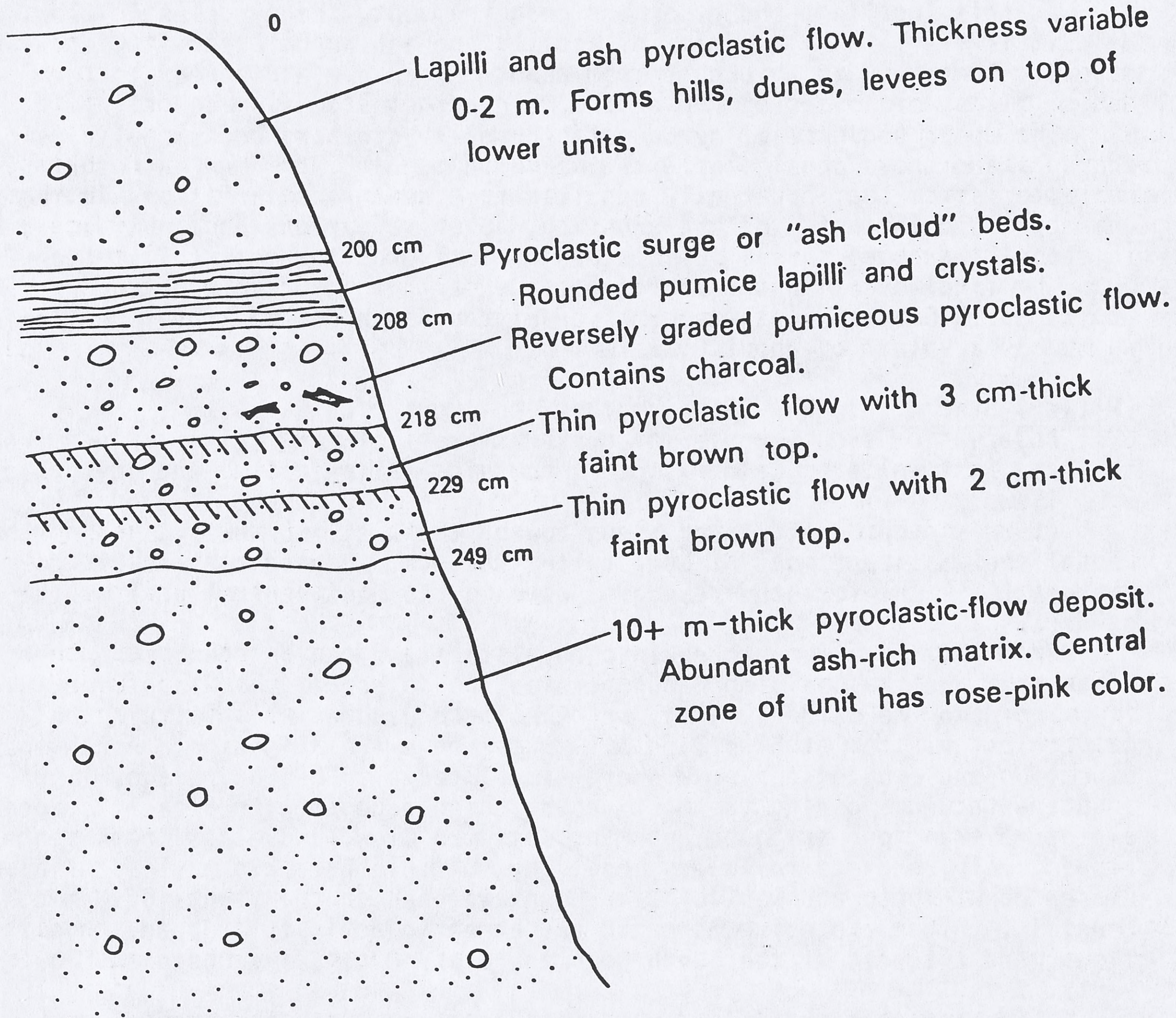

FIGURE 5.--Sketch of stratigraphic section exposed along road into the south Deadman Creek Campground about 1/2 km north of South Deadman Dome. Section shown is above road and represents upper part of sequence that overlies the main South Deadman pyroclastic flow seen at Stop 2. The upper section is 1-2.5 m thick and represents a succession of near-vent pyroclastic-flow and-surge deposits that form dunes, hills, and levees on top of the main body of the pyroclastic flow.

THIS MANUSCRIPT HAS BEEN ACCEPTED FOR PUBLICATION IN GEOLOGY AND IS EXPECTED TO COME OUT IN JANUARY 1985. ANY CITATION OF THESE DATA SHOULD BE REFERRED TO GEOLOGY, (IN PRESS).

Holocene eruptions at the Inyo Volcanic chain, California--Implications for possible eruptions in Long Valley Caldera

C. Dan Miller U.S. Geological Survey, P. O. Box 25046, Denver Federal Center, M.S. 903, Denver, Colorado 80225

ABSTRACT

The 11-km-long Inyo volcanic chain consists of 6 magmatic and more than 15 phreatic eruptive centers alined along a north-trending fracture. About 0.8 km^3 of rhyolitic-rhyodacitic magma erupted along the chain during at least three eruptive episodes during the last several thousand years. Pyroclastic deposits make up about 40 percent of this volume. The chemical similarities, timing of eruptions, and alinement of magmatic and phreatic vents suggest that the third eruptive episode, about 650-550 yrs ago, occurred when a vertical, tabular, silicic magma body was emplaced at a shallow depth. A similar dikelike intrusion may explain an increase in seismicity and deformation in the south moat of Long Valley Caldera. Events about 650-550 yrs ago at the Inyo chain provide a model for possible events during future eruptions in the south moat of the caldera.

INTRODUCTION

The Inyo volcanic chain consists of 6 magmatic and more than 15 phreatic eruptive centers alined along a north-trending 16-km-long fracture located east of the Sierra Nevada in central eastern California (Fig. 1). The Inyo vents extend from the south end of the Mono Craters into the northwest corner of the Long Valley Caldera (Fig. 2), a large elliptical depression formed by eruption of the Bishop Tuff about 700,000 yrs ago (Bailey et al., 1976).This paper describes the age, nature, and sequence of Holocene eruptions at the Inyo chain and discusses their implications with regard to possible future eruptions in the south moat of Long Valley Caldera, where seismicity and deformation have increased in 1980-83.

HOLOCENE ERUPTIONS

The location and alinement of vents in the Inyo volcanic chain is apparently due to repeated injection of magma into north-trending fractures at the base of the Sierra Nevada escarpment. The alinement of vents forms an 11-km-long north-south chain that coincides with a 16-km-long north-trending zone of faults and cracks (Fig. 2) resulting from east-west crustal extension. Many Inyo vents are within small grabens a few hundred meters wide; the chain as a whole is within a broad, shallow, poorly defined graben 2-3 km wide. North-trending fissures near several vents, and others west of Mammoth Lakes (Fig. 2), are tens to hundreds of meters long and vary in width from less than one to several meters wide. Many fissures are draped with thick pyroclastic debris in which elongate sags and sinkholes have developed. Field relations between deposits of the last eruptive episode and ground cracks suggest that crustal extension preceded and probably accompanied the rise of magma and resulting eruptions.

Figure 1. Index map of the Long Valley-Mono Lake area, east-central California.

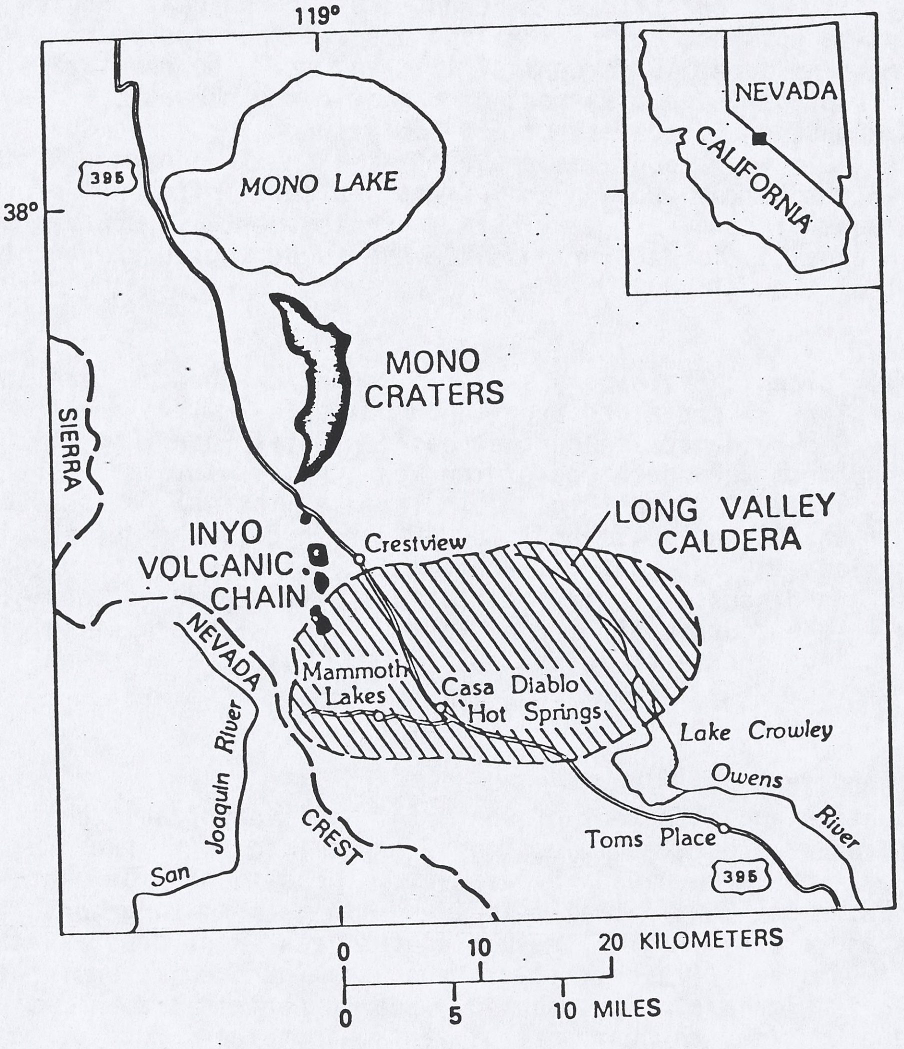

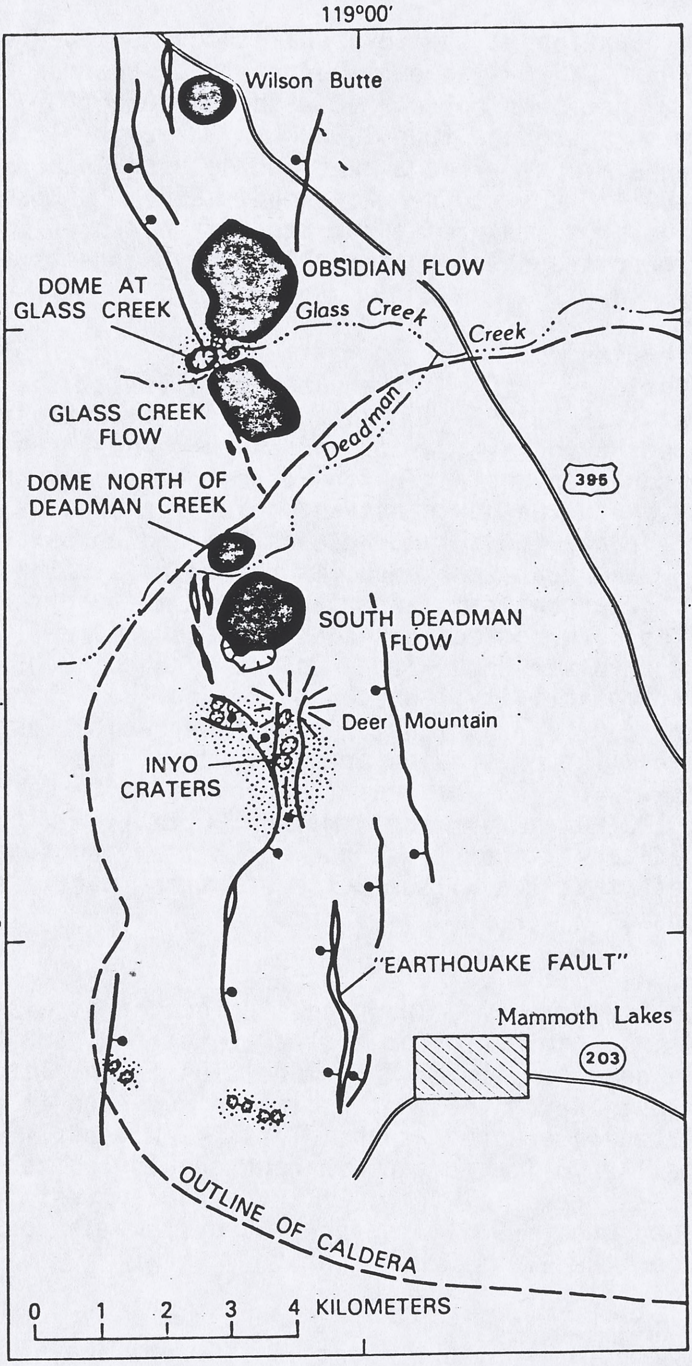

Figure 2. Map of Inyo volcanic chain and western part of Long Valley Caldera (heavy dashed line). Black areas = Inyo rhyolite domes and flows. Circles with hachures = phreatic vents. Stipple = phreatic explosion debris (after Bailey and Koeppen, 1977). Elongate lens-shaped patterns = fissures.

Early Eruption

The earliest eruption at the Inyo chain occurred when a rhyolite dome with a volume of about 0.04 km^3 was emplaced north of Deadman Creek. No explosive magmatic activity has been correlated with this eruption. The dome is morphologically more subdued than 1,200- to 1,350-yr-old Wilson Butte and is overlain by tephra erupted from a vent in the Mono Craters chain that has been dated at 1,190±80 ^{14}C yrs (tephra 2: Wood, 1977). Comparison of obsidian-hydration data of Wood (in press) for the dome north of Deadman Creek with other volcanic deposits dated during this study suggests that this dome is about 6,000 yrs old.

Wilson Butte Eruption

The Wilson Butte vent (Fig. 2) erupted rhyolite at the north end of the Inyo chain about 1,350-1,200 ^{14}C yrs ago. Initial explosive eruptions produced near-vent pyroclastic-fall and -surge deposits several meters thick and a thin widespread pyroclastic-flow deposit. The pyroclastic-flow deposit can be traced 9 km to the northeast and covers an area of at least 60 km^2. Assuming their average total thickness is 1 m and porosity is 35 percent, the pyroclastic-flow and near-vent deposits represent a combined magma volume of about 0.04 km^3. Charcoal samples collected from the pyroclastic-flow deposit at two localities have radiocarbon ages of 1,380±70 and 1,330±50 yrs B.P. Wilson Butte, a rhyolite dome with a volume of about 0.05 km^3, was emplaced after the explosive activity. Wilson Butte and the Wilson Butte pyroclastic-flow deposit are overlain by the 1,190±80 ^{14}C-yr-old tephra 2 of Wood (1977). No weathering or erosion are apparent at the contact of the tephra and pyroclastic flow. The dome was thus erupted after about 1350 ^{14}C yrs ago and prior to 1,190±80 ^{14}C yrs ago. Wilson Butte lies within a broad young graben and is adjacent to at least one north-trending fissure (Fig. 2); these relations suggest that the Wilson Butte eruptions were associated with active east-west extension.

Other Eruptions

A small rhyolite dome of unknown age is located at Glass Creek. The dome is 700 m across, has an explosion crater at the top, and a volume of about 0.002 km^3. The dome is similar in composition to rhyolite erupted at the Obsidian Flow vent during the most recent episode and it is overlain by a thick cover of tephra erupted at the Glass Creek vent.

A second small rhyolite dome of unknown age is located near the southwest edge of the Glass Creek flow (Fig. 2). The dome, first identified by D. E. Sampson (Pers. commun., 1984), is about 50 by 100 m across and is overlain by tephra erupted at the Glass Creek vent.

Most Recent Eruptions

Explosive magmatic eruptions about 650-550 yrs ago at the South Deadman, Obsidian Flow, and Glass Creek vents (Fig. 2) produced thick blankets of near-vent pyroclastic-fall, -flow, and -surge deposits (Table 1). One or more lobes of air-fall tephra, deposited downwind from each vent, consist of varying proportions of juvenile pumice, crystals, glass, denser microvesicular rhyolite, and accidental lithic fragments. All explosive products from the most recent Inyo eruptions overlie the 1,190±80 ^{14}C-yr-old tephra 2 of Wood (1977).

TABLE 1. CHARACTERISTICS OF DEPOSITS FROM MAGMATIC ERUPTIONS ABOUT 650-550 YR AGO AT THE GLASS CREEK, OBSIDIAN FLOW, AND SOUTH DEADMAN VENTS

Vent	Tephra			Pyroclastic flows			Domes	
	Length (km)	Area (km^2)	Volume (km^3)	Length (km)	Area (km^2)	Volume (km^3)	Area (km^2)	Volume (km^3)
Glass Creek vent	>190	>9,000	0.10	--	---	----	1.0	0.10
Obsidian Flow vent	>25	>140	0.02	<2	---	----	1.8	0.17
South Deadman vent								
SSW lobe	>25	>140	0.04					
NE lobe	>20	>80	0.01	6	>15	0.05	1.1	0.13

Explosive magmatic activity at these vents occurred during a short time and was followed closely by multiple phreatic explosions at sites along Glass Creek, south and west of Deer Mountain, and on the north and northeast flanks of Mammoth Mountain (Fig. 2). After explosive magmatic and phreatic activity stopped, rhyolite flows were extruded at the South Deadman, Glass Creek, and Obsidian Flow vents.

South Deadman Eruptions

Eruptions of the most recent episode began at the South Deadman vent (Fig. 2) and deposited a lobe of rhyolitic tephra more than 20 km long toward the northeast (Fig. 3A). The tephra is more than 2 m thick near the vent, covers an area of more than 80 km^2, and assuming a porosity of 35 percent, represents a magma volume of about 0.01 km^3. Pumiceous pyroclastic-flow deposits immediately overlie the tephra deposit near the source (Fig. 3A). The pyroclastic-flow deposits are more than 10 m thick along Deadman Creek, where they consist of multiple flow units with interbedded surge deposits. The deposits extend 6 km to the northeast and several km to the west, cover an area of about 15 km^2, and represent a magma volume of about 0.05 km^3.

The second tephra lobe produced by the South Deadman vent trends south-southwest (Fig. 3B). This tephra is more than 4 m thick near the vent and extends more than 25 km to the south into the High Sierra. The minimum area covered by the deposit is 140 km^2, and the volume of magma represented is about 0.04 km^3. Lack of erosion between strata and dating suggest that the south-southwest lobe was emplaced soon after the northeast lobe.

Radiocarbon dates on charcoal collected from fragmental deposits erupted at the South Deadman vent during the two eruptive pulses give ages in radiocarbon years of: 510±100, 655±120, 670±60, 740±70, 750±60, and 770±120 B.P. Jeffrey pine stumps rooted in pyroclastic flows of this episode have cross-dated ring counts (David Yamaguchi, written commun., 1983), that indicate a minimum calendar age of A.D. 1369 for these eruptions. This tree-ring date approximates the age of the deposits because the fine-grained matrix of the deposits should have allowed rapid establishment of seedlings, and trees on these deposits are at least 100 years younger than the maximum lifespan of Jeffrey pine in the region (David Yamaguchi, written commun., 1984).

Obsidian-Flow Eruptions

Eruptions soon after the initial eruption at South Deadman, at the Obsidian-Flow vent about 5 km to the north (Fig. 2), began with an explosive eruption that deposited a lobe of rhyolitic tephra to the northeast (Fig. 3C). The lobe can be traced more than 25 km, covers an area of more than 140 km^2, and represents a magma volume of about 0.02 km^3. Thin, small-volume pyroclastic-flow and -surge deposits overlie the tephra near the vent.

No radiocarbon dates have been obtained for these fragmental deposits. The deposits overlie the north-northeast-trending tephra lobe from the South Deadman vent, and cross-dated Jeffrey pines growing on them indicate a minimum calender age of A.D. 1433 (David Yamaguchi, written commun., 1983).

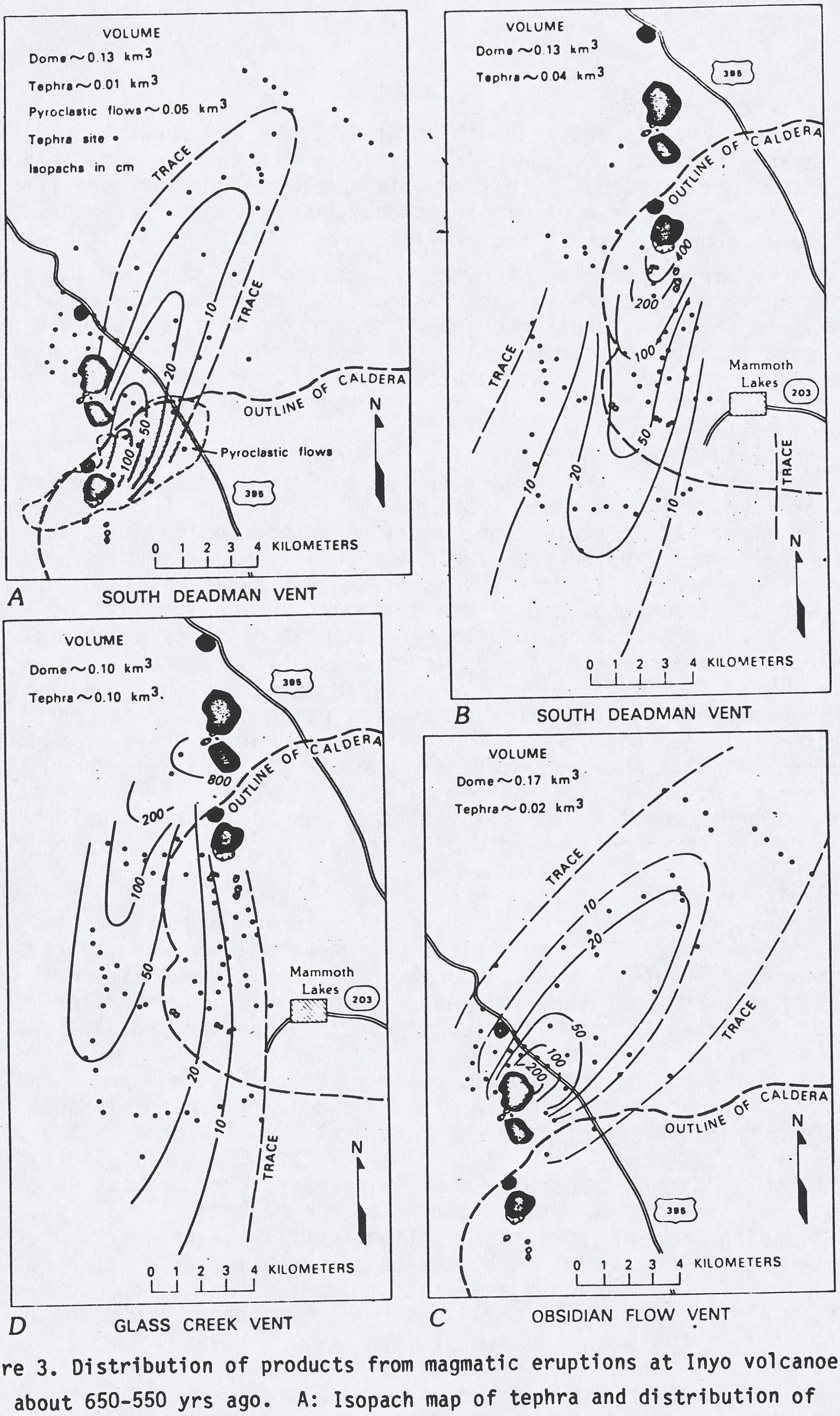

A SOUTH DEADMAN VENT

B SOUTH DEADMAN VENT

D GLASS CREEK VENT

C OBSIDIAN FLOW VENT

Figure 3. Distribution of products from magmatic eruptions at Inyo volcanoes about 650-550 yrs ago. A: Isopach map of tephra and distribution of pyroclastic flows from first eruption at South Deadman vent. B: Isopach map of tephra from second eruptive pulse at South Deadman vent. C: Isopach map of tephra erupted at Obsidian Flow vent. D: Isopach map of near-vent eastern part of Glass Creek tephra lobe.

Glass Creek Eruptions

The next vent to erupt, south of Glass Creek and about 1.5 km south of the Obsidian-Flow vent, produced a rhyolitic tephra that is more than 10 m thick near the vent (Fig. 3D). This deposit can be traced for more than 190 km to the south, covers an area of more than 9,000 km^2, and represents a magma volume of about 0.1 km^3 (Wood, 1977).

Poorly sorted pumiceous flowage deposits, at least one unit of which is incipiently welded, are exposed along Glass Creek. These deposits have an aggregate thickness of as much as 25 m near the source vent, and can be traced for several kilometers downvalley. Although they resemble deposits of pumiceous pyroclastic flows, these strata were probably generated from thick, near-vent accumulations of Glass Creek tephra that avalanched down steep slopes west of the vent.

The Glass Creek tephra was first described by Wood (1977) who named it tephra 1; he determined its age to be 720±60 ^{14}C yrs B.P. and suggested that it was erupted from the South Deadman vent, based on its trace-element composition. Its distribution, and a detailed isopach map (fig. 3D) indicate that the tephra erupted from the Glass Creek vent, and it is here renamed the Glass Creek tephra, after its source; new ^{14}C dates obtained during this study suggest it is somewhat younger than thought by Wood.

The Glass Creek tephra overlies fragmental deposits erupted from both the South Deadman and Obsidian-Flow vents and killed a forest west of its source vent. Wood samples from the forest yield dates of 530±50 and 650±100 ^{14}C yrs B.P. Cross-dating of Jeffrey pines growing on Glass Creek tephra indicates a minimum calender age of A.D. 1472 for this eruption (David Yamaguchi, written commun., 1983). Thus, the calender age of this tephra is somewhat older than 512 yrs (in 1984) and may be several tens of years older, because the coarse, matrix-poor deposit at the site of the oldest dated tree would be expected to be colonized by seedlings only after a period of decades or longer.

Phreatic Eruptions

Contemporaneous with and soon after explosive magmatic activity ceased at the Inyo volcanoes, phreatic eruptions occurred along the north-south alinement of vents (Fig. 2). Phreatic craters along Glass Creek, between the Glass Creek and Obsidian-Flow vents, formed prior to and after magmatic tephras erupted at nearby vents; at least one crater predates extrusion of Obsidian Flow.

Following explosive magmatic activity at the South Deadman and Glass Creek vents, at least three phreatic eruptions occurred south of South Deadman flow to form the Inyo craters; three additional phreatic craters that appear to be similar in age formed west of the Inyo craters (Fig. 2). The explosion craters lie within two small, complex grabens, one of which is alined north-south and lies directly on the trend of the magmatic vents (Fig. 2).

Deposits from the phreatic eruptions overlie tephras from South Deadman and Glass Creek vents. Radiocarbon dates on uncharred wood in phreatic debris from south Inyo crater suggest that at least one eruption occurred about 550±60 ^{14}C yrs ago (Wood, 1977). Huber and Rinehart (1967) noted that Jeffrey pines and firs growing within the Inyo craters have as many as 400 growth rings.

Phreatic explosion craters on the north and northeast flank of Mammoth Mountain (Fig. 2) were recognized by Huber and Rinehart (1967). Debris from one of these was dated (Bailey and Koeppen, 1977; R. A. Bailey, written commun., 1983) at 500±200 ^{14}C yrs B.P.

Effusive Eruptions

After all explosive magmatic activity and all or most phreatic activity stopped, extensive rhyolite flows issued from the South Deadman, Glass Creek, and Obsidian Flow vents and covered areas of 1-2 km^2 with volumes of 0.1-0.2 km^3 (Table 1). No magmatic or phreatic tephra have been found on any of the rhyolite flows; all explosive activity along the chain had apparently ceased before eruption of any of the flows. These observations suggest that the entire eruptive episode occurred within a short time because effusive eruptions often begin soon after explosive activity stops.

No radiocarbon or closely limiting tree-ring dates have been obtained for the Inyo rhyolite flows. Previous attempts to date the flow rocks by K/Ar-dating techniques (Dalrymple, 1967) have yielded ages that greatly exceed the radiocarbon ages of fragmental deposits that preceded eruption of the flows.

Timing of the Most Recent Eruptive Episode

Radiocarbon dates for the episode range from 500±200 to 770±120 ^{14}C yrs B.P. Minimum ages derived from tree-ring counts range from about 615 yrs for the earliest eruption to about 512 yrs for the youngest explosive magmatic activity. Extrusion of the three lava flows after all explosive activity had ceased suggests a short time interval for the entire eruptive episode. Finally, there is no evidence for erosion, or weathering between any of the strata deposited in this episode.

GEOMETRY OF FEEDER CONDUIT

Characteristics of the most recent eruptions suggest that events about 650-550 yrs ago resulted when a vertical dikelike body was emplaced into a zone of crustal extension. Evidence includes (1) alinement of vents, (2) "simultaneous" eruptions along a chain of vents, (3) chemical similarities of alined-vent magmas (Bailey et al., 1983), (4) paired zones of tensional cracks (Fink and Pollard, 1983), and (5) graben structures (Fink and Pollard, 1983).

Studies of the petrology and chemistry of the Inyo flows and domes by Bailey et al. (1983) led them to suggest that magmas erupted during the last eruptive episode, and probably earlier episodes as well, came from a single chemically zoned magma chamber. They noted that rhyolite magmas erupted at the Obsidian Flow, Glass Creek, and South Deadman vents are chemically and petrographically heterogeneous; each flow typically includes a sparsely porphyritic marginal facies and a coarsely porphyritic core. From Obsidian Flow vent southward to the South Deadman flow, the proportion of the coarsely porphyritic facies increases. Alternatively, Sampson et al. (1983) suggested that chemical heterogeneities displayed by the Inyo magmas cannot be explained by fractional crystallization of a single magma body and that distinctly separate magmas are involved. These data suggest that magmatic phases erupted during the last series of Inyo eruptions were supplied in different proportions within a single elongate conduit system.

Paired zones of tensional cracks and fissures and graben structures, (Fig. 2), are similar to surface deformation related to dikelike feeder conduits and alined-vent eruptions elsewhere (e.g., Medicine Lake Highland, Fink and Pollard, 1983; South Sister, Scott, 1983).

Nearly "simultaneous" eruption of Inyo volcanic vents and their proximity to parallel-trending grabens and extensional features imply the existence of a dike or a set of subparallel dikes that acted as feeders for the last series of magmatic eruptions and as a heat source for associated phreatic explosions. Surface extensional cracks that continue south of the Inyo craters along the so-called "Earthquake Fault" (Fig. 2) suggest that subsurface dike(s) extend south of the South Deadman vent to an area just west of the town of Mammoth Lakes; thus, the Inyo volcanoes may be underlain by a dikelike feeder system as long as 13 km.

IMPLICATIONS FOR FUTURE ACTIVITY IN LONG VALLEY CALDERA

Events about 650-550 yrs ago in the Inyo volcanic chain provide a model for possible future eruptions in the south moat of Long Valley Caldera. Ground-surface extension, uplift of a resurgent dome, and increased seismicity in Long Valley Caldera during 1980-83 (Ryall and Ryall, 1982; Miller et al., 1982; Miller and Newhall, 1983; Cockerham and Savage, 1983) have increased the concern about possible future eruptions in that area. Cockerham and Savage (1983) interpreted the seismicity and ground-surface deformation southeast of Mammoth Lakes during 1983 as due to intrusion of a dike into the south ring fracture of the caldera.

If a dike is being intruded under the south moat of Long Valley Caldera, events 650-550 yrs ago at the Inyo volcanoes provide insights into tectonic and eruptive events that might occur if such a dike moves toward the surface. Past events at the Inyo chain suggest that dikelike conduits, such as the one postulated under the south moat, could produce extensive surface faulting and both explosive magmatic and phreatic eruptions closely spaced in time at many vents. The sequence of activities expected would be (1) surface deformation above a rising dike, (2) phreatic eruptions as a dike approaches the surface, (3) a series of magmatic and phreatic eruptions at several to many points along the trend of a dike, and (4) extrusion of lava at magmatic vents.

The analogy between past volcanic events in the Inyo chain and recent changes in the south moat of Long Valley Caldera is discussed here because, at both locations, injection of magma is postulated to take place into zones of weakness resulting from crustal extension or deformation. The size and nature of future eruption(s) in the Long Valley epicentral zone will depend on such factors as the nature of magma being injected, including its volume, composition, volatile content, and other physical characteristics. All these factors are unknown, and thus a wide range of activity--eruptive and noneruptive--is possible within the epicentral area at Long Valley Caldera.

REFERENCES CITED

Bailey, R. A., Dalrymple, G. B., and Lamphere, M. A., 1976, Volcanism, structure, and geochronology of Long Valley Caldera, Mono County, California: Journal of Geophysical Research, v. 81, p. 725-744.

Bailey, R. A., and Koeppen, R., 1977, Preliminary geologic map of Long Valley Caldera, Mono County, California: U.S. Geological Survey Open-File Map 77-468, scale 1:62,500.

Bailey, R. A., MacDonald, R. A., and Thomas, J. E., 1983, The Inyo-Mono Craters: Products of an actively differentiating rhyolite magma chamber, eastern California [abs.]: EOS (American Geophysical Union Transactions), v. 64, p. 336.

Cockerham, R. S., and Savage, J. C., 1983, Earthquake swarm in Long Valley, California, January 1983 [abs.]: EOS (American Geophysical Union Transactions), v. 64, p. 890.

Dalrymple, G. B., 1967, Potassium-argon ages of recent rhyolites of the Mono and Inyo Craters, California: Earth and Planetary Science Letters, v. 3, p. 289-298.

Fink, J. H., and Pollard, D. D., 1983, Structural evidence for dikes beneath silicic domes, Medicine Lake Highland volcano, California: Geology, v. 11, p. 458-461.

Huber, N. K., and Rinehart, C. D., 1967, Cenozoic volcanic rocks of the Devils Postpile quadrangle, eastern Sierra Nevada, California: U.S. Geological Survey Professional Paper 554-D, p. D1-D21.

Miller, C. D., Mullineaux, D. R., Crandell, D. R., and Bailey, R. A., 1982, Potential hazards from future volcanic eruptions in the Long Valley-Mono Lake area, east-central California and southwest Nevada--A preliminary assessment: U.S. Geological Survey Circular 877, 10 p.

Miller, C. D., and Newhall, C. G., 1983, Volcanic-hazards implications of recent seismicity, deformation, and hydrothermal activity, Long Valley Caldera, California, USA [abs.]: 1983 International Union of Geodesy and Geophysics Program and Abstracts, p. 363.

Ryall, F., and Ryall, A., 1982, Propagation of effects and seismicity associated with magma in the Long Valley Caldera, eastern California: Earthquake Notes, v. 53, no. 1, p. 46-47.

Sampson, D. E., Ardito, C. P., Kelleher, P. C., Cameron, K. L., and Bullen, T. D., 1983, The geochemistry of Quaternary lavas from the Inyo-Mono chain: Evidence for several magma types: EOS (American Geophysical Union Transactions), v. 64, p.889.

Scott, W. E., 1983, Character and age of Holocene rhyodacite eruptions at South Sister volcano, Oregon: EOS (American Geophysical Union Transactions), v. 64, p. 899-900.

Wood, S. H., 1977, Distribution, correlation, and radiocarbon dating of late Holocene tephra, Mono and Inyo Craters, eastern California: Geological Society of America Bulletin, v. 88, p. 89-95.

_____in press, Chronology of late Pleistocene volcanics, Long Valley and Mono Basin geothermal areas, eastern California: U.S. Geological Survey Open-File Report, 55 p.

ACKNOWLEDGMENTS

Reviewed by P. W. Lipman, R. P. Hoblitt, and M. K. Reagan, who made valuable comments that led to improvement of the paper. I thank M. K. Reagan, W. E. Scott, and R. P. Hoblitt for assistance and valuable discussions in the field.

2019.8.48

HETCH HETCHY DOME
Miguel Mdw
O'Shaughnessy Dam
Poopenaut Valley
LE CONTE POINT
RANCHERIA MOUNTAIN
GRAND CANYON OF THE TUOLUMNE RIVER
SMITH PEAK
Smith Meadow
HOOPER PK
ELBOW HILL
COLD MTN
Cold Canyon
MT CONNESS
RAGGED PEAK
COLBY MTN 9631
FALLS RIDGE
Ranger station
BASE LINE
DOUBLE ROCK
MORAINE FLAT
YOSEMITE NATIONAL PARK
White Wolf Pack Station
BALD MOUNTAIN 7261
Long Gulch
Ackerson Mdw
Aspen Valley
TUOLUMNE PEAK
LEMBERT DOME
FAIRVIEW DOME
Tuolumne Meadows
POLLY DOME 9810
MOUNT HOFFMANN 10005
Cathedral Pk
UNICORN PEAK
JOHNSON PEAK
Snow Flat
Porcupine Flat
Cathedral Pass
CATHEDRAL RANGE
RAFFERTY PEAK
Long Meadow
11282
Tuolumne Pass
MT WATKINS
SUNRISE MTN
INDIAN ROCK
BOUNDARY HILL
Lookout tower
Gin Flat
Tamarack Flat
YOSEMITE
Tenaya Canyon
CLOUDS REST
PARSONS
VOGELSANG PEAK
SIMMONS PEAK
NORTH DOME
Yosemite Village
EAGLE PEAK
HALF DOME
EL CAPITAN
Camp Curry
Glacier Point
BUNNELL POINT
Little Yosemite Valley
Ranger Station
MT FLORENCE
MARIPOSA CO
MADERA CO
TAFT POINT
Clark Canyon
Foresta
Power plant
EAGLE PEAK
MOUNT STARR KING 9092
El Portal
Rancheria Flat
140
OSTRANDER ROCKS
MT CLARK
CLARK RANGE
FOERSTER PEAK
Badger Pass
Peregoy Meadow
GRAY PK
APPROXIMATE
Chinquapin
RED PEAK 11699
YOSEMITE NATIONAL PARK
BROWN PEAK
CATHEWOOD SADDLE
PINOCHE PEAK
Isberg Pass
TRIPLE DIVIDE PEAK
Empire Meadow
MERCED PEAK
Merced Pass
HORSE RIDGE
SIERRA NATIONAL FOREST
BUENA VISTA CREST
Cabin
MORAINE MTN
Fernandez Pass
TIMBER KNOB
CHOWCHILLA MOUNTAINS
Devil Gulch
FOOTMAN RIDGE
WAWONA DOME
North Wawona
Wawona
GALE PEAK
SING PEAK
RED TOP
SIERRA
DEVIL PEAK Lookout tower
Chiquito Pass
MADERA PEAK
Gravelly Ford Mine
KIRBY PEAK
WAWONA PT
RAYMOND MTN
QUARTZ MTN
Clover Meadow Forest Sta
Cem
HOGAN MOUNTAIN
WHITE CHIEF MOUNTAIN
Campground
Fish Camp
Muglers Meadow
Miller Meadow
IRON MOUNTAIN 9165
JACKASS BUTTE
Elliott Corner
Ranch
Campground
Camp
PALONI MTN
Sonny Meadows
Ranger Station
41
SPECKERMAN MTN
FRESNO DOME
TEXAS FLAT
Graveyard Meadow
STUMPFIELD MTN
Sugar Pine
Nelder Grove
McSwain Mines
PILOT PEAK
SILVER KNOB
Beasore Meadow
JACKASS ROCK
MIAMI MTN 4327
Lookout tower
Nelson Cove
Nipinnawassee
Metcalf Gap
INDIAN PEAK
Gooseberry Flat
SIVELS MTN 5813
Ranger station
Meadow
LITTLE SHUTEYE